STRATEGIES FOR USING MICROORGANISMS AND ENZYMATIC SYSTEMS IN BIOREMEDIATION

Francesca Pennacchio

Dottorato in Scienze Biotecnologiche – XXI ciclo
Indirizzo Biotecnologie Industriale
Università di Napoli Federico II

Dottorato in Scienze Biotecnologiche – XXI ciclo
Indirizzo Biotecnologie Industriale
Università di Napoli Federico II

STRATEGIES FOR USING MICROORGANISMS AND ENZYMATIC SYSTEMS IN BIOREMEDIATION

Francesca Pennacchio

Dottoranda: Francesca Pennacchio

Relatore: Prof. Alberto Di Donato

Coordinatore: Prof. Giovanni Sannia

INDEX

SUMMARY

Environmental pollution caused by the release of a wide range of xenobiotic compounds has assumed serious proportions. Bioremediation techniques, utilizing microorganisms to reduce the concentration and toxicity of various chemical pollutants such as petroleum hydrocarbons, polycyclic aromatic hydrocarbons, polychlorinated biphenyls, industrial solvents and pesticides, are the most promising strategies for the restoration of polluted environments.

Several bacterial strains with promising degradative abilities have already been isolated and characterized. However, the full exploitation of the potential of bioremediation strategies requires not only the isolation of a large number of strains with wide degradative abilities but also an accurate characterization of these strains both at the microbiological and biochemical/genetic level. This knowledge is necessary to perform a rational planning of bioremediation interventions.

The present work describes two research lines which illustrate the two different approaches:

1. Engineering of catechol 2,3-dioxygenase (C2,3O) a crucial enzyme in degradative pathway for aromatic compounds of *Pseudomonas* sp. OX1, a well-studied microorganism.
2. Isolation of new strains able to degrade aromatic hydrocarbons directly from polluted environments by means of appropriate selection procedures.

Ring cleavage dioxygenases catalyze the oxygen dependent cleavage of catecholic compounds, a critical step in the aerobic degradation of aromatic compounds. Their specificity and regioselectivity control the range of molecules degraded through the catabolic pathway of microorganisms able to use aromatic hydrocarbons as growth substrates. Catechol-2,3-dioxygenase from *Pseudomonas* sp. OX1 can cleave effectively only 3,4-dimethylcatechol (DMC), a catechol which derives from the hydroxylation of *o*-xylene, and not 3,5- and 3,6-DMC, the hydroxylation products of *m*- and *p*-xilene, respectively. Thus, the restricted specificity of C2,3O is the primary metabolic determinant which limits the ability of *Pseudomonas* sp. OX1 to efficiently grow on xylene mixtures. Thus, understanding the molecular determinants that control substrate binding in *Pseudomonas* sp. OX1 C2,3O could allow to develop mutated enzymes with a wider substrate specificity and eventually engineered microorganisms with enhanced ability to grow on substituted aromatic compounds. In this thesis we describe the preparation of several C2,3O variants with mutations at positions 249, 270, 267 and/or 198 designed with the aim of obtaining a mutated enzyme with both a good affinity and a high catalytic efficiency on 3,5-DMC, and 3,6-DMC.

In the second section we describe the isolation from surface seawater samples and the characterization of a new *Sphingomonadales*, *Novosphingobium* sp. PP1 Y. The strain PP1Y is able to use a surprisingly large number of mono- and polycyclic aromatic compounds as the sole carbon and energy sources but shows also a very interesting and effective adaptation to grow on complex mixtures of aromatic compounds dissolved in oil phases like gas-oil and gasoline.

RIASSUNTO

Per "*bioremediation*" si intende l'utilizzo di organismi viventi, in particolare microrganismi quali batteri, funghi e lieviti, per la degradazione di composti chimici tossici.

Alcune tipologie di composti che possono essere trattate con le tecniche di bioremediation sono gli idrocarburi alifatici, quelli aromatici e gli idrocarburi aromatici policiclici (IPA). Ancora, i composti policiclici aromatici alogenati (diossine, PCB, dibenzofurani, dibenzotiofeni, ecc.), i composti organici clorurati non aromatici (cloruro di vinile, policloroetileni, ecc.), fenoli e ammine aromatiche, composti utilizzati in agricoltura (diserbanti, pesticidi, fungicidi, ecc.), e infine svariati reflui industriali (solventi, sgrassanti, detergenti, reagenti per la produzione dei polimeri, ecc.).

A causa della loro tossicità, ed in alcuni casi della loro cancerogenicità, gli idrocarburi aromatici, i loro derivati e le molecole aromatiche eterocicliche destano particolare preoccupazione e sono quindi stati oggetto di numerosi studi.

L'eccezionale adattabilità dei microrganismi fa si che, dopo un tempo sufficientemente lungo, in un ambiente inquinato compaiano ceppi adattati capaci non solo di tollerare i composti inquinanti ma di utilizzarli come fonte di nutrimento. Questi ceppi possono essere utilizzati, singolarmente o in consorzi composti da numerosi ceppi, per ridurre o eliminare composti chimici presenti in acque dolci o salate, suoli, sabbia e fondali marini.

Sono stati già isolati e caratterizzati numerosissimi ceppi batterici capaci di degradare un'ampia varietà di composti xenobioticiquali ad esempio gli Sfingomonadali (capaci di degradare idrocarburi alifatici e aromatici, IPA, diossine e dibenzofurani), i Micobatteri (capaci di degradare gli IPA), gli Pseudomonadali (capaci di degradare idrocarburi alifatici e aromatici, IPA, fenoli e ammine aromatiche, detergenti, solventi) e gli Attinomiceti (capaci di degradare idrocarburi alifatici e aromatici, IPA, diossine e dibenzofurani).

Gli interventi di bioremediation possono svolgersi *in situ* o *ex situ*. Nel primo caso, se nell'ambiente da trattare si è già sviluppata una microflora con capacità degradative, l'attività della microflora indigena può essere stimolata mediante una serie di interventi volti ad ottimizzare parametri ambientali quali ad esempio la disponibilità di nutrienti (mediante fertilizzazione con azoto, fosforo, zolfo ecc.), l'aerazione (mediante aratura, pompaggio forzato di aria ecc.), l'umidità (mediante irrigazione) e la temperatura (mediante pompaggio forzato di aria calda). Nel caso in cui nell'ambiente da trattare non si sia ancora sviluppata una microflora con capacità degradative, la microflora endogena può essere arricchita inoculando opportuni ceppi coltivati in laboratorio. Negli interventi *ex situ* il substrato inquinato (acqua, terreno, sabbia, limo di fondali, ecc.) viene asportato e trattato in opportuni impianti (bioreattori, vasche, ecc.). Tutti i parametri fondamentali (temperatura, pH, umidità, ossigenazione, salinità, ecc.) possono essere monitorati costantemente e modificati all'occorrenza. Questo tipo di intervento, dal costo più elevato, è adatto alla decontaminazione di volumi relativamente piccoli di substrato inquinato.

I protocolli di trattamento vanno ottimizzati caso per caso. La programmazione dell'intervento di bonifica deve partire dall'analisi della tipologia degli inquinanti e dei parametri chimico-fisici del substrato da trattare (disponibilità di nutrienti minerali,

temperatura, pH, umidità, ossigenazione, salinità, ecc.) in modo da scegliere la combinazione più opportuna di ceppi e trattamenti. Il successo degli interventi di bonifica dipende quindi in larga parte dalla disponibilità di un'ampia scelta di ceppi microbici.

Molti ceppi particolarmente promettenti per impieghi nelle bioremediation sono già disponibili (molti sono coperti da brevetto), tuttavia, l'isolamento di nuovi ceppi utili è relativamente semplice dal punto di vista tecnico.

Il presente lavoro di tesi si inserisce in un progetto più ampio il cui scopo è l'ottenimento di microrganismi e sistemi enzimatici da utilizzare per le strategie di bioremediation intese sia per interventi *in situ* ed *ex situ* che per l'impiego in bioreattori progettati per lo smaltimento di reflui industriali quali ad esempio acque reflue contenenti elevati livelli di idrocarburi aromatici e/o loro derivati. Per conseguire questo obiettivo sono in corso di svolgimento sia linee di ricerca indirizzate all'isolamento da ambienti inquinati di nuovi ceppi dotati di specifiche capacità degradative naturali e alla loro caratterizzazione che linee di ricerca il cui scopo è studiare, al fine di poter manipolare, le capacità catalitiche degli enzimi dei pathway degradativi e a più lungo termine progettare microrganismi ingegnerizzati dotati di più ampie capacità degradative o più adatti all'impiego in campo e nei sistemi bioreattoristici.

Il lavoro di tesi persegue entrambe le linee di ricerca esposte e si articola in due parti che illustrano i due differenti approcci.

La prima parte descrive la progettazione, la realizzazione e la caratterizzazione di mutanti della catecolo 2,3-diossigenasi (C2,3O) da *Pseudomonas* sp. OX1 dotati di una più ampia specificità di substrato. Nella seconda parte viene descritto l'isolamento e la caratterizzazione di un nuovo microrganismo, *Novosphingobium puteolanum* PP1Y, in grado di degradare una delle più ampie varietà di idrocarburi aromatici descritte in letteratura.

Le catecolo diossigenasi ed in generale le "ring cleavage dioxygenases" (RCD) svolgono un ruolo cruciale nella degradazione dei substrati aromatici essendo responsabili del taglio dell'anello aromatico. Tuttavia la loro specificità di substrato, spesso ristretta, pone un limite alla varietà di composti aromatici che un ceppo può degradare. *Pseudomonas* sp. OX1 è un interessante esempio. Questo ceppo infatti, capace di utilizzare benzene, toluene, *o*-xilene e tutti i fenoli che da essi derivano come unica fonte di carbonio ed energia, è stato impiegato con successo nella realizzazione di un bioreattore per il trattamento di reflui contenenti idrocarburi aromatici realizzato grazie ad una collaborazione con il gruppo di ricerca dei Professori Salatino e Marzocchella del Dipartimento di Ingegneria Chimica dell'Università di Napoli Federico II. Tuttavia il ceppo OX1 non è in grado di degradare *m*- e *p*-xilene spesso associati a benzene, toluene, *o*-xilene. Questa incapacità è stata attribuita al fatto che il 3,5- e il 3,6-dimetilcatecolo (DMC), che vengono prodotti dall'azione degli enzimi dell'*upper pathway* su *m*- e *p*-xilene, non sono substrati per la C2,3O di questo ceppo. Da ciò nasce l'esigenza di ampliare lo spettro di substrati che possono essere degradati dalla C2,3O per poi sviluppare ceppi ingegnerizzati di *Pseudomonas* sp. OX1 capaci di degradare miscele di isomeri dello xilene.

Lo studio del modello del sito attivo della C2,3O ha permesso di individuare nel loop G247-L248-T249 i determinanti molecolari che impediscono l'accesso al sito attivo di 3,5- e 3,6-DMC.

La caratterizzazione dei mutanti della posizione T249, (T249S)-, (T249A)- e (T249G)-C2,3O, ha confermato che l'ingombro sterico, dato dalla catena laterale della T249, è il principale responsabile dell'incapacità della C2,3O di legare efficientemente i dimetilcatecoli, ma ha anche mostrato che il gruppo ossidrilico della catena laterale di questo residuo svolge un ruolo essenziale nella catalisi.

Qualsiasi intervento di mutagenesi sito diretta per compensare la diminuzione dell'efficienza catalitica mostrata dai mutanti della posizione 249, richiede ovviamente la preliminare comprensione del ruolo svolto dal gruppo ossidrilico della T249 nella catalisi. L'analisi approfondita delle strutture cristallografiche disponibili, nonché la preparazione di modelli dei complessi C2,3O/substrati, ha permesso di ipotizzare l'esistenza di un sito di legame per una molecola d'acqua, che si disporrebbe a ponte fra il substrato e il gruppo ossidrilico della T249 creando un reticolo di legami a idrogeno. Questa ipotesi è estremamente interessante sia dal punto di vista teorico che da quello applicativo. Infatti, finora, la possibilità che la molecola d'acqua visibile nei siti attivi delle RCD, abbia un significato funzionale, non è mai stata investigata ed avrebbe profonde implicazioni per quanto riguarda la comprensione del meccanismo catalitico di questa famiglia di enzimi. Dal punto di vista pratico, l'ipotesi dell'esistenza di una molecola d'acqua con funzione catalitica, suggerisce una possibile via per la preparazione di mutanti che non solo leghino ad alta affinità il 3,5- ed il 3,6-DMC, ma che ne catalizzino efficientemente il taglio. Proprio sulla base di queste considerazioni sono stati selezionati quattro residui, A1 98, G251, F267 e G270, che circondano il sito ipotetico per la molecola d'acqua catalitica e quindi rappresentano bersagli per ulteriori interventi di ingegneria proteica. Mediante mutagenesi *in silico* ed esperimenti di docking sono state scelte tre mutazioni, F267H, G270E e G270Q, che nel mutante (T249G)-C2,3O potrebbero ripristinare il sito di legame della molecola d'acqua catalitica e quindi generare un mutante multiplo che combini la capacità di legame dei dimetilcatecoli di (T249G)-C2,3O con l'efficienza catalitica della C2,3O *wt*.

L'analisi informatica ha anche mostrato che il tipo di conformazione adottato dalle catene laterali di glutammina e glutammato in posizione 270 è determinato dalla natura dei due residui in posizione 198 e 267 adiacenti al residuo 270. Per questo motivo si è deciso di combinare le mutazioni già descritte con mutazioni dei residui A1 98 e F267 per restringere o aumentare le possibilità di movimento delle catene laterali di glutammato e glutammina. In particolare si è deciso di mutare il residuo di alanina in glicina, per ridurre l'ingombro sterico, o in serina, per aumentarlo. Il residuo di fenilalanina è stato invece sostituito con leucina.

La tecnica di mutagenesi scelta ha permesso di creare una *library* contenente le combinazioni desiderate di mutazioni a partire dal vettore contenente la sequenza codificante il mutante (T249G)-C2,3O, mentre lo "screening" mediante PCR ha permesso la rapida identificazione dei cloni di interesse.

I mutanti realizzati sono stati espressi in *E. coli*, purificati e successivamente caratterizzati su quattro substrati catecolo, 3-metilcatecolo, 3,5- e 3,6-dimetilcatecolo. La caratterizzazione cinetica dei doppi mutanti (T249G, F267H)-, (T249G, G270E)- e (T249G, G270Q)-C2,3O ha mostrato che i due mutanti, (T249G, F267H)- e (T249G, G270E)-C2,3O mostrano un sensibile miglioramento dei valori di $_{kcat}$ per il 3,5- e il 3,6-DMC, suggerendo che l'ipotesi iniziale sul coinvolgimento di una molecola di acqua nella catalisi e l'analisi informatica successiva siano valide.

L'analisi cinetica ha però anche rivelato effetti parzialmente inattesi delle due mutazioni. In particolare la mutazione G270E causa un aumento di 2-3 volte nei valori di K_M per tutti i substrati utilizzati rispetto al mutante di riferimento (T249G)-

C2,3O. Questo effetto è probabilmente dovuto al fatto che la sostituzione di una glicina con glutammato crea ingombro nel sito attivo ed in particolare con i residui del loop 197-199.

Al contrario della mutazione G270E, la mutazione F267H lascia invariato o riduce il valore di K_M per il 3,5-DMC e per il 3,6-DMC e provoca contemporaneamente un aumento della $_{kcat.}$ Conseguentemente nel mutante (T249G, F267H)-C2,3O il valore di K_S aumenta di un ordine di grandezza

Infine, è da sottolineare che la simultanea presenza dei residui E270 e H267 provoca una riduzione del valore della K_M per il 3,5 e il 3,6-DMC rispetto al mutante (T249G, G270E)-C2,3O, mentre i valori di $_{kcat}$ sono confrontabili ai valori osservati per il mutante che presenta la sola mutazione in posizione 270. E' interessante notare che la mutazione fenilalanina → istidina riduce l'ingombro in posizione 267 e questo può in parte compensare l'aumento di ingombro causato dalla mutazione glicina → glutammato a cui è stato attribuito l'aumento del valore di K_M nel mutante (T249G, G270E)-C2,3O.

Ulteriori analisi hanno mostrato che mutazioni di due residui adiacenti alla posizione 270, A1 98 e F267, possono essere usate per modificare le possibilità di movimento delle catene laterali dei residui di glutammato o glutammina in posizione 270. Queste ultime, secondo i modelli molecolari, dovrebbero collocarsi proprio al centro delle catene laterali dei residui in posizione 198 e 267. La mutazione A198G, ad esempio, riducendo l'ingombro in posizione 198 potrebbe favorire l'avvicinamento della catena laterale di E270 a questa posizione mentre la mutazione A198S potrebbe avere l'effetto opposto.

Al contrario la mutazione F267L riducendo l'ingombro della catena laterale presente in posizione 267 potrebbe permettere alla catena laterale di E270 o Q270 di avvicinarsi a questo residuo allontanandosi dalla catena laterale in posizione 198.

Sono stati analizzati gli effetti delle mutazioni A198G e A198S inserite nella sequenza del doppio mutante (T249G, G270E)-C2,3O e gli effetti della mutazione F267L inserita sia nella sequenza del doppio mutante (T249G, G270E)-C23O che del doppio mutante (T249G, G270Q)-C2,3O. La mutazione A1 98G ha determinato un peggioramento, talvolta anche significativo, di tutte le costanti catalitiche sia impiegando il catecolo o il 3-MC che i dimetilcatecoli.

Al momento l'ipotesi più plausibile è che la mutazione A198G alteri la conformazione del loop K197-A198-H199 che contribuisce alla formazione del sito catalitico diminuendo così sia l'affinità per i substrati che l'efficienza catalitica.

La mutazione A198S, invece, ha determinato lievi miglioramenti dei valori delle costanti catalitiche per i substrati fisiologici (catecolo e 3-MC) ma non ha modificato i parametri catalitici misurati utilizzando i dimetilcatecoli. I risultati ottenuti mostrano chiaramente che la sostituzione del residuo A198 non è adatta allo scopo di migliorare le performance catalitiche della C2,3O sui dimetilcatecoli.

Decisamente più incoraggianti sono gli effetti della mutazione F267L. Contrariamente alle mutazioni della posizione 198, questa mutazione ha effetti trascurabili sui parametri catalitici misurati utilizzando catecolo e 3-MC ma migliora notevolmente i parametri catalitici misurati utilizzando i dimetilcatecoli.

In particolare i valori di K_S aumentano di 10-70 volte a seconda del substrato e della natura del residuo in posizione 270 (Glu o Gln). Considerando invece i valori assoluti della costante K_S riportati in tabella 2 si può notare che il mutante (T249G, F267L, G270E)-C2,3O è attualmente il miglior catalizzatore disponibile del taglio dei dimetilcatecoli.

La seconda parte del lavoro di tesi descrive l'isolamento e la caratterizzazzione del microrganismo *Novosphingobium puteolanum* PP1Y.

Il ceppo PP1Y è stato isolato mediante una procedura di arricchimento con fenantrene da campioni di acqua superficiale prelevati in un bacino interno del porto di Pozzuoli. Dopo diversi passaggi in terreno minimo contenente cristalli di fenantrene i campioni sono stati piastrati su piastre di M9G/agar contente fenantrene come unica fonte di carbonio ed energia. Su alcune piastre sono state osservate colonie di colore giallo circondate da aree in cui l'agar - reso lattescente dai microcristalli di fenantrene - era tornato trasparente indicando l'avvenuta degradazione del fenantrene. Il ceppo PP1Y è stato isolato a partire da una di queste colon ie.

Il sequenziamento parziale del gene per l'RNA ribosomale 16S ha mostrato che il ceppo PP1Y è uno sfingomonadale strettamente imparentato (2 nucleotidi di differenza) con *Novosphingobium pentaromativorans* US6-1, un ceppo isolato da una baia in Korea capace di crescere su composti policiclici aromatici con un numero di anelli compreso tra 3 e 5, e con *Novosphingobium* sp. Phe-8 (5 nucleotidi di differenza). Tuttavia la caratterizzazione microbiologica mostra che il ceppo PP1Y differisce dal ceppo US6-1 per alcune proprietà rilevanti quali condizioni ottimali di crescita, composizione degli acidi grassi di membrana, caratteristiche metaboliche, spettro di composti aromatici degradati e morfologia di crescita; ciò fa supporre che il ceppo PP1Y sia probabilmente una nuova specie del genere *Novosphingobium* affine alle due specie citate.

Le cellule di *Novosphingobium puteolanum* PP1Y hanno la forma di corti bastoncelli negativi alla colorazione di Gram. Possono essere mobili (presumibilmente flagellate) o non-mobili. Le cellule non-mobili possono presentarsi in forma libera o formare aggregati cellulari che in alcuni casi divengono macroscopici presentandosi sotto forma di "flocculi" ramificati. Queste caratteristiche sono state riscontrate anche in altri sfingomonadali che mostrano quello che viene definito "di morfismo planctonico/sessile". Tali sfingomonadali dimorfici possono esistere in forma aggregata (forma "sessile") e in forma libera (forma "planctonica"). L'esistenza della forma sessile è dovuta alla presenza della capsula polisaccaridica che fa da collante fra le cellule.

I flocculi del ceppo PP1Y mostrano alcune caratteristiche che non sono state descritte nel caso di altri sfingomonadali dimorfici. I flocculi aderiscono spontaneamente alle superfici idrofobiche quali i polimeri plastici e adsorbono, concentrandoli, molecole idrofobiche quali coloranti idrofobici e IPA. Il ceppo PP1Y forma spontaneamente su superfici idrofobiche, sia solide che liquide, un "biofilm" che appare come una versione strutturata dei flocculi amorfi che si formano in coltura liquida.

Sono state analizzate le potenzialità degradative del ceppo PP1Y, effettuando delle crescite del microrganismo e fornendo come substrato derivati del petrolio. Il ceppo PP1Y è in grado di crescere utilizzando benzina e gasolio come uniche fonti di carbonio ed energia. In particolare il gasolio permette velocità di crescita quasi confrontabili a quelle registrate in mezzo ricco con estratto di lievito e triptone. Il gasolio è ben tollerato almeno fino ad un rapporto 2:1 = acqua:gasolio. La crescita è circa 2-5 volte più lenta nel caso della benzina. In un sistema bifasico acqua/gasolio o acqua/(paraffina-benzina) il ceppo PP1Y è responsabile della formazione di una emulsione stabile della fase oleosa che viene frammentata in goccioline con diametro inferiore a 1 mm. L'analisi al microscopio a contrasto di fase delle gocce di gasolio ha mostrato che esse sono rivestite da uno strato di biofilm contente cellule

batteriche la cui densità superficiale aumenta con il progredire dell'incubazione. Dopo incubazione prolungata (>10 giorni) nelle colture sono stati individuati aggregati che contengono più strutture sferiche rivestite di batteri legate fra loro da materiale rifrangente simile a quello che compone i flocculi ottenuti in terreno ricco.

Benzina e gasolio sono miscele estremamente complesse di decine se non centinaia di idrocarburi saturi, insaturi ed aromatici. Pertanto risulta piuttosto complesso determinare direttamente quali idrocarburi vengono degradati da *Novosphingobium puteolanum* PP1Y impiegando tali miscele come fonti di carbonio ed energia. Conseguentemente si è deciso di verificare quali idrocarburi puri potessero essere usati dal ceppo PP1Y come singole fonti di carbonio ed energia.

Il ceppo PP1Y non è in grado di utilizzare nessuno degli idrocarburi saturi impiegati quali ad esempio pentano, esano, decano, dodecano, tetradecano, pentadecano, paraffina a bassa viscosità (*low viscosity paraffin*, LVP) e paraffina ad alta viscosità (*high viscosity paraffin*, HVP) che sono miscele di numerosi alcani. Pertanto si può concludere che gli alcani non sono substrati utilizzabili per la crescita. Al contrario, il ceppo PP1Y è capace di crescere utilizzando una varietà molto ampia di composti aromatici sia mono- che policiclici. Con l'eccezione del benzene e dell'1 ,2,3-trimetilbenzene, tutti i più comuni alchilbenzeni presenti nei derivati del petrolio possono essere utilizzati come uniche fonti di carbonio ed energia, tra questi, toluene, etilbenzene, i tre isomeri dello xilene e dell'etiltoluene, 1,2,4- e 1,3,5-trimetilbenzene. Gli IPA che possono essere utilizzati come unica fonte di carbonio ed energia dal ceppo PP1Y includono bifenile, naftalene, 1- e 2-metilnaftalene, 1,2-, 1,3- e 2,6-dimetilnaftalene, fenantrene, antracene, pirene, crisene, benz[a]antracene, fl uorantene, acenaftene, fluorene, tetralina (tetraidronaftalene), di benzofurano.

Allo scopo di verificare l'effettiva degradazione degli idrocarburi aromatici da parte di *Novosphingobium puteolanum* PP1Y, una fase organica, costituita da dodecano, tetradecano, LVP o HVP contenente un singolo idrocarburo aromatico policiclico, è stata incubata in presenza di terreno salino inoculato con cellule del ceppo PP1Y.

L'analisi delle fasi organiche ha mostrato che il microrganismo è in grado di degradare il 90% del fenantrene in tre giorni, che la degradazione del naftalene è rapida e completa in circa venti ore mentre nel caso del bifenile e del pirene in venti giorni è stato degradato circa il 50% ed il 20%, rispettivamente.

In conclusione va sottolineato che l'insieme di caratteristiche microbiologiche del ceppo PP1Y lo rendono particolarmente adatto all'impiego in interventi *in situ*. In primo luogo la presenza di miscele complesse di idrocarburi aromatici non solo non ostacola la degradazione ma favorisce la crescita, infatti, benzina e gasolio sono i migliori substrati per la crescita. Inoltre la capacità di formare biofilm su superfici di varia natura favorisce l'adesione del ceppo ai substrati da trattare (sabbia, limo, ecc.) riducendo la dispersione e il dilavamento delle cellule da parte di pioggia e onde e quindi riduce la necessità di ripetere frequentemente gli inoculi di cellule. La capacità di formare emulsioni stabili riduce la necessità di aggiungere detergenti e surfattanti. E' interessante notare che incapsulando piccole gocce di olio ed estraendone gli idrocarburi aromatici il ceppo PP1Y può ridurne la dispersione nell'ambiente, cosa che invece si verifica in presenza di ceppi che degradano efficientemente gli idrocarburi saturi ma non quelli aromatici. Infine, la capacità di crescere in ampi intervalli di pH, temperatura e soprattutto salinità ne rende possibile l'impiego in una varietà di ambienti incluse le zone salmastre costiere quali lagune e delta di fiumi. Attualmente è in corso il sequenziamento e l'analisi del genoma del ceppo PP1Y in collaborazione con i gruppi del Prof. F. Salvatore (CEINGE S.r.l.) e del Prof. G. Paolella (Dipartimento di Biochimica e Biologia Molecolare, Università di Napoli

Federico II). Lo studio del genoma completo non solo faciliterà la comprensione delle basi molecolari delle peculiari proprietà del ceppo PP1Y ma consentirà anche di progettare modifiche per potenziarne le abilità degradative ed ampliarne ulteriormente i possibili campi di utilizzo.

INTRODUCTION

Bioremediation techniques exploit microorganisms, like bacteria, fungi, and yeasts, to degrade pollutants [1]. Environmental pollutants (mainly xenobiotics) which could be treated using bioremediation techniques include:

a) aliphatic and aromatic hydrocarbons;
b) polycyclic aromatic hydrocarbons (PAH);
c) polycyclic aromatic halogenated compounds like polychlorobiphenils (PCB) and polychlorodioxines;
d) alogenated aliphatic hydrocarbons like vinyl chlorides;
e) (poly)phenols and aromatic amines;
f) industrial wastes containing organic solvents, degreasers, detergents, residual reagents etc..

It should be underlined that aromatic compounds, because of their high toxicity for all living organisms, are considered particularly dangerous and have been the subject of several studies [1].

Due to the well known adaptability of microorganisms, polluted environments eventually develop an adapted micro-flora composed not only by strains which tolerate pollutants but also by microorganisms which are able to use pollutants as sources of energy, carbon, nitrogen, or sulfur for their growth [1-4]. These strains can be used, individually or as consortia, to reduce or to remove pollutants from soils, waters, urban and industrial wastes.

Several bacterial strains with promising degradative abilities have already been isolated and characterized. They belong to several different genus of both Gram(-) and Gram(+) bacteria. Some examples are *Pseudomonadales* (which degrade aliphatic and aromatic hydrocarbons, PAH, phenols, aromatic amines, detergents, solvents, etc.) [5, 6]; *Sphingomonadales* (which degrade aliphatic and aromatic hydrocarbons, PAH, phenols, aromatic amines, heterocyclic aromatic compounds, etc.) [7-9]; *Mycobacteria* (which degrade PAH) [3, 10, 11]; *Actinomycetes* (which degrade aliphatic and aromatic hydrocarbons, PAH, phenols, aromatic amines, heterocyclic aromatic compounds, etc.) [12, 13].

The majority of the strains with effective degradative abilities are aerobic and use mono and dioxygenase to start degradation of xenobiotics [14, 15]. A few number of anaerobic degraders are also known. However, it should be underlined that several anaerobic bacteria show the ability to de-halogenate polyhalogenated-hydrocarbons thus improving their biodegradability by aerobic bacteria [16, 17].

Bioremediation interventions can be carried out *in situ* or *ex situ*. In the first case, if the polluted environment has already developed an adapted micro-flora, indigenous strains can be stimulated through optimization of crucial parameters like nutrients availability (fertilization with nitrogen, sulfur, phosphorus, etc.), aeration (ploughing, venting), humidity (irrigation), pH and temperature (pumping of warm air). If the polluted environment has not yet developed adapted strains, indigenous micro-flora can be enriched by inoculating selected laboratory-grown strains including engineered strains. In the case of *ex situ* interventions polluted materials, like water, soil, sand or mud, are removed and treated in plants (bioreactors, settling tanks, etc.) where the parameters that can influence biodegradation (temperature, pH, humidity, oxygen concentration, salinity) are constantly monitored and changed when needed. This strategy is obviously more expensive and allows treatment of smaller amounts of polluted material.

Thus, bioremediation strategies should be studied case by case starting from the analysis of pollutants and their chemical-physical parameters in order to select the most appropriate combination of strains for each application. Therefore, the success of bioremediation interventions largely depend on the availability of a wide panel of strains which are able not only to degrade several xenobiotics but also to be metabolically active under different conditions of temperature, salinity, pH, oxygen and water availability.

The present work is part of a wider research project aiming at obtaining microbial strains and enzymatic systems which could be used both in *in situ* or *ex situ* bioremediation interventions and in bioreactors for the treatment of industrial wastes like, for example, wastewaters containing high levels of aromatic hydrocarbons and their derivatives. Two different strategies for making available new or improved strains for biodegradation are currently under evaluation: (i) isolation and characterization of strains with specific degradative abilities directly from polluted environments, and (ii) production of engineered strains. These latter can be produced after characterization of the catalytic machineries of enzymes involved in the degradation of xenobiotics in order to design mutated enzymes and later engineered strains with improved and/or wider abilities or better suited to their use in bioreactors.

The present work describes two research lines which illustrate the two different approaches:

3. Engineering of catechol 2,3-dioxygenase (C2,3O) a crucial enzyme in degradative pathway for aromatic compounds of *Pseudomonas* sp. OX1, a well-studied microorganism.
4. Isolation of new strains able to degrade aromatic hydrocarbons directly from polluted environments by means of appropriate selection procedures.

In the following sections we will describe the state of the art and aims of these two strategies.

Protein engineering of the catechol 2,3-dioxygenase from Pseudomonas sp. OX1.

Pseudomonas sp. OX1 is an ideal model organism for studies of metabolic engineering since it can utilize benzene, toluene, and *o*-xylene, but not *m*- and *p*-xylene, as the sole sources of carbon and energy trough a single, well-characterized degradative pathway [2]. Moreover, in collaboration with the research group of Professor Salatino and Marzocchella (Dipartimento di Ingegneria Chimica, Università di Napoli Federico II), the strain has already been used to set up a bioreactor for the treatment of wastewaters containing aromatic hydrocarbons [18]. Two NADH-dependent monooxygenases – toluene/*o*-xylene-monooxygenase (ToMO) and phenol hydroxylase (PH) – act sequentially in the degradative pathway [19] to convert aromatic hydrocarbons to the corresponding catechols. The two monooxygenases form the so-called *upper pathway*. Catechols are successively converted to non-cyclic molecules by C2,3O, an "*extradiol ring cleavage dioxygenase*" (ECD), which cleaves one of the C-C bond adjacent to the diol moiety of catechols [20, 21] (Fig. 1). ToMO and PH are able to convert *o*-xylene as well as *m*-xylene and *p*-xylene to 3,4-DMC, 3,5-DMC and 3,6-DMC, respectively. However, *Pseudomonas* sp. OX1 C2,3O can cleave effectively only 3,4-DMC [22] yielding a non-cyclic compound which can be further metabolized through the so-called *lower pathway*. This is not possible in the case of 3,5-DMC and 3,6-DMC because of the very low activity of C2,3O towards these compounds [22]. Thus, the restricted specificity of C2,3O is the primary metabolic determinant which limits the ability of

Pseudomonas sp. OX1 to efficiently grow on xylene mixtures. Moreover, the inability of *Pseudomonas* sp. OX1 to cleave 3,5- and 3,6-DMC has also an adverse consequence on the metabolism of the microorganism since the NADH consumed by the monooxygenase-catalyzed hydroxylations of *m*- and *p*-xylene cannot be restored by the *lower pathway* reactions. This inefficiency results in a loss of metabolic reducing power when *Pseudomonas* sp. OX1 grows on xylene mixtures.

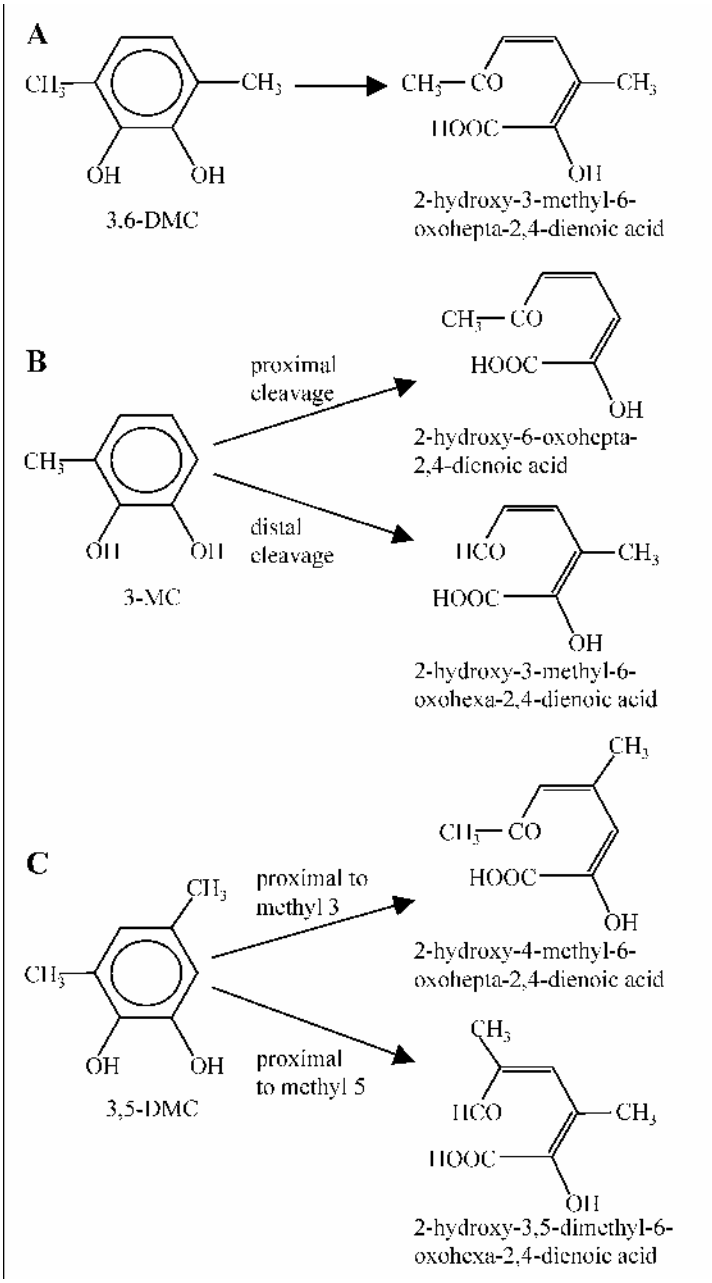

Fig. 1. Possible extradiol cleavage reactions for 3,6-DMC A), 3-MC B) and 3,5-DMC C). Wild type C2,3O catalyzes effectively only the proximal cleavage of 3-MC and at very low efficiency the cleavage of 3,6-DMC and the cleavage of 3,5-DMC proximal to methyl 5.

Thus, understanding the molecular determinants that control substrate binding in *Pseudomonas* sp. OX1 C2,3O could allow to develop mutated enzymes with a wider substrate specificity and eventually engineered microorganisms with enhanced ability to grow on substituted aromatic compounds.

The structure of *Pseudomonas* sp. OX1 C2,3O was modeled by homology using the crystal structure of *P. putida* MT2 C2,3O (1 mpy, [23]) as template. Successively, in order to hypothesize which residues of C2,3O are involved in substrate recognition, the structures of two ECDs, 2,3-dihydroxybiphenyl-1 ,2-dioxygenase

(DHBD) from *Pseudomonas* KKS102 (1eim, [24]) and the 3,4-di hyd roxyphenylacetate 2, 3-d ioxygenase (H PCD) from *Brevibacterium fuscum* (1 q0c, [25]), crystallized in their active Fe(II) form with the substrate bound to the catalytic metal, were used as templates for an *homology docking* of catechols into the active site of C2,3O. These complexes where chosen because available data suggested that they represent the catalytically competent enzyme/substrate complex [24, 25]. This strategy revealed that substrate CH groups at positions 3 and 4 point toward small cavities, indicated as sub-sites 1' and 2' in Fig. 2, which are defined by residues Ile204, Phe302, Ile291 and Leu248. These cavities are large enough to accommodate methyl substituents at positions 3 and 4 of a catechol molecule as verified by the docking of 3-MC, 4-MC and 3,4-DMC. Instead, the CH groups at positions 5 and 6 of the substrate point toward the backbone of Leu-248 and the side-chain of Thr-249, respectively (Fig. 2A-B). Apparently, the close contacts between these two residues and the edge of the substrate ring prevent binding of 3,6- and 3,5-DMC.

As CH atoms at position 6 contact the side chain of residue Thr249, we hypothesized that a reduction in the volume of this side chain might provide room for housing a methyl substituent at this position and allow for the binding of 3,6-DMC or 3,5-DMC as depicted in Figures 2D and 2F, respectively.

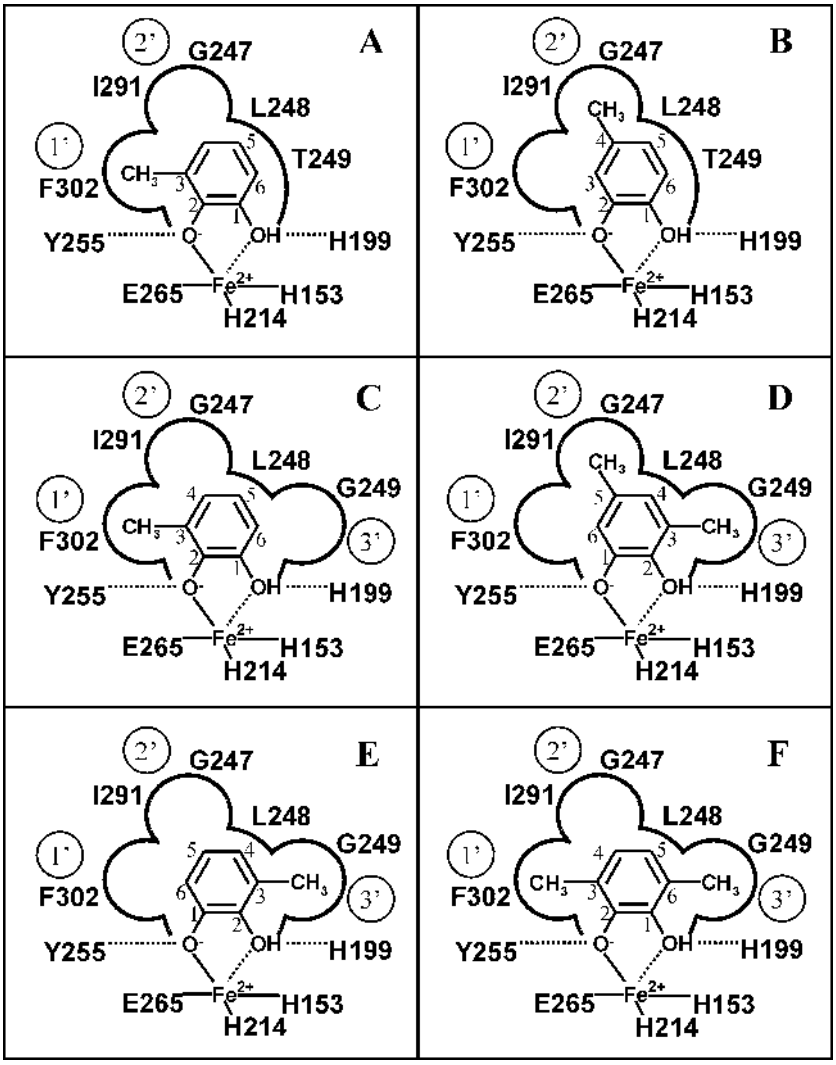

Fig. 2. Scheme of possible binding of 3-MC, 3,5-DMC and 3,6-DMC to C2,3O active site. A) and B), binding of 3-MC and 4-MC, respectively, into the active site of wild type *P. stutzeri* C2,3O. C) and E) show two possible orientations for the binding of 3-MC to the active site of (T246G)-C2,3O. D) and F), binding of 3,5-DMC and 3,6-DMC, respectively, to the active site of (T246G)-C2,3O.

Based on the observations above, residue Thr-249 was substituted *in silico* with serine, alanine and glycine, and the molecular contacts of docked 3,6- and 3,5-DMC were re-inspected. The progressive reduction of the side chain of residue 249 created a new cavity (sub-site 3', Fig. 2C-F) adjacent to CH atoms at position 6, resulting in the reduction of steric hindrance between a methyl group at this position and the protein. When glycine is present at position 249 the closest contact between the methyl group in the sub-site 3' and residue 249 increased from 1.7 Å to 3.9 Å.

The three mutants (T249S)-, (T249A)-, and (T249G)-C2,3O were produced by site-directed mutagenesis and assayed on catechol, 3-MC, 3,5-DMC, and 3,6-DMC. As expected the K_M values showed a progressive increase as the volume of side chain at position 249 decreased in the case of catechol, 3-MC, whereas a progressive decrease of the K_M values was observed in the case of 3,5-DMC, and 3,6-DMC (Fig. 3A). These data suggested that the creation of the hypothetical 3' sub-site improves the binding of the two larger substrates and reduces affinity for the two smaller catechols. Surprisingly, mutations T249A and T249G, which remove the hydroxyl group from the side chain at position 249, caused also a strong decrease in the k_{cat} values (Fig 3B). This reduction counterbalances the improved binding of 3,5-DMC and 3,6-DMC. As a consequence mutants (T249A)-, and (T249G)-C2,3O are not more efficient than wild type C2,3O in the cleavage of 3,5-DMC, and 3,6-DMC.

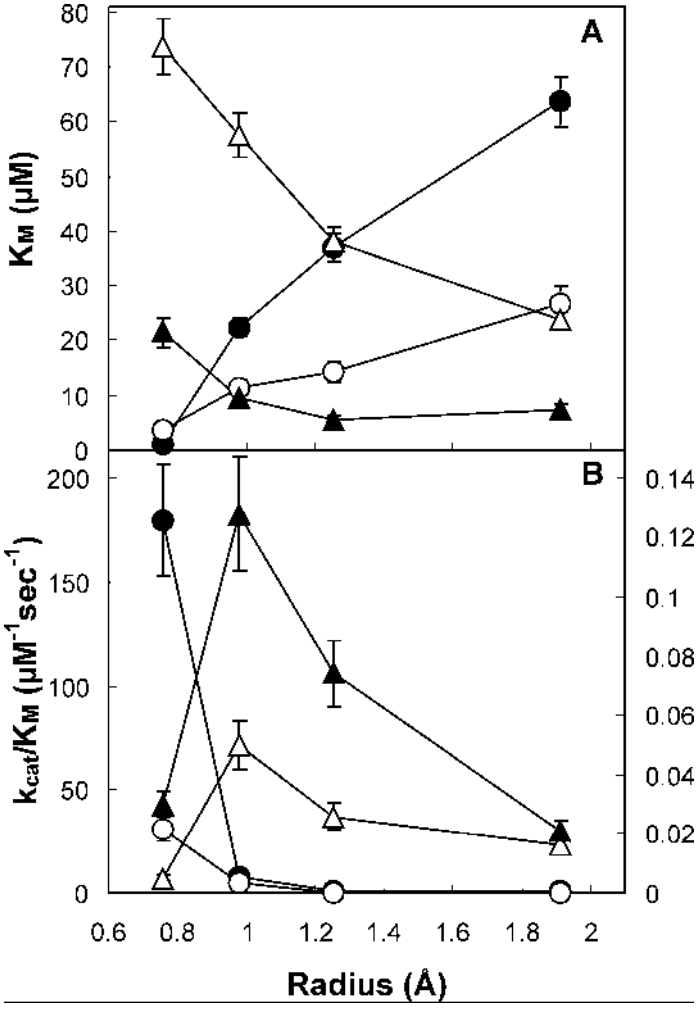

Fig. 3. Catalytic parameters of wild-type and mutant C2,3Os measured at pH 7.5 are shown as function of the radius of the radius of sub-site 3' shown in Fig. 5 (radius are: 0.76, 0.98, 1.25 and 1.91 Å for wt, (T249S)-, (T249A)-, and (T249G)-C2,3O, respectively). Filled circles, catechol; open circles, 3-MC; filled triangles, 3,6-DMC; open triangles, 3,5-DMC.For clarity in (B) the k_{cat}/K_M values on catechol and 3-MC and the values on 3,5-DMC and 3,6-DMC are reported on different scales – on the left and on the right, respectively.

A possible explanation of these findings is that mutations T249A and T249G cause the loss of a water molecule bound to the hydroxyl group of Thr-249 visible in

the crystal structure of C2,3O. A water molecule in the same position has been found also in the crystal structures of several ECDs/substrate complexes]. Moreover, docking experiments performed in our laboratory suggested that the water molecule could stay in the active site during catalysis by bridging through H-bonds Thr-249 side chain and substrate. These observations suggested that T249 and the bound water could play a previously unsuspected role in catalysis [26].

In this thesis we describe the preparation of several (T249G)-C2,3O variants with further mutations at positions 270, 267 and/or 198 designed with the aim of restoring the water binding site into the active site of this mutant and to obtain a mutated enzyme with both a good affinity and a high catalytic efficiency on 3,5-DMC, and 3,6-DMC.

Isolation of new strains from polluted environments

New strains with the ability to degrade xenobiotics are usually isolated by using enrichment techniques. The appropriate substrate is added to samples to increase the relative abundance of the desired microorganisms, successively enriched samples are used to inoculate selective culture broths containing the appropriate substrate as the sole carbon, nitrogen, sulphur or energy source. The success of this approach depends on the accurate choice of the environmental sample and of isolation conditions.

In order to isolate new strains with the ability to degrade PAH, samples of surface seawater were collected inside the harbour of Pozzuoli (Naples, Italy) which is heavily polluted by fuel oils due to the high number of small boats in the harbour. Like all derivatives of petroleum, gasoline and gas-oil contain relevant amounts of aromatic hydrocarbons. Gasoline contains about 25% of mono- and up to 10% polycyclic aromatic hydrocarbons [27]. Gas-oil, on the contrary, contains a larger fraction of PAHs – up to 15% – and only 5-6% alkylbenzenes [28]. These aromatic fractions are extremely complex including tens if not hundreds of molecules belonging to (poly)alkyl-benzenes, PAHs and (poly)alkyl-PAHs, naphthenes (i.e. polycyclic compounds with fused aromatic and saturated rings) and nitrogen, sulphur or oxygen-containing heterocyclic compounds.

Fuel oils degrading bacterial strains are largely diffused in the environment. The so-called “obligate hydrocarbonoclastic bacteria” (O HCB), like *Alkanivorax*, *Marinobacter* and *Oleispira* [29], are among the most effective oil degraders. However, these bacteria degrade prevalently or exclusively the saturated fraction of petroleum and fuels. The most effective degraders of aromatic compounds belong to *Pseudomonadales* (Gram-), *Sphingomonadales* (Gram-) and *Mycobacteria* (Gram+) [1]. *Sphingomonadales* are unusual alpha-proteobacteria which contain glycosphingolipids instead of the more common lipopolysaccharides in the outer membrane. This peculiarity makes their cell surface more hydrophobic than those of the other Gram- strains and this is considered one of the reasons why several *Sphingomonadales* have developed the ability to degrade mono and polycyclic aromatic compounds. Likely, another reason is the fact that many *Sphingomonadales* harbor several large conjugative plasmids (up to six plasmids with lengths ranging from less than 50 kbp to more than 500 kbp) [30, 31]. Due to these megaplasmids several *Sphingomonadales* have “collected” genes for the degradation of xenobiotics and continuously exchange them with other strains. Some interesting examples are *Novosphingobium aromaticivorans*, which can use alkyl-benzenes as the sole carbon and energy sources [32], *Novosphingobium pentaromativorans* US6-1, which degrades PAHs with 3-5 rings [4], *Sphingomonas paucimobilis* EPA505, which

degrades several polycyclic compounds [33], and *Sphingomonas wittichii* R1, which can grow using dibenzofuran and dibenzo-*p*-dioxin and co-metabolizes mono and dichloro-derivatives of these toxic aromatic compounds [34].

In this thesis we will describe the isolation from surface seawater samples and the characterization of a new *Sphingomonadales*, *Novosphingobium* sp. PP1 Y. The strain PP1Y not only uses a surprisingly large number of mono and polycyclic aromatic compounds as the sole carbon and energy sources but shows also a very interesting and effective adaptation to growth on complex mixtures of aromatic compounds dissolved in oil phases like gas-oil and gasoline.

MATERIALS AND METHODS

Bacterial strains

E.coli strain BL21(DE3) F^-, *omp*T, *hsd*S(r_{B^-},m_{B^-}),*dcm*, *gal,* (DE3). The strain was purchased by Novagen and used for proteins expression.
E.coli strain CJ236. The strain was purchased by Bio-Rad and used for site-direct mutagenesis.
E.coli Top F'10 strain (F'{lacIq Tn*10* (Tet^R)} *mcr*A (*mrr-hsd*RMS-*mcr*BC) φ80*lacZ* M15 *lac*X74 *rec*A1 *deo*R *ara*D139 (*ara-leu*)7697 *gal*U *gal*K *rps*L (Str^R) *end*A1 *nup*G). The strain was purchased by Invitrogen and used for genetic manipulation.

Medium

LB (Luria-Bertani) and M9 medium, solid and liquid, were prepared as described by Sambroook *et al*.[35]
KPSA medium was prepared as follows: 20 mM potassium phosphate (pH 6.9), 10 mM sodium chloride and 18.7 mM ammonium chloride.

C-Goodies were added in KPSA medium at 0.5% (v/v) and were prepared as described in the following table:

MgO	10.75 g
$CaCO_3$	2.0 g
$FeSO_4$ x $7H_2O$	7.0 g
$ZnSO_4$ x 7 H_2O	1.44 g
$MnSO_4$ x H_2O	1.12 g
$CuSO_4$ x 5 H_2O	0.25 g
$CoSO_4$ x 7 H_2O	0.28 g
H_3BO_3	0.06 g
HCl	51.3 ml
$MgSO_4$	60.2 g
$NiCl_2$ x 6 H_2O	4 mg
Na_2MoO_4 x 2 H_2O	6 mg
H_2O	1000 ml

Antibiotics

Ampicillin, chloramphenicol and Kanamycin were purchased from Sigma and were used at concentration of 100 µg/mL, 30 µg/mL and 70 µg/mL respectively.

Vectors

pET22b(-I-)XN/C2,3O and pET22b(-I-)XN/C2,3O(T249G), coding for C2,3Owt and (T249G)-C2,3O mutant, were available in laboratory and were used to prepare library of C2,3O mutants.

Substrates

3,5- and 3,6-dimethylcatechol were synthesized by Doc. A. Pezzella (Dipartimento di Chimica organica e Biochimica, Napoli Università Federico II) according procedure described by Pezzella *et al* [42].

Synthesis of oligonucleotides
Oligonucleotides used for site-direct mutagenesis were synthesized at MWG-Biotech (http//ecom.mwgdna.com).

Plasmid DNA
Plasmids coding for C2,3O mutants, were prepared using QIAprep^{R} Spin Miniprep Kit (QIAGEN) and sequenced at MWG-Biotech (http//ecom . mwgdna.com).

Transformation of *E. coli* TOP F'10 cells by electroporation
1 mL of an over-night culture of *E. coli* TOP F'10 was inoculated in 100 mL of LB medium and incubated at 37 °C on a shaker. The cells were grown up to $O.D._{600\ nm}$= 0,6-0,8. and place on ice for 30 min and then haversted by centrifugation. The pellet was gently resuspended in 50 mL of cold sterile H_2O. After second centrifugation the cells were resuspended in 25 mL of cold sterile H_2O. The third washing was performed in 2 mL of 15% glycerol; the cells were then haversted by centrifugation and pellet was resuspended in 0.5 mL of 15% glycerol.

Aliquot of cells was mixed with 1 µL of mutagenesis reaction, incubated for 1 min on ice and transferred into pre-chilled cuvette. High voltage electroporation (25 µF) was performed wirh a BioRad Gene Pulser Xcell^{TM} at a field strength of 2.5 kV/cm and 200 Ohm a shock pulse was applied to competent cells producing pulse length of 4.8-5.0 ms. Immediately after electroporation 1 mL of LB medium was added and the cells were incubated at 37 °C for 1 h in a shaker. The cells were then plated onto selective solid medium with 100 µg/mL ampicillin.

Transformation of E.coli BL21(DE3) cells
Single colony of E.coli BL21(DE3) was inoculated in 10 mL of LB medium. Cells were incubated at 37 °C on a shaker and grown up to midlogarithmic phase and then haversted by centrifugation. The pellet was washed in 2.5 mL of 0.1 M $MgCaCl_2$ and haversted by centrifugation. The pellet was re-suspended in 5 mL of 0.1 M $CaCl_2$ and stored on ice for 60 min. The cells were collected by centrifugation and re-suspended in 3,5 mL of cold 0.1 M $CaCl_2$, 10% glycerol. 100 µL o competent cells were mixed with 20 ng of plasmid DNA and stored on ice for 1 h. Heat shock was performed by incubating cells at 42 °C for 2 min, followed by 1 min on ice and then diluted to 1 mL with LB medium. An incubation for 1 h at 7 °C was perfomed before plating the cells onto selective solid medium supplemented with 100 µg/mL ampicillin.

Site-direct mutagenesis
The site-direct mutagenesis was performed using the kit Muta-gene (Bio-rad) based on method described by Kunkel [36]. This system is based on the use of uracils-contaning single strand DNA, synthesized in a *dut, ung* double mutant bacterium (*E. coli* strain CJ236). This uracil-containing strand is then used as the template for the synthesis *in vitro* of a complementary strand primed by an oligonucleotide containing the desired mutation. The resulting double-stranded DNA is transformed into a strain with a functional N-glycosidase, thus selecting against the parental strand.

Preparation of uracil-containig single-strand DNA
4 ng of plasmid pET22b(+).XN/C2,3O(T249G) were transformed into 100 µL of CJ236 as described in this section and the cells were then plated onto selective solid medium with 100 µg/mL ampicillin and incubated for 20 h at 37 °C. It was prepared uracils-contaning single strand DNA as described in *Sambrook et al.* [35].

Mutagenesis reaction

Mutagenesis reactions were prepared in a final volume of 10 µL containing 200 ng of stranded uracil containing DNA, 10 pmol of phosphorilated mutagenic oligonucleotide (table 1) and 1 µL of 10x annealing buffer (200 mM Tris-HCl pH7.4, 20 mM $MgCl_2$, 500 mM NaCl). The reactions were incubated at 70 °C for 5 min and then cooled slowly, after the reactions were placed in an ice-water bath for 5 min. It was added 1 µL of 10x synthesis buffer (5 mM dNTP, 10 mM ATP, 100 mM Tris/HCl pH 7,4, 50 mM $MgCl_2$, 20 mM DTT), 3 U of T4 DNA ligase and 4 U of T4 DNA polymerase. The reaction were incubated on ice for 5 min followed by another 5 min at 25 °C, and finally at 37 °C for 90 min. The reactions were stopped adding 90 µL of stop solution (10 mM Tris-HCl pH 7,4, 50 mM EDTA). 1 µL of reactions was used to transform Top F' 10 and the cells were plated on LB agar with 100 µg/mL ampicillin and incubated for 20 h at 37 °C.

The clones harbouring the desired mutations were identified by DNA sequencing. The sequences of all the clones were successively verified by sequencing.

Table 1.

Mutagenic primer	Sequence	
mutP198	**5' -GCCACGTCGTGCGGCTTGGTCGACAG-3'**	P198
mutG198	**5' -GCCACGTCGTGACCCTTGGTCGACAG-3'**	G198
mutS198	**5' -GCCACGTCGTGTGACTTGGTCGACAG-3'**	S198
mutEQ270	**5' -GGTAGTTGTAATCCTSCCCGCAGAACA-3'** **G *(Gln)*** **C *(Glu)***	E/Q 270
mutHLEO	**5' -GGTAGTTGTAATCCTS CCGCAAW CACTTCGTTGCG-3'** ***(Gln)* G A *(Leu)*** ***(Gln)* G T *(His)*** ***(Glu)* C A *(Leu)*** ***(Glu)* C T *(His)***	H/L 267: E/Q 270
mutH267	**5' -CTCCCCCGCAATGCACTTCGTTGCG- 3'**	H267

Expression of C2,3Os

E. coli strain BL21 (DE3), transformed with pET22b(+).XN containing the sequences coding for the C2,3O mutants, was growth at 37 °C in LB medium containig ampicillin (100 µg/mL) until optical density at 600 nm was 0,6-0,7. Induction was performed by adding IPTG and $Fe(NH_4)_2(SO_4)_2$ at final concentration of 0,5 mM and 100 µM, respectively. After 3 h, cells were haversted by centrifugation at 4000 x g for 20 min at 4 °C, washed with 50 mM Tris/HCl (pH 7.5), and collected by centrifugation. Cell paste was stored at -80 °C until use.

Purification

The bacterial pellet was suspended in buffer A (50 mM Tris/HCl (pH 7.5) containing 0,08 M NaCl, 10%(v/v) glycerol, 10% (v/v) ethanol and 2 mM dithiothreitol) in the

presence of 100µM $Fe(NH_4)_2(SO_4)_2$ and was disrupted by sonication. Cell debris was removed by centrifugation (12,000 × g, 1 h at 4 °C).The supernatant was loaded at 4 °C onto a 15 mL Q-Sepharose column equilibrated previously in buffer A and washed with 30 mL of equilibration buffer. Elution was carried out with 260 mL of buffer A with a NaCl linear gradient ranging from 0.08 to 0.5 M at a flow rate of 13 mL/h. Fractions containing dioxygenase activity were pooled and added 10% (v/v) glycerol and stored at -80 °C under nitrogen atmosphere.

Determination of the protein concentration

The protein concentration was determined according to the Bradford's method. The coomassie Brilliant (sigma) was added to the samples and the absorbance at 595 nm was monitored. A solution of bovine serum albumin was used as a standard.

SDS-PolyAcrylamide Gel Electrophoresis

Gel electrophoresis under denaturing condition was performed as described by Laemmli. The resolving gel was prepared at 18% acrylamide and the stacking gel was prepared at 6% acrylamide.[37]

Iron determination of C2,3O mutants

The iron content of C2,3O mutants was determined by using the iron-chelating reagent Ferene S, which forms a complex with ferrous iron [Fe(II)].

The samples were incubated at room temperature for 10 min and 25 µL of 50% (w/v) trichloracetic acid were added. Precipitated proteins were removed by centrifugation, the supernatants were transferred and 50 µL of 45% sodium acetate were added. 450 µL of Ferene S reagent [0.8 mM Ferene S, 10 mM ascorbic acid and 45% sodium acetate] were added to the samples, in presence of ascorbic acid trivalent iron [Fe(III)] dissociated from proteins becomes reduced to divalent iron [Fe(II)], which forms a complex with Ferene S, then it was determined iron total content of protein. If Ferene S reagent was prepared without adding ascorbic acid, it was determined Fe(II) concentration in proteic samples. The absorbance at 593 nm were measured and Fe(II) concentration was calculated using as molar extinction coefficient 34320 $M^{-1}cm^{-1}$.

Enzyme assay

All assay were performed at 25 °C in 50 mM Tris/HCl (pH 7.5) in a final volume of 1 mL by spectrophotometric determination of the product of the reaction. Wild-type and mutant C2,3Os were used to start the reaction.

The amount of the fission products was measured spectrophotometrically using their absorption extinction coefficient at the respective ε_{max} values. These coefficients were as follows: ε_{375} = 33,000 $M^{-1}cm^{-1}$ for 2-hydroxymuconic semialdehyde, the product of catechol; ε_{388} = 13,400 $M^{-1}cm^{-1}$ for 2-hydroxy-6-oxohepta-2,4-dienoic acid, the product of 3-methylcatechol; ε_{393} = 8,230 $M^{-1}cm^{-1}$ for 2-hydroxy-3,5-dimethyl-6-oxohexa-2,4-dienoic acid, the product of 3,5-dimetylcatechol; and ε_{393} = 15,200 $M^{-1}cm^{-1}$ for 2-hydroxy-3-methyl-6-oxoepta-2,4-dienoic acid, the product of 3,6-dimetylcatechol.

Kinetics parameters were determined by the program GraphPad Prism (GrapfPad Software; www.graphpad.com). One unit of enzyme activity was defined as the amount of enzyme required to form 1 µmol of the metacleavage product per minute under assay conditions.

Identification of Strain PP1Y

To identify strain PP1Y, 16S rDNA gene was sequenced at BRM Genomics. The sequence was compared with sequences available in GenBank database using the BLAST search system.

Optimal salt concentration, pH and temperature for growth of PP1Y

In order to find out the optimum salt concentration for growth of PP1Y, 10 µL of pre-inoculum grown in LB medium were inoculated in 10 mL of liquid medium containing 5 g/L of tryptone, 2,5 g/L of yeast extract, 20 mM potassium phosphate (pH 6.9) and different sodium chloride concentrations, 0%, 0,5%, 1%, 2%, 3%, 4% and 5% (w/v) and then incubated at 30 °C in shaker. The optimal pH for the growth of PP1Y was determined using a liquid medium containing 5 g/L of tryptone, 2,5 g/L of yeast extract ,20 mM potassium phosphate and the pH of solution was adjusted at 5.6, 6.3, 7.0, 7.5 and 8.0. The optimum temperature was determined inoculating cells of strain PP1Y in LB medium and incubating at different temperature. Growths were monitored by measuring the optical density at 600 nm.

Growth on aromatic compounds

In order to verify the ability of strain PP1Y to use gas-oil and gasoline as the sole source of carbon and energy, 15 µL of pre-inoculum of PP1Y grown in LB medium were inoculated in 15 mL of KPSA medium containing C-Goodies and 0,5 mL of gas-oil was added. The growth in presence of gasoline was performed in biphasic system, the cells of strain PP1Y were inoculated in 15 mL of mineral liquid medium (KPSA+ C-Goodies) and 0.1 mL of gasoline dissolved in 0,4 mL of paraffin was added. The cultures were incubated on shaker at 30 °C. Bacterial growth was followed by measurement of absorbance of cultures at 600 nm.

The utilization of individual aromatic compound as growth substrates was determined either in biphasic cultures supplementing mineral liquid medium with the compound dissolved in C_{12}, C_{14}, LVP or HVP or providing substrate in pure form. For inoculum preparation PP1Y was grown overnight in LB medium, 10 µL of cells were inoculated in 10 mL of KPSA medium containing substrates at concentrations ranging from 0.2 to 2.0% (w/v) and were incubated at 30 °C.

Degradation of paraffin-dissolved aromatic hydrocarbons

Degradation of aromatic compounds was determined in 50 mL polyethylene tubes containing 10 mL of mineral liquid medium (KPSA+Goodies) supplemented with 0,4 mL of oil phase (C_{12}, C_{14}, LVP or HVP) containing 0.05% (w/v) phenanthrene, naphthalene, biphenyl or pyrene.

At increasing times, aliquots of paraffin drops were collected and analyzed. The degradation of aromatic hydrocarbons was examined by normal-phase high performance liquid chromatography (HPLC) by determining the percentage of aromatic hydrocarbons remaining in the oil phase.

HPLC system was equipped with a Waters 1525 binary pump coupled to a Waters 2996 photodiode array detector. Polycyclic substrates were separated using Waters Spherisorb 5µm CN-NP column (4.6 x 250 mm) and the absorbance of eluate was monitored at 270 nm. Analysis was carried out at a flow of 0.5 mL/min by using a two-solvent system comprising 0.1% isopropyl alcohol in hexane (solvent A) and 20% isopropyl alcohol in hexane (solvent B). Polycyclic substrates were separated using a 10 min isocratic elution with 100% of solvent A, followed by elution with a

linear 100% to 90% solvent A gradient in 15 min and then an isocratic 90% solvent A step. Nitrobenzene was used as internal standard.

RESULTS & DISCUSSION

Part 1: Protein engineering of the catechol 2,3-dioxygenase from *Pseudomonas* sp. OX1.

1.1. Design of C2,3O mutants.

In collaboration with Dr. Eugenio Notomista (Department of Structural and Functional Biology, Naples University Federico II) (dimethyl)catechols and water were simultaneously docked into the active site of the model of wild type C2,3O and into the model of the first generation mutant (T249G)-C2,3O by using a Monte Carlo-Energy minimization (MC-EM) strategy. Docking of 3-MC into the active site of wild type C2,3O confirmed the hypothesis that a water molecule can bind into the active site forming a H-bonds network involving Thr-249 and the substrate molecule (Fig. 1.1).

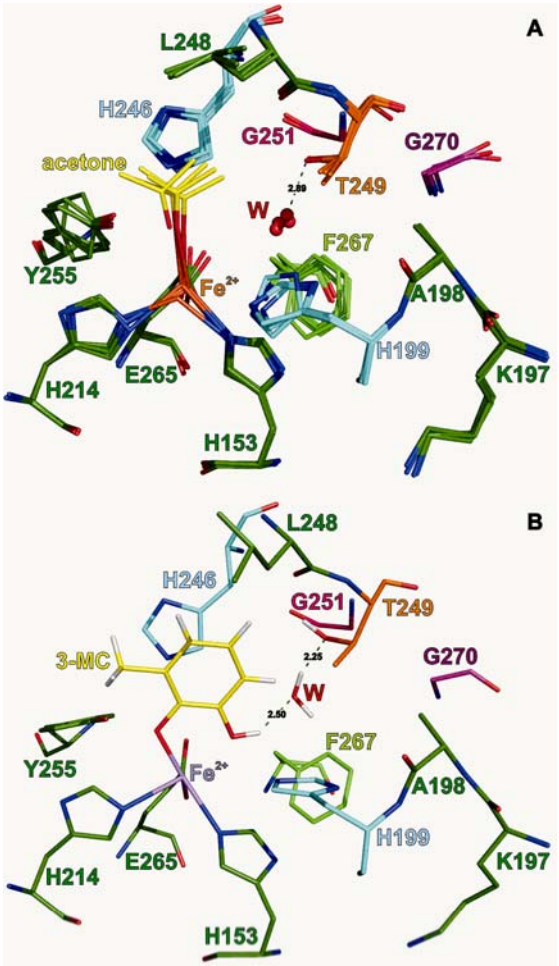

Fig. 1.1. A) Superimposion of the four non-equivalent subunits of C2,3O from P. putida MT2 (pdb code 1MPY). B) MC-energy minimized model of the complex wild type C2,3O/3-MC/water. Nitrogen atoms are coloured blue, oxygen are coloured red and hydrogen atoms, when shown, are coloured white. Carbon atoms of different residues are coloured with different colours. W = water molecule. Hydrogen bonds are shown as green broken lines. Hydrogen bond distances are in Å. In (A) only the shortest Thr-249/W H-bond is shown.

Docking procedure showed that also His-199 and His-246 provide an important contribution to water binding trough electrostatic interactions (Fig. 1.1). Interestingly, docking of a water molecule and 3,6-DMC into the active site of (T249G)-C2,3O showed that the water molecule can still bind into the active site but at a different position, closer to Glu-265 than in the case of wild type C2,3O. This shift of the water molecule inside the active site could impair its contribution to catalysis and provide a molecular explanation for the low $_{kcat}$ values measured for this mutant on all substrates.

In order to design C2,3O mutants with improved catalytic efficiency on 3,5-DMC and 3,6-DMC, (T249G)-C2,3O was chosen as starting point because, among the first generation mutants, it showed the lowest K_M values – and hence the highest apparent affinity – on both DMCs.

Besides residue Thr-249, four other side-chains face the hypothetical water binding site: Gly-250, Gly-270, Ala-198 and Phe-267 (Fig. 1.1). These four positions are possible targets for site-directed mutagenesis. By using the Deep-View and PyMol protein visualization and modeling softwares the four residues were mutated *in silico* to find a combination of side-chains able to restore the hypothetical water molecule binding site without hindering the sub-site for the binding of the methyl group at position 6 of 3,6-DMC. The most promising mutants were further examined by the MC-EM strategy.Residue at position 250 was judged not suitable for mutagenesis because it is to close to the water binding site and even a serine residue at this position could partially hinder the sub-site for methyl binding (not shown).
On the contrary, mutation of more distant Gly-270 residue to glutamate or glutamine could position the hydrophilic side-chains of these residues to H-bond distance from a water molecule located at a position similar to that found in the complex between wild type C2,3O and 3-MC (Fig. 1.2).

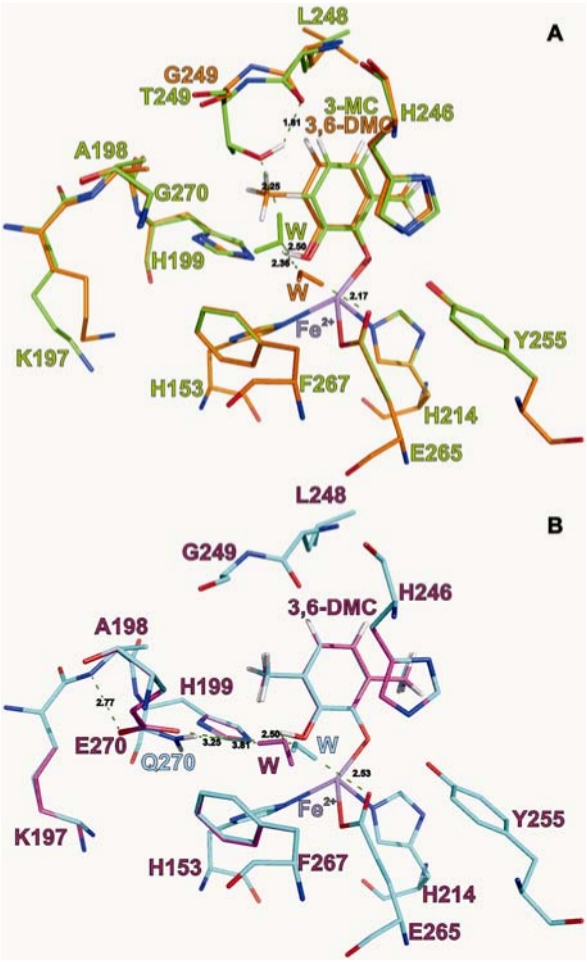

Fig. 1.2. A) Comparison between the model complexes wild type C2,3O/3-MC/water and (T249G)-C2,3O/3,6-DMC/water. B) Comparison between the model complexes (T249G, G270E)-C2,3O/3,6-DMC/water and (T249G, G270Q)-C2,3O/3,6-DMC/water W = water molecule. Atoms and H-bonds are coloured as in Fig. X1 except carbon atoms which are coloured green (wild type C2,3O), orange [(T249G)-C2,3O], purple [(T249G, G270E)-C2,3O], and cyan [(T249G, G270Q)-C2,3O]. All the atoms of each water molecule are coloured like the carbon atoms of the same complex.

Models of C2,3O with mutations G270E or G270Q also showed that the large side-chains of glutamate and glutamine were closely packed between the side-chains of residues at positions 198 and 267 (Fig. 1.2). Therefore, mutations at these two positions could be used to control the positioning of the side-chains of Glu-270 and

Gln-270. For example, mutation A198G, reducing the hindrance, could allow closer contacts between the backbone of this residue and the side-chains of Glu-270/Gln-270, whereas, mutations A1 98S and A1 98P could exert the opposite effect. Similarly, a reduction of the bulky side-chain of Phe-267 could allow the shifting of the side-chains of Glu-270/Gln-270 toward the water binding site. Two types of mutations at position 267 were considered: (i) mutations F267L and F267A reduce the volume of the side-chain preserving its hydrophobic nature, whereas, (ii) mutations F267H, F267N, and F267S insert hydrophilic side-chains which could form hydrogen bonds with the side-chain of Glu-270/Gln-270 and also directly with the water molecule (Fig. 1.3).

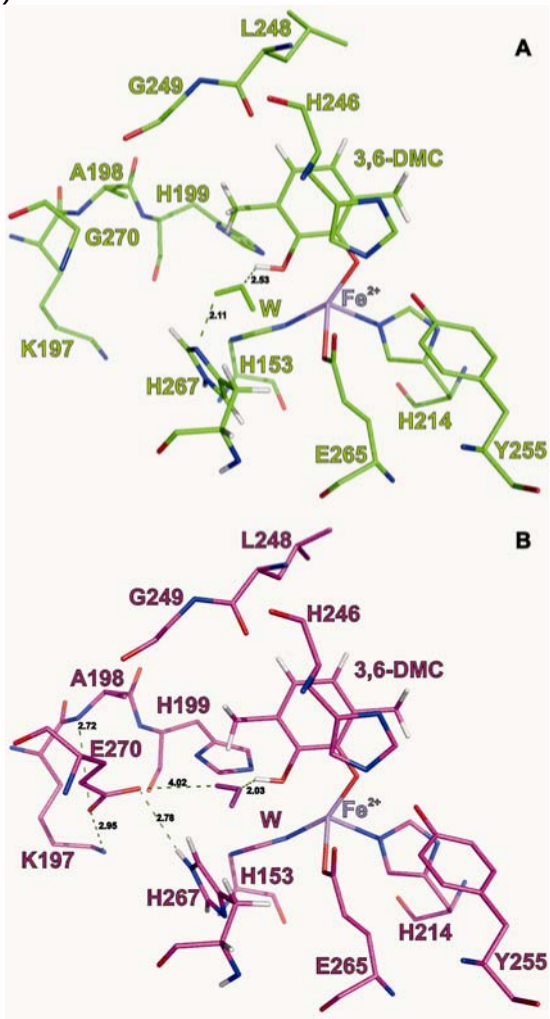

Fig. 1.3. A) Model of the complex (T249G, F276H)-C2,3O/3,6-DM C/water. B) Model of the complex (T249G, F276H, G270E)-C2,3O/3,6-DMC/water. W = water molecule. Atoms and H-bonds are coloured as in Fig. X1 except carbon atoms which are coloured green [(T249G, F276H)-C2,3O/3,6-DMC/water] and purple [(T249G, F276H, G270E)-C2,3O/3,6-DMC/water]. All the atoms of each water molecule are coloured like the carbon atoms of the same complex.

Table 1.1 shows the combination of mutations which were considered particularly promising on the basis of the modeling experiments.

1.2. Preparation of the C2,3O mutants.

Due to the very high number of combinations (Table 1.1) we decided to prepare the expression vectors for the mutants of C2,3O using the Kunkel strategy and a series of degenerated oligonucleotides whose combinations allow to obtain all the desired mutations at positions 198, 267, and 270 (see Materials and Methods). For example, by using simultaneously the degenerated mutagenic oligonucleotides for positions 198 and 270 we prepared a small library containing the expression vectors coding for the six possible triple mutants at these positions (lane 8 in table 1.1).

Table 1.1

	Positions*				
protein	**198**	**249**	**267**	**270**	**Number of mutants**
(T249G)	A	**G**	F	G	1
double	A	**G**	F	**E/O**	2
mutants	A	**G**	**H/N**	G	2
triple	A	**G**	**H/N/S**	**E/O**	6
mutants	A	**G**	**A/L**	**E/Q**	4
	G/S/P	**G**	F	**E/Q**	6
quadruple mutants	**S/P**	**G**	**A/S**	**E/Q**	8
Number of double-quadruple mutants					28

* mutated residues are shown in bold.

Identification of mutations present in each clone was performed by PCR adapting a procedure used in prenatal diagnosis which allows to discriminate two sequences differing by a single base pair. The procedure is based on the use of a PCR primer whose 3' nucleotide binds the nucleotide which differs in the wild type and mutant sequences. As *Taq* polymerase lacks the 3'->5' exonucleasic activity, if the nucleotide at the 3' end of the oligonucleotide is not correctly paired to the template the oligonucleotide is not recognized as primer by the polymerase. The sequences of all the clones were successively confirmed by sequencing.

This strategy allowed to prepare in short time thirteen double and triple mutants. In the following section we will describe the kinetic characterization of three double mutants – (T249G, G270E)-, (T249G, G270Q)- and (T249G, F267H)-C2,3O – and five triple mutants – (A198G, T249G, G270E)-, (A198S, T249G, G270E)-, (T249G, F267H, G270E)-, (T249G, F267L, G270E)-, and (T249G, F267L, G270Q)-C2,3O.

1.3. Expression, purification and characterization of C2,3O mutants.

All the double and triple mutants were expressed in the *E. coli* strain BL21 (DE3) and purified by ion exchange chromatography on the strong anion exchanger Q-sepharose as described in the Material and Methods section. The first generation mutant (T249G)-C2,3O was purified and used as a control. Fig. 1.4 shows a typical chromatogram with a single major peak containing the C2,3O mutant. The fractions of the peak were pooled and analyzed by SDS-PAGE. All mutant C2,3O showed about 95% purity. Proteins were not purified further as every attempt to obtain purer samples lead to loss of enzyme activity (not shown).

At the end of the purification procedure all mutants were assayed to determine the iron content. All mutants showed a ratio moles of iron/moles of monomers very close to 1 (typically 1.1 ± 0.1), as expected. Moreover, all the iron was present in the catalytically productive Fe(II) state.

Kinetic characterization was done using catechol, 3-MC, 3,5-DMC and 3,6-DMC as described in Materials and Methods.

The comparison between the K_M values of the single mutant (T249G)-C2,3O and of the double mutants (T249G, G270E)-, (T249G, G270Q)- and (T249G, F267H)-C2,3O suggests that mutation of residue Gly-270 to Glu and Gln determines a significant decrease of the apparent affinity for all the substrates, whereas mutation

F267N has the opposite effect (the K_M values on catechol and 3-MC decrease 3 and 6 fold, respectively). As already discussed in section 1.2 the rather bulky side-chain of Glu(Gln)-270 inserts among the side-chains of residues Ala-1 98, His-1 99, Phe-267 and the substrate (Fig. 1 .2), therefore, it is likely that it interferes with substrate binding directly or indirectly slightly deforming the active site cavity.

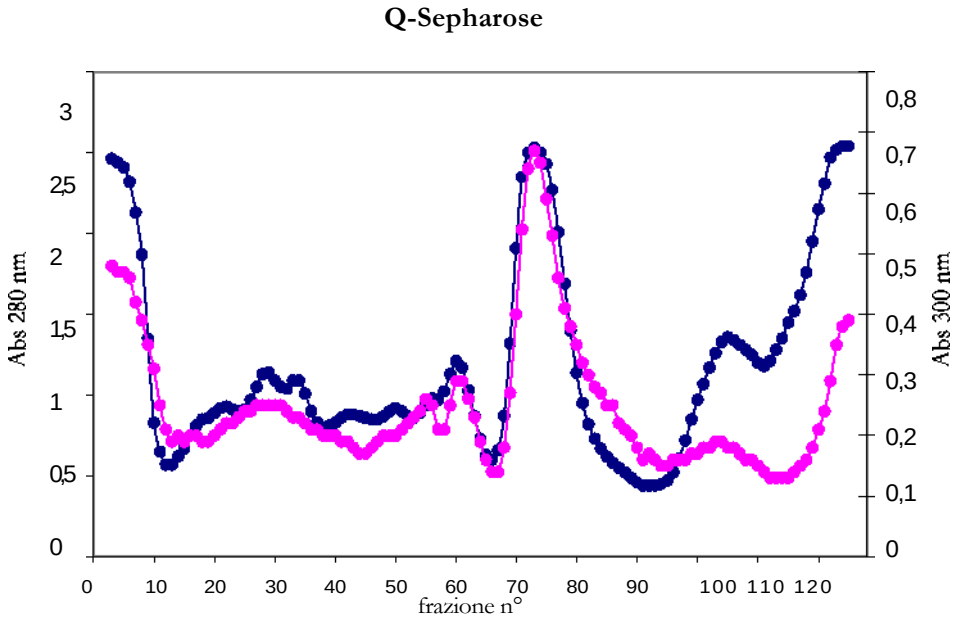

Fig. 1.4

The effect of mutation F267H is less easy to explain as it does not change significantly the volume of the side-chain and is not expected to interact directly with the substrates. An intriguing hypothesis is that the His residue at position 267 partly restores the water binding site contributing indirectly to improve substrate binding and catalysis as discussed below.

As for the $_{kcat}$ values mutation G270E has negligible effects in the case of catechol and 3-MC, whereas it determines a 6 and 12 fold increase in the case of 3,6-DMC and 3,5-DMC, respectively. On the contrary, the apparently similar G270Q mutation determines a decrease of the $_{kcat}$ values on catechol and 3-MC, 6 and 4 fold, respectively, and a slight increase only in the case of 3,5-DMC. Mutation F267H, like G270E, has negligible effects in the case of catechol and 3-MC, whereas it determines 8 and 80 fold increases in the case of 3,6-DMC and 3,5-DMC, respectively.

These findings suggest that both F267H and G270E, can restore the water binding site as predicted by the MC-EM procedures (Fig 1.2 and 1.3). In fact, the MC-energy minimized models of mutants (T249G, F267H)- and (T249G, G270E)-C2,3O showed that both mutation F267H and G270E could provide a H-bond acceptor alternative to Thr-249 Oγ (Oε and Nδ in the case of Glu-270 and His-267, respectively).

The MC-energy minimized model of mutant (T249G, G270Q)-C2,3O showed that the side-chain of glutamine could orient the carbonyl moiety toward the backbone of Ala-198 (forming an H-bond) and the $–NH_2$ group toward the water site (Fig. 1 .2B). If an efficient catalysis requires that the water molecule is bound by a H-bond acceptor – as it has been observed in the cases of the model complexes wild type C2,3O/3-

MC/water, (T249G, F267H)-C2,3O/3,6-DMC/water and (T249G, G270E)-C2,3O/3,6-DMC/water (Fig. 1.1B, 1.2A, 1.3A) – the orientation of the glutamine side chain could be less effective than glutamate and histidine thus explaining the negligible effects on catalysis shown by mutation G267Q.

Looking at the K_S values in Table 1.2 it is clear that, among the three double mutants, (T249G, F267H)-C2,3O is the most efficient catalyst for the cleavage of dimethylcatechols.

The triple mutant (T249G, F267H, G270E)-C2,3O combines the two mutations, F267H and G270E, which increase significantly the catalytic efficiency. This mutant shows a $_{kcat}$ value similar to that of (T249G, G270E)-C2,3O, but a K_S value similar to that of (T249G, F267H)-C2,3O, therefore the combination of the two mutations fails to provide a more effective catalyst. Again this finding could depend on the hindrance of Glu-270 side-chain, an hypothesis supported also by the features of the triple mutant (T249G, F267L, G270E)-C2,3O discussed below. An alternative explanation was provided by the MC-EM analysis. The MC-energy minimized models showed that, when His-267 and Glu-270 are simultaneously present, His-267 could bind directly the carboxylate of Glu-270 so that the water molecule would interact only with Glu-270 (Figure 1 .3B).

As discussed in section 1.1 the triple mutants (A198G, T249G, G270E)-, (A198S, T249G, G270E)-, (T249G, F267L, G270E)-, and (T249G, F267L, G270Q)-C2,3O were prepared with the aim of controlling the positioning of the side-chain of residue Glu(Gln)-270. In particular, mutations A198G and F267L were chosen to try to increase the mobility of the glutamate(glutamine) side-chain.

The comparison between the catalytic constants of mutant (T249G, G270E)-C2,3O and of triple mutant (A198G, T249G, G270E)-C2,3O shows that mutation A198G determines a decrease of the apparent affinity for all the substrates – with the exception of 3-MC. The decrease is particularly high in the case of catechol and 3,5-DMC and less pronounced in the case of 3,6-DMC. Moreover, mutation A198G reduces the $_{kcat}$ values 3 fold in the case of 3-MC and ten fold in the case of 3,5- and 3,6-DMC. As a consequence mutation A1 98G determines a marked decreases of the specificity constant for all the substrate and is the worst catalyst for the cleavage of dimethylcatechols. The effect of this mutation has not been investigated throughly by MC-EM, however, at the moment the most likely explanation is that the presence of a Gly residue at position 198 changes the conformation of the loop Lys-197/Ala-198/His-1 99 impairing the participation to catalysis of His-199, a residue essential for the catalytic activity of C2,3Os [21]. Interestingly, mutation A198S has opposite effects. In fact, it slightly decreases the K_M values (2.5 fold in the case of catechol) suggesting an improved binding of the substrates. Moreover, it increases the k_{cat} value on catechol and 3-MC two and three fold, respectively. Unfortunately, mutation A1 98S determines a decrease of the $_{kcat}$ values measured on dimethylcatechols. The comparison between the MC-energy minimized complexes of (A198G, T249G, G270E)-C2,3O with 3-MC and 3,6-DMC indicates that the hydroxyl group of Ser-198 could form a hydrogen bond with the side-chain of Glu-270 anchoring it in a conformation suitable to reconstitute the water binding site, but at the same time it would interact closely with the second methyl group of 3,6-DMC (Fig. 1.5A). This could prevent optimal positioning of dimethylcatechols for catalysis and determine the observed selective decrease of the $_{kcat}$ values for these substrates.

At difference with mutation A1 98S, which selectively improves the catalytic constants for the physiologic substrates, mutation F267L was found to improve the catalytic constants for dimethylcatechols, when coupled with G270E and G270Q mutations. In

fact, the K_S values for catechol and 3-MC increased 3-5 fold in the case of (T249G, F276L, G270E)-C2,3O and 10 fold in the case of (T249G, F276L, G270Q)-C2,3O. Moreover, the K_S values for 3,5-DMC increased 72 fold in the case of (T249G, F276L, G270E)-C2,3O and 11 fold in the case of (T249G, F276L, G270Q)-C2,3O. Finally, the K_S values for 3,6-DMC increased 21 fold with both mutants. In all cases the increase in the K_S values was due to both a decrease in the K_M values and an increase in the $_{kcat}$ values indicating that mutation F276L improves substrate binding and substrate transformation.

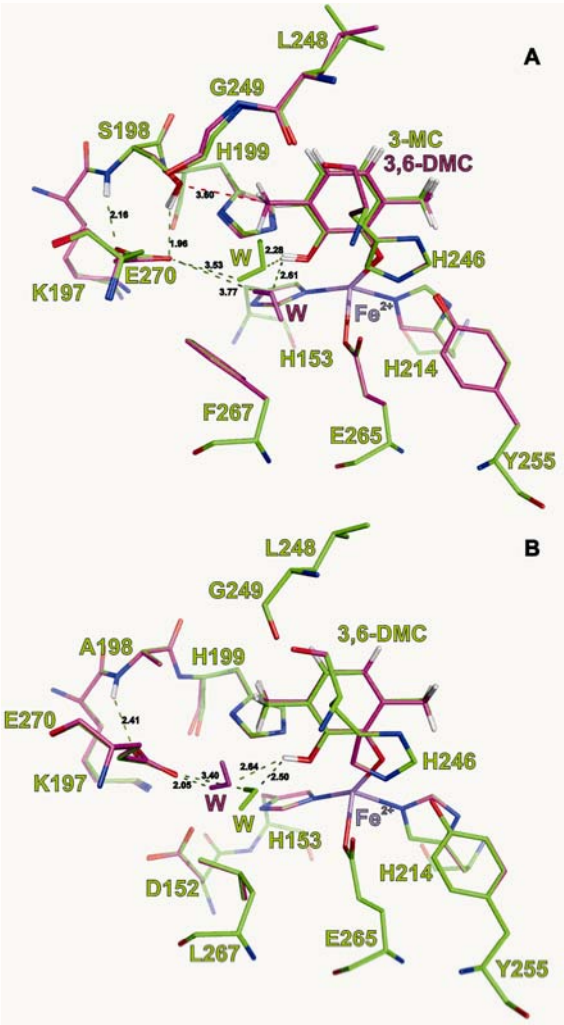

Fig. 1.5. A) Comparison between the model complexes (A198S, T249G, G270Q)-C2,3O/3-MC/water and (A1 98S, T249G, G270Q)-C2,3O /3,6-DMC/water. B) Comparison between two different model complexes (T249G, F267L, G270E)-C2,3O/3,6-DMC/water. W = water molecule. Atoms and H-bonds are coloured as in Fig. X1 except carbon atoms which are coloured green [(A198S, T249G, G270Q)-C2,3O/3-MC/water and the first model (T249G, F267L, G270E)-C2,3O/3,6-DM C/water] or purple [(A1 98S, T249G, G270Q)-C2,3O/3,6-DMC/water and the second model (T249G, F267L, G270E)-C2,3O/3,6-DMC/water]. All the atoms of each water molecule are coloured like the carbon atoms of the same complex.

The comparison of the MC-energy minimized models of (T249G, G270E)- and (T249G, F276L, G270E)-C2,3O showed that in the triple mutant the water molecule could dock into two slightly different positions. One of the two positions corresponds to that observed in the model of the double mutant (not shown). The second position, closer to the carboxylate of Glu-270 and characterized by a strong H-bond between this group and the water molecule, is made possible by the reduced steric hindrance of Leu-267 with respect to Phe-267 (Fig.1 .5B). Interestingly, in this complex the water molecule is in a bridging position between Glu-270 and the 3,6-DMC OH group and the orientation of the OH bonds of the water molecule is very similar to that observed in the case of the wild type C2,3O/3-MC complex (Fig.1.5B). Even if this second complex is about 1 kcal/mol less stable than the first one it could give a contribution

to catalysis explaining the increased catalytic efficiency of the mutants bearing the mutation Leu-267.
Thus it can be concluded that mutant (T249G, F276L, G270E)-C2,3O is the best available catalyst for the cleavage of 3,5-DMC and 3,6-DMC.
At the moment we are preparing and characterizing further mutants with residues smaller than leucine at position 267, as for example asparagine, alanine and serine. These mutations have been chosen to try to stabilize the second water site observed in (T249G, F276L, G270E)-C2,3O. These mutants will allow to verify if further reducing the hindrance at position 267 and, hence, increasing the mobility of Glu(Gln)-270 side-chain and of the water molecule, will provide more efficient catalysts for the cleavage of dimethylcatechols.

Table 1.2

	Substrate											
	CAT			3-MC			3,5-DMC			3,6-DMC		
Protein	K_M [a]	k_{cat} [b]	K_S [c]	K_M [a]	k_{cat} [b]	K_S [c]	K_M [a]	k_{cat} [b]	K_S [c]	K_M [a]	k_{cat} [b]	K_S [c]
wild type	1.0	180	180	3.8	118	31	74	0.36	0.005	21.5	0.66	0.03
(T249G)	52.3	66	1.26	44.1	8.1	0.18	34	0. 025	0.0073	10.2	0. 042	0.004
(T249G, G270E)	163	60	0.37	72.5	9.1	0.13	119	0.3	0.0025	27.1	0.23	0.008
(T249G), G270Q)	83.7	11.4	0.14	32.1	2.4	0.076	104	0.13	0.0012	48.8	0.05	0.001
(T249G, F267H)	29	28	0.95	7.6	6.7	0.93	34.5	2.2	0.063	9.2	0.35	0.038
(T249G, F267H, G270E)	19.5	19	0.98	37	5.6	0.15	67	0.75	0.011	11.2	0.21	0.019
(A198G, T249G, G270E)	286	40.4	0.14	54.5	3.03	0.055	231	0.0022	$9,5*10^{-5}$	55.6	0.025	$4,5*10^{-4}$
(A198S, T249G, G270E)	66	126	1.9	51	28	0.55	96	0.048	$5*10^{-4}$	28	0.026	$9*10^{-4}$
(T249G, F267L, G270E)	55	70	1.3	31	19	0.62	28	5.0	0.18	8.0	1.35	0.17
(T249G, F267L, G270Q)	33	45	1.37	32	15.4	0.48	64	0.85	0.013	23	0.49	0.021

RESULTS & DISCUSSION

Part 2: Isolation of new strains from polluted environments

Seawater samples were collected in six different areas inside the harbor of Pozzuoli (NA) (Fig. 2.1). All samples were collected at the surface and close to oil stains. The area indicated by number 1 in Fig. 2.1 is a bay for the mooring of small boats connected to the port by a narrow canal.

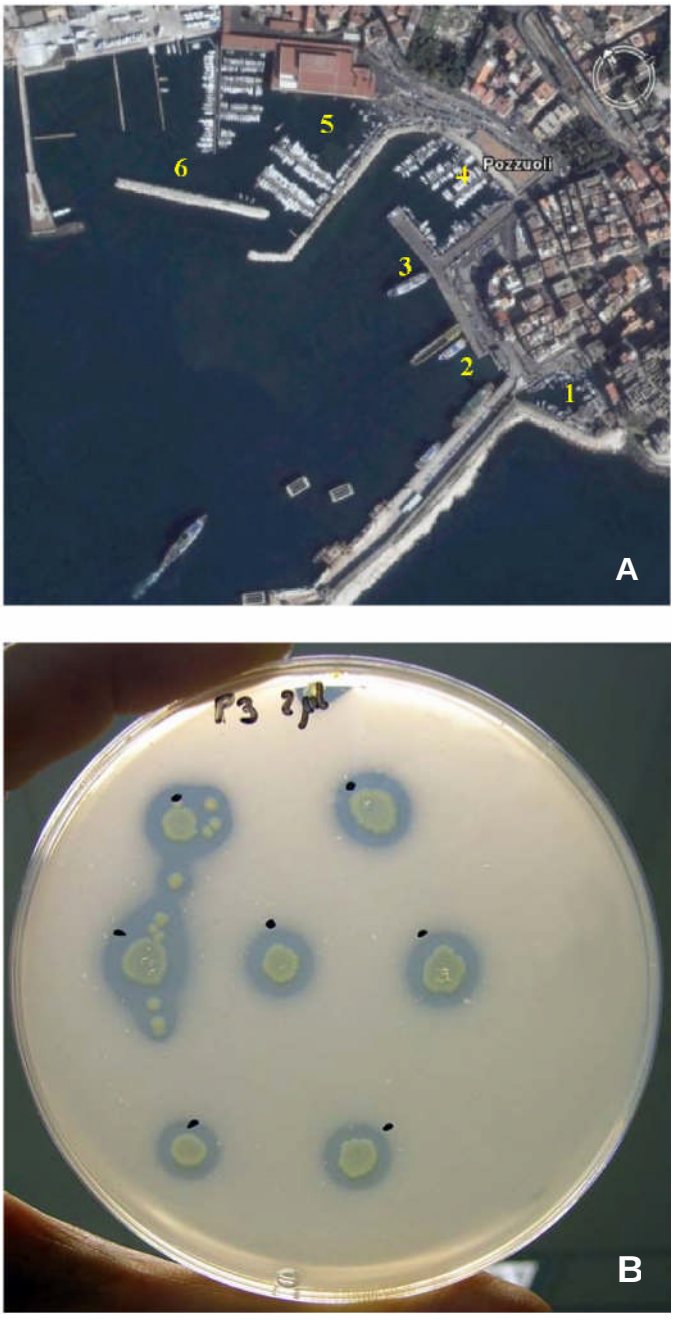

Fig. 2.1. A) Satellite picture of Pozzuoli harbour showing the points where water samples were collected. B) PP1Y colonies surrounded by a clear halo on M9G-Agar plate containing phenanthrene as the sole carbon source incubated 7 days at 25°C.

In order to favor the growth of microorganisms able to use aromatic hydrocarbons as energy and carbon source, naphthalene, phenanthrene and anthracene crystals, separately or as a mixture, were added to seawater samples. After three-six weeks of incubation at 25°C some samples showed the appearance of turbidity and/or brown/yellow color which are indications of microorganisms growth. These samples

were used to inoculate saline solutions (M9G) containing naphthalene, phenanthrene and/or anthracene as the sole source of carbon and energy. After two-four weeks of incubation turbid and/or colored cultures were used to inoculate fresh medium containing PAH as the sole carbon source. After three-four rounds of enrichment, aliquots were spread on agar plates containing phenanthrene as the sole carbon source. Several yellow colonies surrounded by clear halos were observed on plates seeded with samples collected inside area 1 (not shown). The appearance of a clear halo in the milky layer of phenanthrene crystals is an indication that the colony is able to degrade phenanthrene causing dissolution of crystals. Strain PP1Y (Pozzuoli; Phenanthrene; area 1; Yellow) described in this thesis was isolated starting from one of these colonies and purified through four plating cycles on reach medium.
When plated on LB-Agar strain PP1Y formed in 2-3 days bright yellow, mucoid colonies. Small amounts of liquid cultures, deposited on M9G-Agar plates containing phenanthrene as the sole carbon source, formed light yellow colonies surrounded by a clear halo in about 5-7 days at 25°C (Fig. 2.1B).

2.1. Analysis of 16S rDNA gene and identification of strain PP1Y.
A fragment of the 16S rDNA gene (Fig. 2.2), whose sequence was determined by BMR GENOMICS, was used to search the GENBANK database. 98-99% sequence identity was found with the rDNA sequences of several *Novosphingobium* strains, whereas, 90-98% sequence identity was found with the rDNA sequences of several strains of *Sphingomonas*, *Sphingobium* and *Sphingopixis*, which, together with the genus *Novosphingobium*, form the *Sphingomonadaceae* family, the sole proteobacteria (the main group of Gram- bacteria) which do not synthesize LPS.

GCCCCTCGGTTCGGAATAACTCAGGGAAACTTGAGCTAATACCGGATAATGACTTCGGTCCA
AAGATTTATTGCCGAGGGATGAGCCCGCGTAGGATTAGCTAGTTGGTGGGGTAATGGCCTAC
CAAGGCGACGATCCTTAGCTGGTCTGAGAGGATGATCAGCCACACTGGGACTGAGACACGGC
CCAGACTCCTACGGGAGGCAGCAGTGGGGAATATTGGACAATGGGCGAAAGCCTGATCCAGC
AATGCCGCGTGAGTGATGAAGGCCTTAGGGTTGTAAAGCTCTTTTACCAGGGATGATAATGA
CAGTACCTGGAGAATAAGCTCCGGCTAACTCCGTGCCAGCAGCCGCGGTAATACGGAGGGAG
CTAGCGTTGTTCGGAATTACTGGGCGTAAAGCGCGCGTAGGCGGTTACTCAAGTCAGAGGTG
AAAGCCCGGGGCTCAACCCCGGAACTGCCTTTGAAACTAGGTGACTAGAATCTTGGAGAGGT
CAGTGGAATTCCGAGTGTAGAGGTGAAATTCGTAGATATTCGGAAGAACACCAGTGGCGAAG
GCGACTGACTGGACAAGTATTGACGCTGAGGTGCGAAAGCGTGGGGAGCAAACAGGATTAGA
TACCCTGGTAGTCCACGCCGTAAACGATGATAACTAGCTGTCCGGGCACATGGTGTTTGGGT
GGCGCAGCTAACGCATTAAGTTATCCGCCTGGGGAGTACGGTCGCAAGATTAAAACTCAAAG
GAATTGACGGGGGCCTGCACAAGCGGTGGAGCATGTGGTTTAATTCGAAGCAACGCGCAGAA
CCTTACCAGCGTTTGACATCCTGATCGCGGATTAGAGAGATCTTTTCCTTCAGTTCGGCTGG
ATCAGTGACAGGTGCTGCATGGCTGTCGTCAGCTCGTGTCGTGAGATGTTGGGTTAAGTCCC
GCAACGAGCGCAACCCTCGTCCTTAGTTGCCATCATTTGGTTGGGCACTCTAAGGAAACTGC
CGGTGATAAGCCGGAGGAAGGTGGGGATGACGTCAAGTCCTCATGGCCCTTACACGCTGGGC
TACACAC GT GC TACAAT GGC GGT GACAGT GGGCAGC GAGT GC GC GAGCACAAGC TAAT C T C C
AAAAGCCGTCTCAGTTCGGATTGTTCTCTGCAACTCGAGAGCATGAAGGCGGAATCGCTAGT
AATCGCGGATCAGCATGCCGCGGTGAATACGTTCCCAGGCCTTGTACACACCGCCCGTCACA
CCATGGGAGTTGGTTTCACCCGAAGGTAGTGCGCTAACCGGCAACGGAGGCAGCTAACCACG
GTGGGATCAGCGACTGGGGTGAAGTC

Fig. 2.2. DNA sequence of a fragment of PP1Y 16S rRNA gene.

Strain PP1Y is closely related to *Novosphingobium pentaromativorans* US6-1^T (two differences in a 1481 bases-long alignment) a strain isolated in Korea and able to degrade PAH with 3-5 rings, and to *Novosphingobium* sp. Phe-8 (five different nucleotides) (data not shown). Therefore on the basis of the 16S rRNA sequences strain PP1Y could be considered a new strain of the species *Novosphingobium pentaromativorans*. However, the microbiological characterization described in the following sections shows that the two strains differ in several relevant physiological features like optimal salinity, metabolic properties, membrane fatty acid composition, growth morphology and range of substrates which can be degraded. For these reasons we suggest that strain PP1Y is a new *Novosphingobium* species and propose the name *Novosphingobium puteolanum* PP1Y.

2.2. Phenotypic characterization.

Novosphingobium puteolanum PP1Y grows effectively in LB medium and in minimal mediums containing casaminoacids or glucose as single carbon sources. Less effectively it can use glycerol, whereas, it does not grow using benzoate or phenol (data not shown).

The strain gave positive results in the assays for the β-galactosidasic, ureasic and arginine-dihydrolase activities and for citrate assimilation. In the same tests the strain US6-1 provides negative results.

Several sphingomonadales produce carotenoids. Nostoxanthin, a yellow carotenoid, is one of the most frequently found in this group of bacteria. The UV-vis spectrum of the yellow pigment produced by *Novosphingobium puteolanum* PP1Y was found to be identical to that of nostoxanthin reported in literature (data not shown). The amount of the pigment depended on the growth substrate, temperature, shaking of the cultures and salinity. The largest amount was observed during growth on solid rich mediums (LB-Agar)

Sphingomonadales are so-called because they produce an atypical outer membrane containing glycosphingolipids (GLS) instead of lipopolysaccharides. For example *S. paucimobilis* outer membrane contains large quantities of GSL-1 and GSL-4 which are formed by a sphingosine molecule bound to a 2-hydroxy fatty acid and to a mono- or tetra-saccharide, respectively. The type and relative abundance of the 2-hydroxy fatty acids is typical of each strain and can be used for tassonomic purposes. The analysis of the fatty acids (Table 2.1) showed that the lipidic composition of the strain PP1Y is more similar to that of the strain *Novosphingobium subarticum* JCM 10398^T than to that of *Novosphingobium pentaromativorans* US6-1^T. Moreover it showed some distinctive features such as the absence of the fatty acid 17:1 and the presence of the fatty acid 18:1 methylated at position 11.

Liquid cultures of strain PP1Y, both in rich and minimal mediums with several growth substrate, became very viscous due to the production of abundant extracellular material likely containing esopolysaccharides (EPS). In fact, it is known that several strains of sphingomonadales produce EPS containing repeated tetrasaccharidic units $(A\text{-}B\text{-}C\text{-}B)_n$ where A is usually rhamnose or mannose, B is glucose and C is glucuronic acid. Sugars at positions A and B usually bind “side-chains” constituted by other sugars or carboxylic acids like acetate and glycerate. Several of these polysaccharides are patented as jellifying agents or thickeners for food industry or scientific research. *Gelrite*, the gel used for the preparation of plates for thermophilic bacteria, is the commercial form of “gellan”, the EPS produced by *Sphingomonas elodea* [38]. Preliminary analysis of the EPS produced by the strain PP1Y performed by Dr. Antonio Molinaro (Dipartimento di Chimica Organica e Biochimica, Università

di Napoli Federico II) showed that it contains, as expected, mainly rhamnose, glucose and glucuronic acid, but also some other less abundant sugars. At the moment we don't know if these sugars are branches of the main polysaccharide or form one or more independent polymers.

Table 2.1. Composition of the membrane fatty acids of the strain PP1Y and of the closely related strains *Novosphingobium pentaromativorans* US6-1 and *Novosphingobium subarticum* JCM1 0398.

Fatty acid	strain US6-1	strain JCM 10398	strain PP1Y
12:0 2-OH	0.8%	-	0.06%
13:0 2-OH	-	-	-
14:0	0.6%	-	0.8%
14:0 2-OH	19.7%	7.6%	4.45%
15:0	-	-	-
15:0 2-OH	0.3%	-	-
16:0	1.0%	10.2%	9.5%
16:0 2-OH	2.5%	2.1%	2.9%
18:0	-	-	0.4%
16:1	8.8%	15.5%	15.1%
17:1	2.0%	3.3%	-
18:1	64.0%	61.1%	65.0%
18:1 11-CH3	-	-	1.1
Others	0.3	0.2	0.7

2.3 Optimal salt concentration, pH and temperature for growth of PP1Y.

As shown in figures 2.3A and 2.3B *Novosphingobium puteolanum* PP1Y was able to grow from 0% to 4% (w:v) NaCl. The highest growth rates were measured at NaCl concentrations between 0.5% and 1.5% (w:v). Growth was very slow at NaCl concentrations above 5%. These features allow the strain PP1Y to grow both in seawater and brackish water, like river estuaries and costal lagoons. It is also interesting to note that the behavior of strain US6-1 is very different [4]. In fact, the highest growth rate for this strain was observed at 2,5% NaCl, moreover, it the strain is not able to grow at NaCl concentrations below 1 %.

As for optimal growth temperature, in LB medium, strain PP1Y was able to grow in a wide range from about 18°C to 42°C. The highest growth rates were observed at about 32-34°C (data not shown).

The effect of pH on the growth rate was studied at 22°C and 28°C (Fig. 2.4). At both temperatures the strain showed the ability to grow in a wide range of pH values (from 5 to about 7.5) even if the optimal pH is slightly more acidic at 22°C (pH 6.0) than at 28°C (pH 7.0).

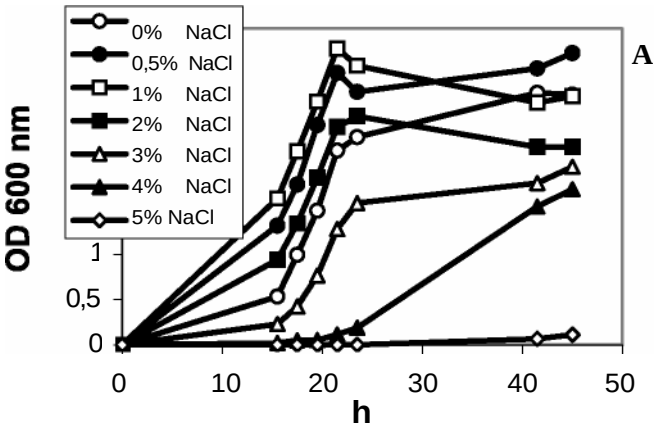

Fig. 2.3. Growth curves of *Novosphingobium puteolanum* PP1Y as function of NaCl concentration.

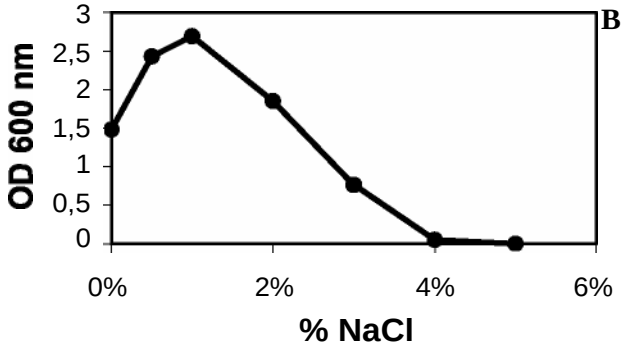

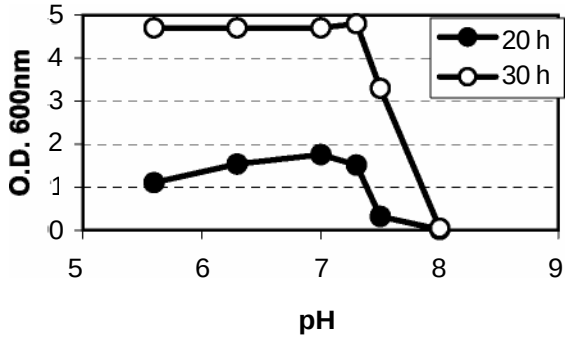

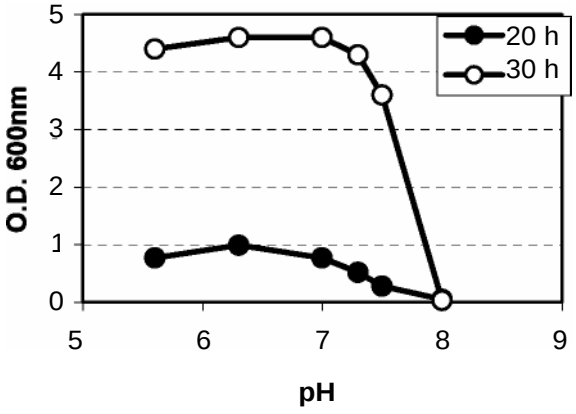

Fig. 2.4. Growth curves of *Novosphingobium puteolanum* PP1Y as function of pH at 28°C A) and 22°C B).

2.4 Morphological analysis of cells and of the "biofilm" of strain PP1Y

Cells of *Novosphingobium puteolanum* PP1Y, observed by phase contrast microscope, appeared as short rods. They could be motile (likely flagellate) or non-motile (Fig. 2.5A). Non-motile cells could form aggregates of different dimensions including macroscopic "flocks" 1-10 mm long. Figure 2.5A shows the border of one of these flocks. The number and dimension of flocks was influenced by several parameters including shaking, temperature and growth substrates. A complete investigation was not performed. However, formation of flocks was found to be favored by slow shaking, high temperature (34°-37°C) and by the presence of casaminoacids. Dried and stained with methylene blue, flocks showed the presence of bunches of cells trapped inside a blue-stained matrix (Figure 2.5B).

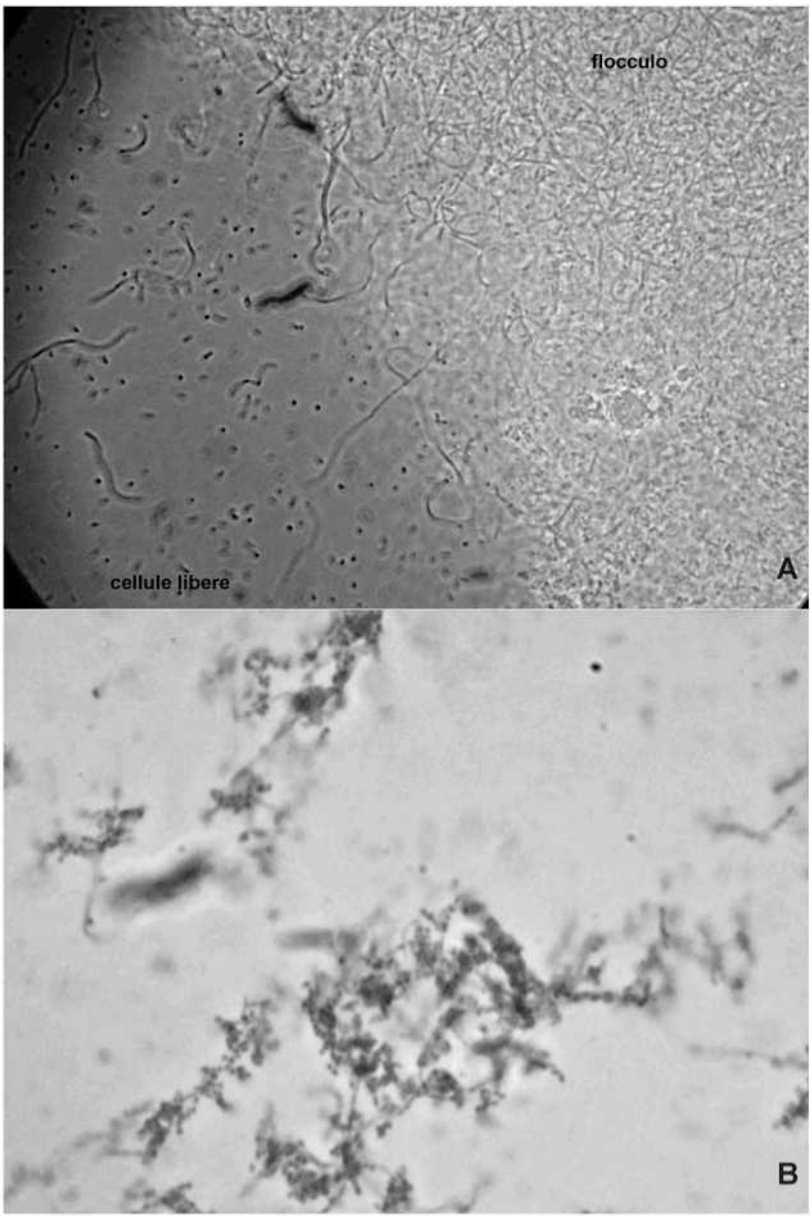

Fig. 2.5 A) Phase contrast microscope picture showing the border of flock (not stained). B) Phase contrast microscope picture showing a flock dried and stained with methylene blue.

A similar behavior has already been described for some other sphingomonadales which show the so-called "planktonic/sessile dimorphism" [39]. These dimorphic strains can exist in a sessile form made up of aggregated cells joined by

polysaccharidic extracellular material, and a planktonic form of free cells. About 5% of the free cells are motile, possessing a single polar flagellum [39]. It is interesting to note that no planktonic/sessile dimorphism has been described for *Novosphingobium pentaromativorans* US6-1^T.
Flocks formed by strain PP1Y showed also some peculiar features. They adsorbed and concentrated hydrophobic molecules like Red Sudan III (Fig. 2.6) and PAH (not shown), and adhered to hydrophobic surfaces as plastic polymers (for example polyethylene and polystyrene).

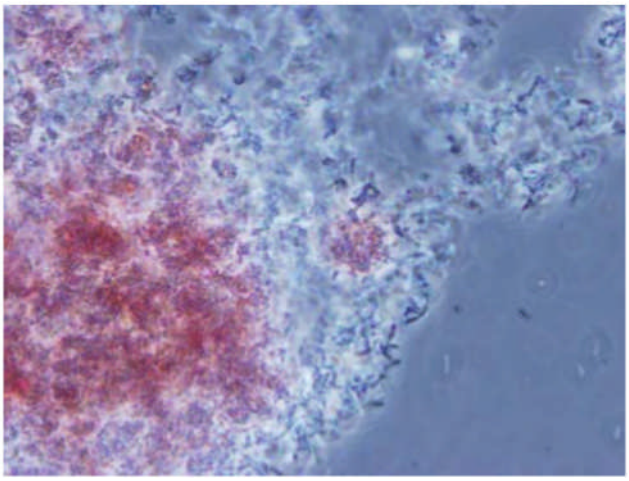

Fig. 2.6 Phase contrast microscope picture showing the border of flock grown in the presence of Sudan III.

Moreover, on several types of hydrophobic surfaces *N. puteolanum* PP1Y formed a "biofilm" which, observed at the phase contrast microscope, appeared as a structured, two-dimensional version of the amorphous flocks. Figure 2.7A shows a polystyrene Petri plate containing 10 ml of LB medium in which *N. puteolanum* PP1Y formed in about 24 h a yellow biofilm layer. After about 48-72 h the plate contained an homogeneous gelatinous layer 3-4 mm thick (not shown). The biofilm, detached from the plate by shaking vigorously, formed gelatinous sheets (shown in Fig 2.7B). Formation of biofilm was observed also on polyethylene surfaces and more surprisingly at the boundary between a liquid aqueous phase and an oil phase as described in the next section.

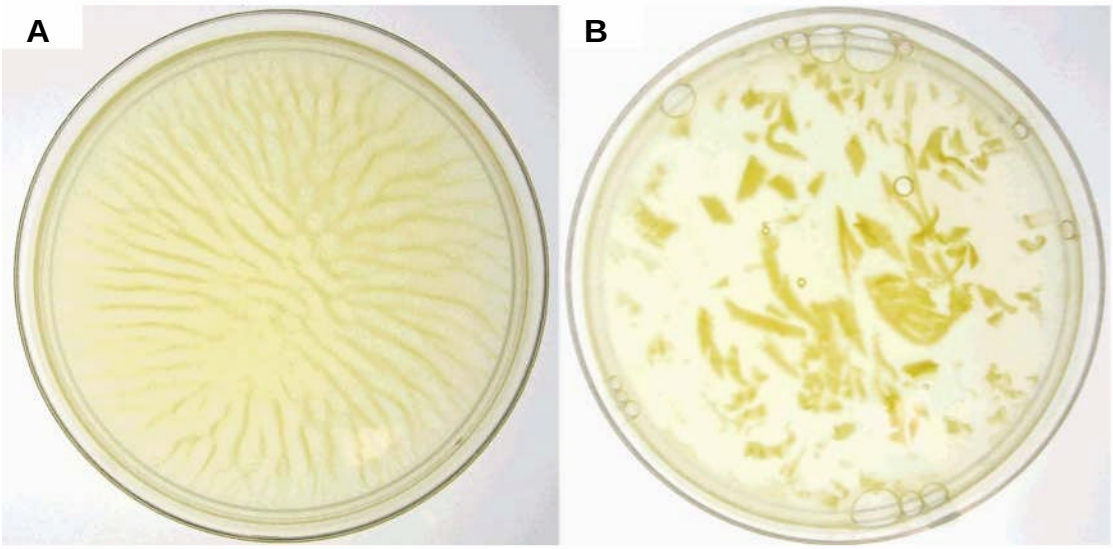

Fig. 2.7 A) Polystyrene Petri plate containing 10 ml of LB medium in which *N. puteolanum* PP1Y formed in about 24 h a yellow biofilm layer. B) PP1Y biofilm detached from the plate by shaking vigorously.

2.5 Growth on oil fuels.

N. puteolanum PP1Y was found to be able to use gas-oil and gasoline as the sole carbon and energy source (Fig. 2.8).

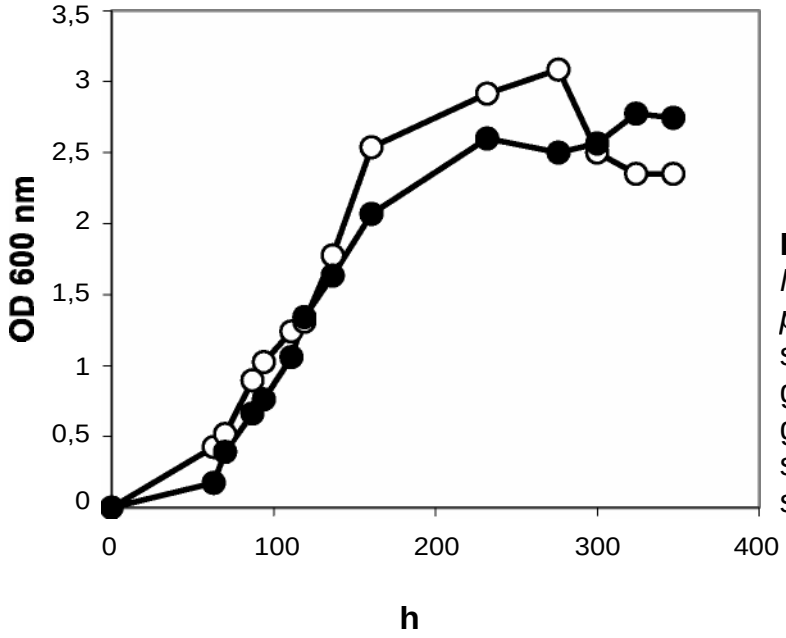

Fig. 2.8 Growth curves of *Novosphingobium puteolanum* PP1Y in saline medium containing gas-oil (void circles) or gasoline (filled circles) as sole carbon and energy sources.

Gas-oil was very well tolerated – at least up to a ratio 2:1 = water:gas-oil – whereas gasoline was more toxic and the highest concentration allowing growth of the strain was found to be 50:1 = water:gasoline. These findings are likely due to the fact that gasoline is a light fraction of petroleum and contains low molecular weight, hydrosoluble hydrocarbons like hexane and heptane which damage cell membranes and proteins [40, 41]. In fact, we observed that gasoline diluted 3-5 fold with liquid paraffin, a mixture of medium and long chain alkanes, which can reduce partitioning of small hydrocarbon to the water phase, was less toxic than pure gasoline and allowed to obtain higher growth rates and higher cell densities (not shown).

In biphasic systems water/gas-oil and water/(gasoline+paraffin) the growth of *N. puteolanum* PP1Y determined emulsification of the oil phase which spread in small drops with a diameter ≤ 1 mm. As shaking was stopped drops stratified at the surface but didn't join together to form an oil phase. Analysis of the drops of gas-oil by phase contrast microscope revealed that each drop was covered by a biofilm containing bacterial cells at a density increasing with the incubation time (Fig 2.9A and B).

Irradiating the sample with UV light the drops appeared enlightened from the inside by an intense blue fluorescence typical of PAH (Fig. 2.10). This finding confirmed that the observed cell-covered drops contained gas-oil.

Due to the strong refraction of the boundaries of oil drops it was not possible to observe directly the existence of an extracellular matrix encapsulating cells. However, several drops showed irregularities or damages to the biofilm (Fig. 2.11A), likely due to collisions with other drops or with the tube, which suggest the existence of a layer of extracellular material. Moreover, in aged cultures "super-aggregates were detected" formed by two or more biofilm-covered drops clearly glued by strongly refractive material similar to that found in the amorphous flocks (Fig 2.11 B). All these finding suggest that *N. puteolanum* PP1Y has developed a "mechanical"

emulsification strategy not based on the secretion of bio-surfactants but on the physical entrapment of small quantities of oil phase.

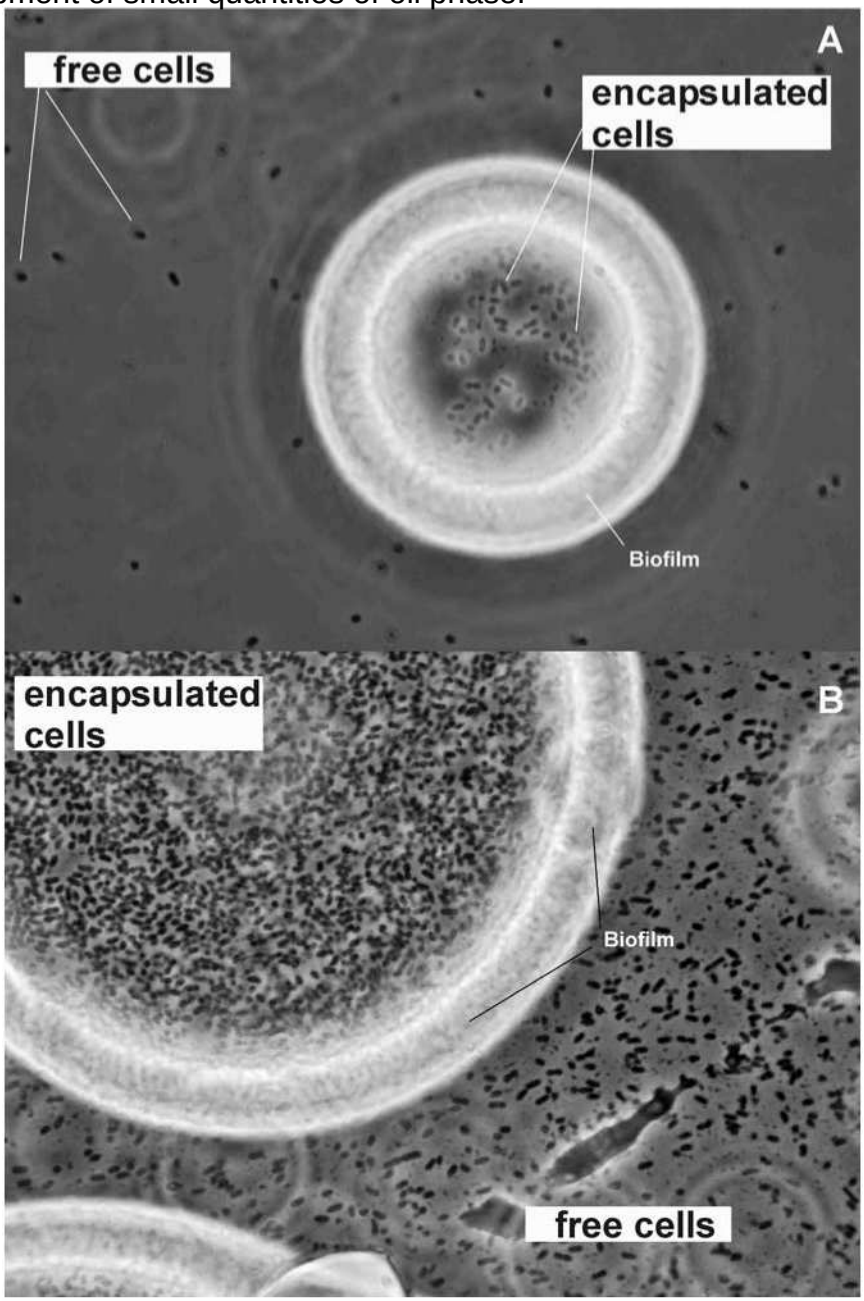

Fig. 2.9 Gas-oil drops covered by biofilm after 3 A) and 10 B) days of incubation.

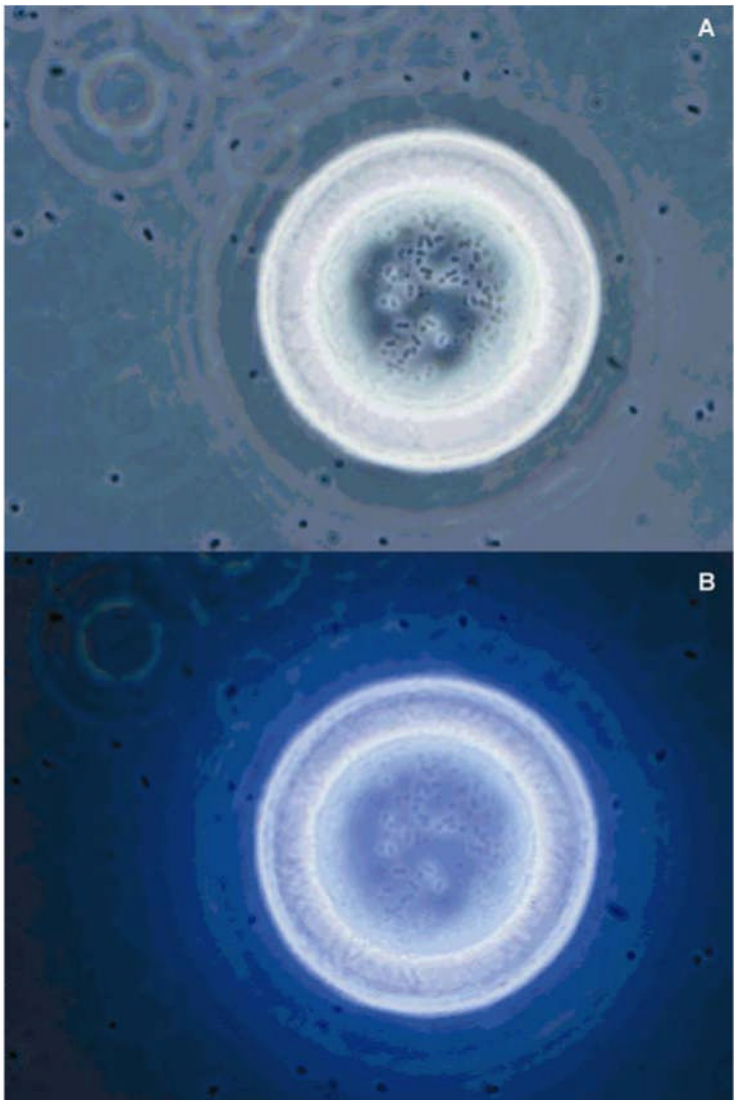

Fig. 2.10 Gas-oil drop covered by biofilm observed at the phase contrast microscope using only visible light A) and both visible and UV light B).

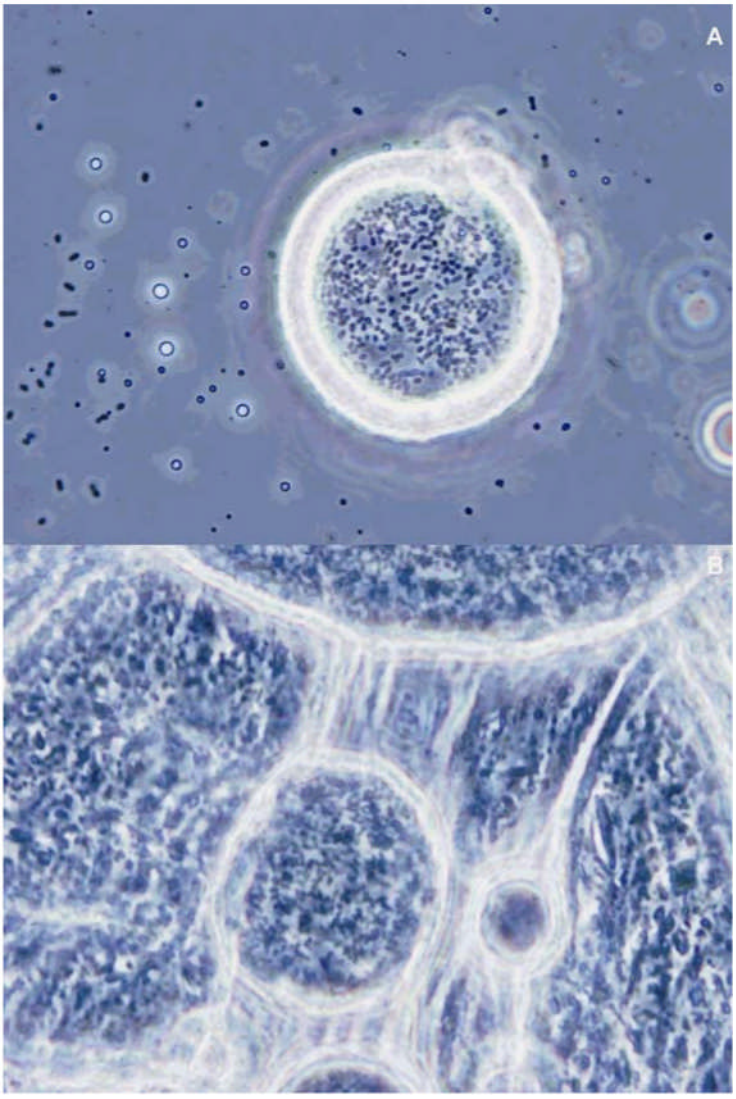

Fig. 2.11 A) Gas-oil drop covered by damaged biofilm observed at the phase contrast microscope. B) Super-aggregates formed by biofilm-covered drops glued by refractive material.

2.6 Analysis of degradative potentialities of *N. puteolanum* PP1Y.

As gasoline and gas-oil contain hundreds aromatic and saturated hydrocarbons, the direct determination of which gas-oil/gasoline components are degraded by *N. puteolanum* PP1Y was too complex. Therefore, we decided to test pure hydrocarbons as the sole carbon and energy sources.

N. puteolanum PP1Y was not able to grow on pure linear alkanes, like hexane, decane (C_{10}), dodecane (C_{12}), tetradecane (C_{14}), pentadecane (C_{15}), on pure cyclic alkanes, like cyclohexane, and on alkane mixtures like *low viscosity paraffin* (LVP) and *high viscosity paraffin* (HVP). On the contrary, it was able to grow on a surprisingly wide range of aromatic hydrocarbons (table 2.2). Except benzene, 1,2,3-trimethylbenzene (1,2,3-TMB), and isopropilbenzene (IB), *N. puteolanum* PP1Y was able to grow on all the (poly)alkylbenzenes commonly found in petroleum-derived fuels (table 2.2). All these monocyclic hydrocarbons, except propylbenzene (PB) and butylbenzene (BB), were good growth substrates provided either in pure form or dissolved in C_{12}, C_{14}, LVP, HVP or silicon oils (polydimethylsiloxane or polymethylphenylsiloxane) at 0.5%-2.0% (w:v) in order to obtain a low complexity

artificial gas-oil, allowing to obtain cultures with $_{O.D.600nm}$ values ≥ 1 in less than one week.

Similar growth rates were observed using as the sole carbon sources biphenyl, naphthalene and all the available (di)methylnaphthalenes in pure or paraffin-dissolved form (table 2.2). Pure phenanthrene crystals – whose water solubility is lower than 1.5 mg/l – allowed a slow growth, whereas, C_{12}-dissolved phenanthrene (2.0% w:v) provided cultures with $_{O.D.600nm}$ values ≥ 1 in about 5-10 days (not shown). Paraffin-dissolved anthracene, pyrene, chrysene, benz[a]anthracene, and fluoranthene showed growth only for incubation times > 14 days. At least in part the slow growth could be attributed to the lower bio-availability of these PAH which not only have water solubility 100-1 0000 lower than that of naphthalene (table 2.2) but have also low solubility in liquid paraffins. For example chrysene solubility in LVP is about 0.2% (w:v), whereas, naphthalenes and phenanthrene can be dissolved in paraffin at concentration 10-20 fold higher.

Analysis of cultures at phase contrast microscope showed that no paraffin-dissolved aromatic hydrocarbon reproduces all the features of the gas-oil grown cultures which contain free cells, tube-attached biofilm, amorphous flocks, biofilm-covered oil drops and their super-aggregates. Even if all mono- and bi-cyclic aromatic hydrocarbons, provided in the paraffin-dissolved form, determined emulsification of the oil phase, oil drops were larger and covered by few cells, whereas a very large number of free cells were visible around the drops (Fig. 2.12A). The less soluble polycyclic substrates like anthracene, chrysene, benz[a]anthracene, and fluoranthene provided cultures with few or none free cells and small drops covered by variable amount of encapsulated cells (not shown).

Some aromatic hydrocarbons, like ethylbenzene, propylbenzene, 3-ethyltoulene, tetrahydronaphthalene, pyrene and the three heterocyclic hydrocarbons dibenzofuran, dibenzothiophene and carbazole (dibenzopyrrole) induced the production of abundant mucilaginous material. Analysis of cultures at phase contrast microscope showed that this material is formed by a sort of refractive sheets containing few cells, sometimes associated in short chains (Fig. 2.12B).

All the features of the gas-oil grown cultures were reproduced using as growth substrate LVP containing 10% (w:v) of a mixture of aromatic hydrocarbons including one monocyclic hydrocarbon (2.0% *p*-X), one bicyclic hydrocarbon (4.0% 2,6-DMN), one tricyclic hydrocarbon (3.6% PHE), and one tetracyclic hydrocarbon (0.8% PYR) (Fig. 2.13A). Mixtures lacking in phenanthrene or pyrene provided oil drops with irregular shape and incomplete biofilm or irregular “hypertrophic” biofilm, respectively (Fig. 2.13B e C). These findings suggest that *N. puteolanum* PP1Y is specifically adapted to grow on aromatic hydrocarbon mixtures and that some PAH, like pyrene, could by involved in the regulation of extracellular matrix/biofilm production.

Table 2.2.

	Hydrocarbons	Abb.	Sol. (mg/l)	logK_{ow}	Growth[a]
	Gas-oil				F,B,T
	Gasoline				F,T
monocyclic aromatic	Benzene	BEN	1760	2.13	-
	Toluene	TOL	515	2.69	F,b
	o-xylene	o-X	178	2.8-3.1	F,b
	m-xylene	m-X	161	3.2	F,b
	p-xylene	p-X	162	3.15	F,b
	Ethylbenzene	EB	152	3.15	f,b,M
	2-ethyltoluene	2-ET	93	3.53	F,b
	3-ethyltoluene	3-ET	94	3.88	f,b,M
	4-ethyltoluene	4-ET	95	3.90	F,b,(M)
	Propylbenzene	PB	60	3.6	M
	Isopropylbenzene	IB	61	3.66	M(*slow*)
	1 ,2,3-trimethylbenzene	1 ,2,3-TMB	75	3.66	-
	1 ,2,4-trimethylbenzene	1 ,2,4-TMB	58	3.65	F,b
	1,3,5-trimethylbenzene	1,3,5-TMB	48	3.42	F,b
	Butylbenzene	BB	50	4.4	b
naphthenes	Indan	IND	109	3.33	-
	Tetrahydronaphthalene	THN	47	3.5-3.8	M
	Acenaphthene	ACE	4	3.92	b
	Fluorene	FLU	2	4.18	b
polycyclic aromatic	Naphthalene	NAP	32	3.36	F,b
	1-methylnaphthalene	1-MN	28	3.87	F,b
	2-methylnaphthalene	2-MN	25	3.86	F,b
	1 ,2-dimethylnaphthalene	1 ,2-DMN	15	4.31	F,b
	1 ,3-dimethylnaphthalene	1 ,3-DMN	8	4.6	F,b
	1 ,7-dimethylnaphthalene	1 ,7-DMN		4.44	f,b,T
	2,3-dimethylnaphthalene	2,3-DMN	3	4.6	F,b
	2,6-dimethylnaphthalene	2,6-DMN	2	4.31	F,b
	Biphenyl	BIP	7.5	4.09	F,b
	Phenanthrene	PHE	1.3	4.57	F,b,T
	Fluoranthene	FAN	0.26	5.22	b
	Pyrene	PYR	0.13	4.88	M
	Anthracene	ANT	0.07	4.5	b
	benzo[a]anthracene	BAN	0.014	5.91	b
	Chrysene	CHR	0.002	5.86	b
heterocyclic	Dibenzofuran	DBF	10	4.17	M
	Carbazol	CAR	1.8	3.72	M
	Dibenzothiophene	DBT	1.47	4.38	M

[a] F = free cells (≥ 1 O.D.600nm) & amorphous flocks; f = free cells (<1 O.D.600nm) & amorphous flocks; B = emulsification & biofilm on oil drops (high cell density); b = emulsification & biofilm on oil drops (low cell density); T = biofilm on the polyethylene tube; M = emulsification & mucilage formation; - = no growth.

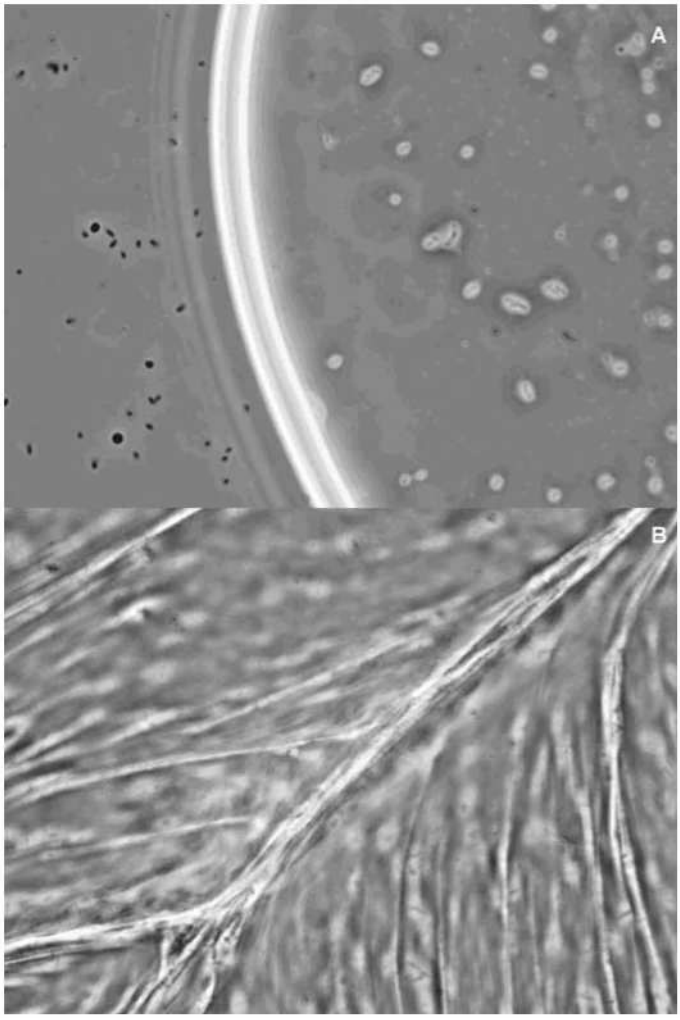

Fig. 2.12 A) *o*-Xylene containing-C14 drop covered by biofilm containing cell at low density. B) Phase contrast microscope picture showing the refractive sheets containing few cells formed by PP1Y growing on pyrene containing-C14 drops.

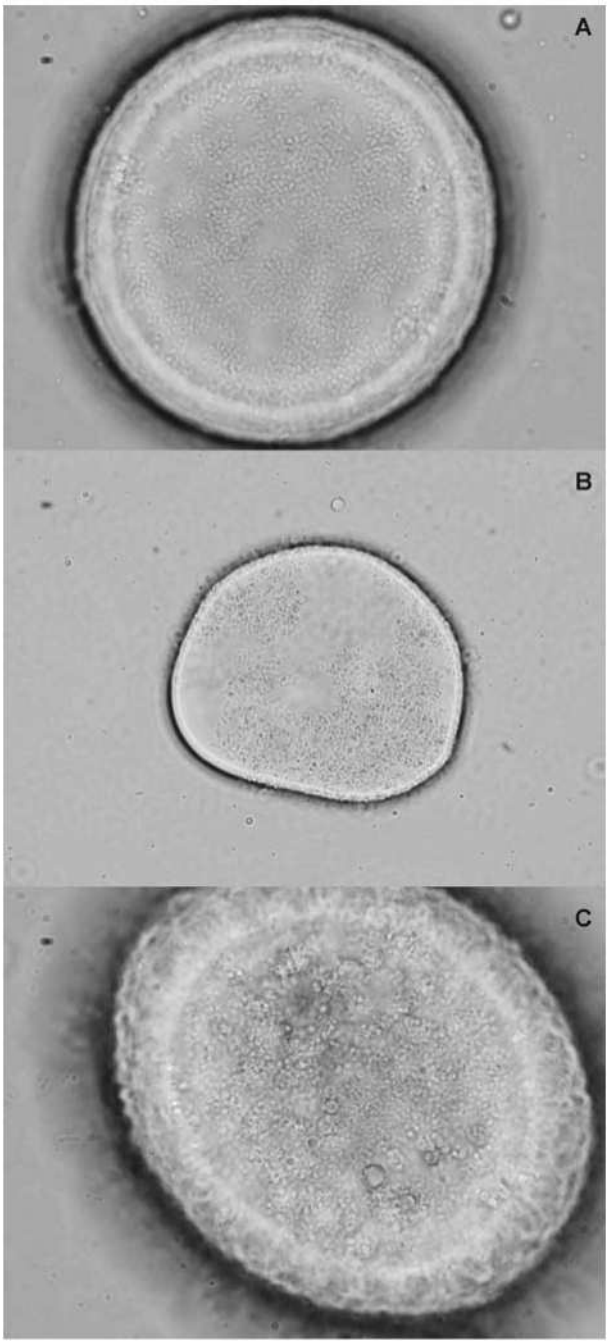

Fig. 2.13 LVP drops containing aromatic hydrocarbon mixtures covered by biofilm. A) LVP drop containing *p*-xylene, 2,3-DMN, phenanthrene, and pyrene. B) LVP drop containing *p*-xylene, 2,3-DMN, and phenanthrene. C) LVP drop containing *p*-xylene, 2,3-DMN, and pyrene.

2.7 Degradation of paraffin-dissolved aromatic hydrocarbons.

In order to verify the degradation ability of *N. puteolanum* PP1Y on aromatic hydrocarbons, single PAH were dissolved in C_{12}, C_{14}, LVP or HVP and incubated at 28°C. At increasing times, aliquots of paraffin drops were collected and the percentage of aromatic hydrocarbon remaining in the oil phase was determined by normal phase HPLC.

Fig 2.14 shows the degradation of C_{12}-dissolved phenanthrene. More than 90% of the initial phenanthrene was degraded in about three days. The slight decrease of phenanthrene concentration in the control sample was likely due to transfer to water phase, evaporation or both. Fig 2.14 shows that the presence of a monocyclic aromatic hydrocarbon (EB) didn't prevent phenanthrene removal.

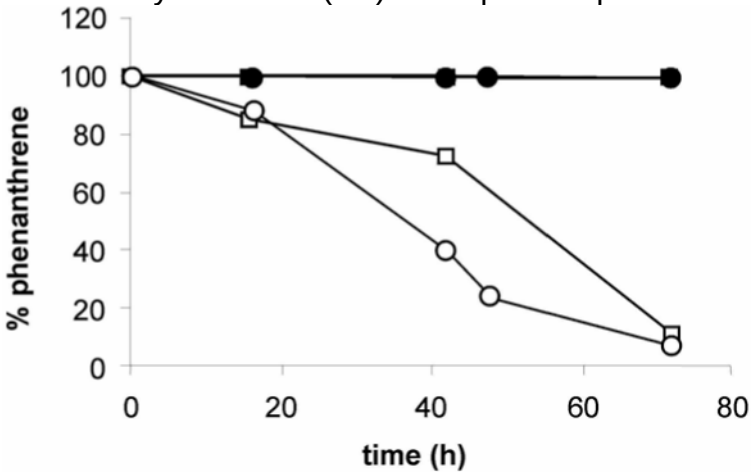

Fig. 2.14 Phenanthrene removal from a C12 oil phase containing phenanthrene (0.5 mg/ml) (empty squares) or phenanthrene (0.5 mg/ml) and ethylbenzene (0.5 mg/ml) (empty circles). Filled symbols show the amount of phenanthrene in control samples lacking cells.

Similar results were obtained using $_{C14,}$ or LVP-dissolved phenanthrene, whereas phenanthrene removal was slightly slower using HVP as organic phase (not shown). It is worth noting that naphthalene removal was complete in less than 24 h also from HVP (Fig 2.15A), whereas, only 50% biphenyl (Fig 2.15B) and 20% pyrene (Fig 2.15C) were removed in 16-20 days from LVP and $_{C12,}$ respectively. Also in this case, at least in part, the observed differences could be due to the different water solubility and $LogK_{ow}$ values (table 2.2) and, hence, to the different bioavailability of the PAH.

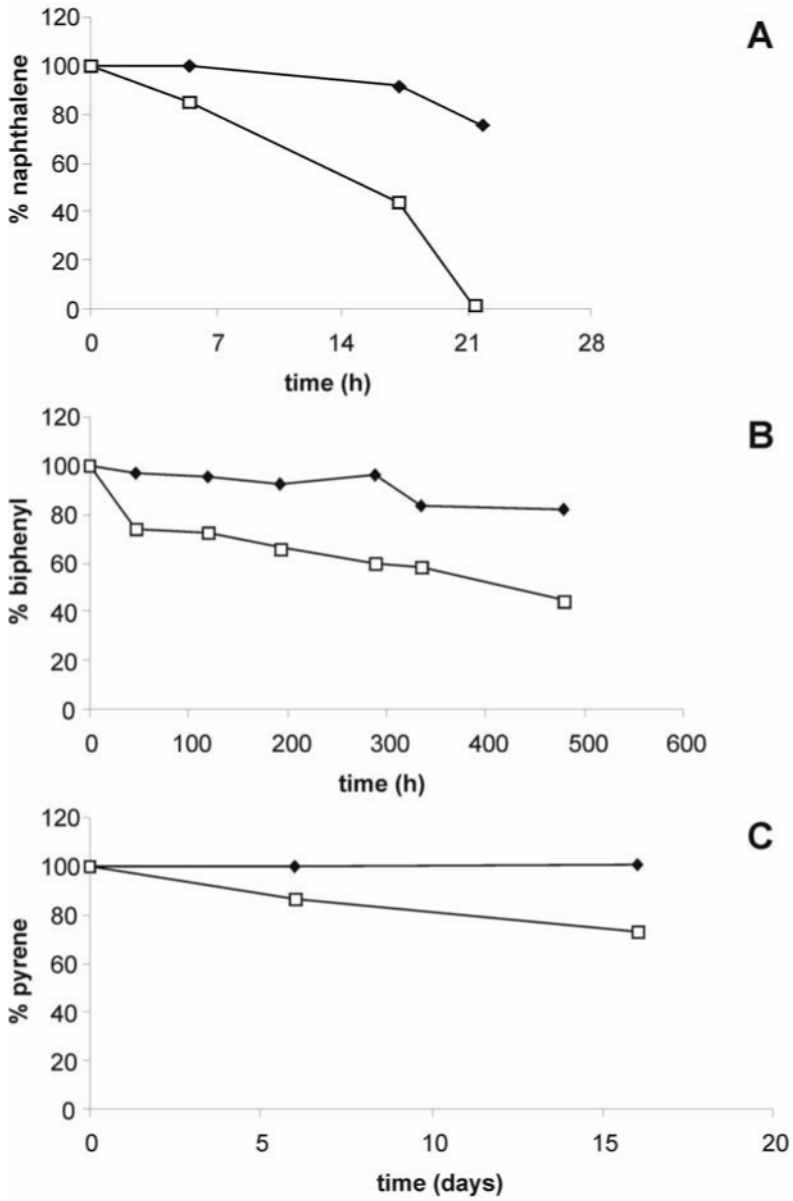

Fig. 2.15 Naphthalene A), biphenyl B), and pyrene C) removal from a C12 oil phase (empty squares). Filled symbols show the amount of PAHs in control samples lacking cells. Initial concentration of PAHs was 0.5 mg/ml of C12.

CONCLUSIONS

Bioremediation techniques are the most promising strategies for the removal of environmental pollutants. In fact, with respect to traditional approaches, they are more effective, less expensive and more environmental-friendly. However, full exploitation of the potential of bioremediation strategies requires not only the availability of a large number of strains with wide degradative abilities but also an accurate characterization of these strains both at the microbiological and biochemical/genetic level. This knowledge is necessary to perform a rational planning of bioremediation interventions. Strains should also be selected on the basis of their ability to proliferate under the specific combination of chemical/physical parameters of the environment to be treated, or to give rise to synergic cooperation. Indeed, a consortium of strains could be able to remove pollutants which are not degraded by any single strain.

Moreover, the knowledge of the molecular systems involved in the degradation of xenobiotics offers the opportunity to prepare engineered microorganisms with improved or widener degradative abilities.

In the present thesis we have described two example of the two different approaches.

Pseudomonas sp. OX1, isolated form wastewaters of an industrial area, shows a very specific adaptation being able to grow with high efficiency, among others, on three monocyclic aromatic hydrocarbons, benzene, toluene, and *o*-xylene but not on similar hydrocarbons like ethylbenzene, *m*- and *p*-xylene. Characterization at the molecular level of the enzymes involved in the degradation of these compounds showed that this specificity is partly due to the first two enzymes of the pathway which convert (alkyl)benzenes to (alkyl)catechols: ToMO and PH. These monooxygenases posses slightly higher affinities for substrates like benzene, toluene, and *o*-xylene than for ethylbenzene, *m*- and *p*-xylene. However, the real bottleneck of the entire degradative pathway is the third enzyme of the pathway i.e. the C2,3O which shows a very restricted substrate specificity. Initial attempts to engineer C2,3O variants with widener substrate specificity allowed to understand that, unfortunately, a single residue – Thr-249 – is involved both in substrate selection and in the catalytic mechanism. The results reported in the first part of the Results & Discussion section show that, using Monte Carlo modeling and site directed protein engineering, it was possible counterbalance the adverse effects of mutation T249G on the catalytic efficiency of the enzyme and obtain mutants which combine a high affinity for dimethylcatechols and a good catalytic efficiency. The best mutant available at the moment, (T249G, F267L, G270E)-C2,3O, shows slightly reduced K_M values and $_{kcat}$ values 30 and 200 fold higher than the first generation mutant (T249G)-C2,3O on 3,6-DMC and 3,5-DMC respectively. If the last group of C2,3O mutants currently under preparation will allow a further increase of one order of magnitude, then these improved mutants could be expressed in the OX1 strain as “isoenzymes” of wild type C2,3O to widen the degradative abilities of the strain. Thus, these improved strains could replace the wild type strain in the bioreactor systems developed in collaboration with Prof. Salatino and Marzocchella of the Dipartimento di Ingegneria Chimica of Naples University Federico II [18].

As for the strategy of searching for new strains, it should be noted that *Novosphingobium putaolanum* PP1Y, the microorganism selected by enrichment from seawater of the harbour of Pozzuoli, is complementary to the OX1 strain in its substrate specificity. In fact, it shows the ability to use a surprisingly wide panel of

mono and polycyclic aromatic hydrocarbons but not benzene or phenols which are good substrates for the strain OX1. Moreover *Novosphingobium putaolanum* PP1 Y posses several features which make it very well suited for the use in *in situ* bioremediations interventions. In fact, the presence of several aromatic hydrocarbons in complex mixtures improves its growth and degradation capabilities rather impairing them. We have observed that gas-oil and gasoline, which are among the most complex known hydrocarbon mixtures, are the best growth substrates. Moreover, its ability to spontaneously form a biofilm on several surfaces could allow the adhesion to soil, sand and mud particles that reducing washing out by atmospheric agents. This feature could reduce the necessity to frequently re-inoculate the strain in the materials under treatment.

Also its ability to form emulsions reduces the need to use detergents which are often required in bioremediation treatments. Moreover, it should be noted that the ability of PP1Y to encapsulate oil drops and to preferentially remove the aromatic fraction may avoid the dispersion of toxic aromatic hydrocarbons in the environment. Finally, the ability of the microorganism to grow in wide ranges of pH, temperature and salinity values allows for the use of *Novosphingobium putaolanum* PP1Y in a variety of environments, including costal lagoons and river estuarines.

In collaboration with the research group of Prof. F. Salvatore (CEINGE S.r.l.) and Prof. G. Paolella (Dipartimento di Biochimica e Biologia Molecolare, Università di Napoli Federico II) we are currently sequencing and analyzing the genome of *Novosphingobium putaolanum* PP1Y. The study of the complete genome will allow to better understand the molecular basis of the unusual features of this strain and to design engineered strains with widened abilities.

BIBLIOGRAPHY

1. Samanta, S.K., O.V. Singh, and R.K. Jain, *Polycyclic aromatic hydrocarbons: environmental pollution and bioremediation.* Trends Biotechnol., 2002. **20**(6): p. 243-8.
2. Baggi, G., et al., *Isolation of a Pseudomonas stutzeri strain that degrades o-xylene.* Appl. Environ. Microbiol., 1987. **53**: p. 2129-2131.
3. Moody, J.D., J.P. Freeman, and C.E. Cerniglia, *Degradation of benz[a]anthracene by Mycobacterium vanbaalenii strain PYR-1.* Biodegradation., 2005. **16**(6): p. 513-26.
4. Sohn, J.H., et al., *Novosphingobium pentaromativorans sp. nov., a high-molecular-mass polycyclic aromatic hydrocarbon-degrading bacterium isolated from estuarine sediment.* Int J Syst Evol Microbiol., 2004. **54**(Pt 5): p. 1483-7.
5. Zhou, H.W., et al., *Different bacterial groups for biodegradation of three- and four-ring PAHs isolated from a Hong Kong mangrove sediment.* J Hazard Mater., 2008. **152**(3): p. 1179-85. Epub 2007 Aug 8.
6. Foght, J.M. and D.W.S. Westlake, *Degradation of polycyclic aromatic hydrocarbons and aromatic heterocycles by a Pseudomonas species.* Can. J. Microbiol., 1988. **34**: p. 1135-1141.
7. Zhao, H.P., et al., *Isolation and characterization of phenanthrene-degrading strains Sphingomonas sp. ZP1 and Tistrella sp. ZP5.* J Hazard Mater., 2008. **152**(3): p. 1293-300. Epub 2007 Aug 8.
8. Willison, J.C., *Isolation and characterization of a novel sphingomonad capable of growth with chrysene as sole carbon and energy source.* FEMS Microbiol Lett., 2004. **241**(2): p. 143-50.
9. Rentz, J.A., P.J. Alvarez, and J.L. Schnoor, *Benzo[a]pyrene degradation by Sphingomonas yanoikuyae JAR02.* Environ Pollut., 2008. **151**(3): p. 669-77. Epub 2007 May 7.
10. Bogan, B.W., et al., *Degradation of straight-chain aliphatic and high-molecular-weight polycyclic aromatic hydrocarbons by a strain of Mycobacterium austroafricanum.* J Appl Microbiol., 2003. **94**(2): p. 230-9.
11. Lopez, Z., et al., *Simultaneous biodegradation of creosote-polycyclic aromatic hydrocarbons by a pyrene-degrading Mycobacterium.* Appl Microbiol Biotechnol., 2008. **78**(1): p. 165-72. Epub 2007 Dec 12.
12. Sorkhoh, N.A., et al., *Crude oil and hydrocarbon-degrading strains of Rhodococcus rhodochrous isolated from soil and marine environments in Kuwait.* Environ Pollut., 1990. **65**(1): p. 1-17.
13. Zeinali, M., et al., *Hydrocarbon degradation by thermophilic Nocardia otitidiscaviarum strain TSH1: physiological aspects.* J Basic Microbiol., 2007. **47**(6): p. 534-9.
14. Coulter, E.D. and D.P. Ballou, *Non-haem iron-containing oxygenases involved in the microbial biodegradation of aromatic hydrocarbons.* Essays Biochem., 1999. **34**: p. 31-49.
15. Dagley, S., *Catabolism of aromatic compounds by micro-organisms.* Adv Microb Physiol, 1971. **6**: p. 1-46.
16. Mogensen, A.S., et al., *Potential for anaerobic conversion of xenobiotics.* Adv Biochem Eng Biotechnol., 2003. **82**: p. 69-1 34.
17. Christensen, N., et al., *Removal of polycyclic aromatic hydrocarbons (PAHs) from sewage sludge by anaerobic degradation.* Water Sci Technol., 2004. **50**(9): p. 237-44.

18. Viggiani, A., et al., *An airlift biofilm reactor for the biodegradation of phenol by Pseudomonas stutzeri OX1.* J Biotechnol., 2006. **123**(4): p. 464-77 Epub 2006 Feb 20.
19. Bertoni, G., et al., *Cloning of the genes for and characterization of the early stages of toluene catabolism in Pseudomonas stutzeri OX1.* Appl Environ Microbiol, 1996. **62**(10): p. 3704-3711.
20. Arenghi, F.L., et al., *Organization and regulation of meta cleavage pathway genes for toluene and o-xylene derivative degradation in Pseudomonas stutzeri OX1.* Appl Environ Microbiol., 2001. **67**(7): p. 3304-8.
21. Viggiani, A., et al., *The role of the conserved residues His-246, His-199, and Tyr-255 in the catalysis of catechol 2,3-dioxygenase from Pseudomonas stutzeri OX1.* J Biol Chem., 2004. **279**(47): p. 48630-9 Epub 2004 Sep 4.
22. Arenghi, F.L., et al., *Organization and regulation of meta cleavage pathway gene for toluene and o-xylene derivative degradation in Pseudomonas stutzeri OX1.* Appl. Environ. Microbiol., 2001. **67**: p. 3304-3308.
23. Kita, A., et al., *An archetypical extradiol-cleaving catecholic dioxygenase: the crystal structure of catechol 2, 3-dioxygenase (metapyrocatechase) from Ppseudomonas putida mt-2.* Structure., 1999. **7**(1): p. 25-34.
24. Sato, N., et al., *Crystal structures of the reaction intermediate and its homologue of an extradiol-cleaving catecholic dioxygenase.* J Mol Biol., 2002. **321**(4): p. 621-36.
25. Vetting, M.W., et al., *Crystallographic comparison of manganese- and iron-dependent homoprotocatechuate 2,3-dioxygenases.* J Bacteriol., 2004. **186**(7): p. 1945-58.
26. Siani, L., et al., *The role of residue Thr249 in modulating the catalytic efficiency and substrate specificity of catechol-2,3-dioxygenase from Pseudomonas stutzeri OX1.* Febs J., 2006. **273**(13): p. 2963-76 Epub 2006 May 30.
27. Sawyer, R.F., *Trends in auto emissions and gasoline composition.* Environ Health Perspect., 1993. **101** (Suppl 6): p. 5-12.
28. Liang, F., et al., *The organic composition of diesel particulate matter, diesel fuel and engine oil of a non-road diesel generator.* J Environ Monit., 2005. **7**(10): p. 983-8. Epub 2005 Aug 8.
29. Yakimov, M.M., K.N. Timmis, and P.N. Golyshin, *Obligate oil-degrading marine bacteria.* Curr Opin Biotechnol., 2007. **18**(3): p. 257-66. Epub 2007 May 9.
30. Basta, T., S. Buerger, and A. Stolz, *Structural and replicative diversity of large plasmids from sphingomonads that degrade polycyclic aromatic compounds and xenobiotics.* Microbiology., 2005. **151** (Pt 6): p. 2025-37.
31. Basta, T., et al., *Detection and characterization of conjugative degradative plasmids in xenobiotic-degrading Sphingomonas strains.* J Bacteriol., 2004. **186**(1 2): p. 3862-72.
32. Romine, M.F., et al., *Complete sequence of a 184-kilobase catabolic plasmid from Sphingomonas aromaticivorans F199.* J Bacteriol., 1999. **181**(5): p. 1585-602.
33. Story, S.P., et al., *Degradation of aromatic hydrocarbons by Sphingomonas paucimobilis strain EPA505.* Arch Environ Contam Toxicol., 2004. **47**(2): p. 168-76.

34. Yabuuchi, E., et al., *Proposal of Sphingomonas wittichii sp. nov. for strain RW1T, known as a dibenzo-p-dioxin metabolizer.* Int J Syst Evol Microbiol., 2001. **51**(Pt 2): p. 281-92.
35. Sambrook, J., E.F. Fritsch, and T. Maniatis, *Molecular Cloning. A Laboratory Manual*. 2nd ed. 1989, Cold Spring Harbor, New York: Cold Spring Harbor Laboratory Press.
36. Kunkel, T.A., *Rapid and efficient site-specific mutagenesis without phenotypic selection.* Proc. Natl. Acad. Sci. USA, 1987. **82**: p. 488-492.
37. Laemmli, U., *Cleavage of structural proteins during the assembly of the head of bacteriophage T4.* Nature, 1970. **227**: p. 680-685.
38. Fialho, A.M., et al., *Occurrence, production, and applications of gellan: current state and perspectives.* Appl Microbiol Biotechnol., 2008. **79**(6): p. 889-900 Epub 2008 May 28.
39. Pollock, T.J. and R.W. Armentrout, *Planktonic/sessile dimorphism of polysaccharide-encapsulated sphingomonads.* J Ind Microbiol Biotechnol., 1999. **23**(4-5): p. 436-441.
40. Goel, S.K., G.S. Rao, and K.P. Pandya, *Hepatotoxic effects elicited by n-hexane or n-heptane.* J Appl Toxicol., 1988. **8**(2): p. 81-4.
41. Mazur, P., K.W. Cole, and A.P. Mahowald, *Critical factors affecting the permeabilization of Drosophila embryos by alkanes.* Cryobiology., 1992. **29**(2): p. 210-39.
42 Pezzella, A., *et al*.An expedient one pot entry catecholestogens and other catechol compounds via IBX mediatec phenolic oxygenation. Tetrahedron Lett., 2005. **46**: p. 3541-3544

PUBLICATION

P1) Izzo, V., Notomista, E., Picardi, A., Pennacchio, F. & Di Donato, A.
The thermophilic archaeon Sulfolobus solfataricus is able to grow on phenol
Research in Microbiology (2005) 156, 677-689

COMUNICATIONS

C1) Cafaro, V, Notomista, E., Scognamiglio, R., Alfieri, F., Bozza, G., Pennacchio, F. & Di Donato, A.
Metabolic Engineering for bioremediation strategies
Japan-Italy Symposium of New Trends in Enzyme Science and Technology Nagoya (2006).

C2) Di Donato, A., Cafaro, V., Izzo, V., Notomista, E., Scognamiglio, R., Alfieri, F., Bozza, G., Pennacchio, F.
Metabolic Engineering: a tool for bioremediation strategies
53° Congresso Nazionale SIB, Riccione (2008).

Available online at www.sciencedirect.com
SCIENCE DIRECT
Research in Microbiology 156 (2005) 677–689
Research in Microbiology
www.elsevier.com/locate/resmic

The thermophilic archaeon *Sulfolobus solfataricus* is able to grow on phenol

Viviana Izzo [a1], Eugenio Notomista [a1], Alessandra Picardi [a], Francesca Pennacchio [a], Alberto Di Donato [ab,*]

[a] *Dipartimento di Biologia strutturale efunzionale, Università di Napoli Federico II, Complesso Universitario di Monte S. Angelo, Via Cinthia, 80126 Naples, Italy*
[b] *CEINGE-BiotecnologieAvanzate S.c.ar.l., Naples, Italy*

Received 11 February 2005; accepted 7 April 2005
Available online 5 May 2005

Abstract

Many eubacteria use aromatic molecules as a carbon and energy source, but only a few archaea have been reported to grow on aromatics. Degradation of aromatic hydrocarbons by aerobic bacteria is generally divided into an upper pathway, which produces dihydroxylated aromatic intermediates by the action of monooxygenases, and a lower pathway that processes these intermediates down to molecules that enter the citric acid cycle. Recently, analysis of the genome of the thermophilic archaeon *Sulfolobus solfataricus* revealed the existence of *orf*s coding for putative enzymes of the degradation pathway of aromatics, i.e., a cluster of *orf*s coding for the subunits of a hypothetical bacterial multicomponent monooxygenase (SsoMO), an *orf* coding for a catechol 2,3-dioxygenase (SsoC2,3O), and an *orf* coding for an enzyme of the lower pathway of the catechol metabolism. In this paper we report that *S. solfataricus* can efficiently grow on phenol as the sole source of carbon and energy. To our knowledge this is the first report of a thermophilic archaeon able to grow on an aromatic compound under aerobic conditions. Moreover, the cloning and heterologous expression and characterization of the thermophilic SsoC2,3O are reported.

Keywords: *Sulfolobus*; Monooxygenase; Dioxygenase; Phenol

1. Introduction

The ability to use aromatic molecules as carbon and energy sources is widespread in eubacteria. Strains able to degrade benzene and phenol derivatives can be found among both Gram-positive and Gram-negative bacteria [10,11,39], among mesophiles and extremophiles [34,35]. The majority of aromatic-degrading microorganisms are aerobic but a few reports of anaerobic degradation have also been published [23,30,47].

The catabolic pathways used by mesophilic bacteria are well characterized and share common features [16,26,28]. The few catabolic pathways known for extremophiles seem to be similar to those found in mesophiles [34,35]. The aromatic ring is first converted to dihydroxylated compounds, usually aromatic vicinal diols (Fig. 1) in the so-called upper pathway. These dihydroxylated molecules undergo ring cleavage reactions producing non-cyclic molecules eventually converted, in the lower pathway, into species that can enter the citric acid cycle (CAC). The initial hydroxylation steps are carried out by mono- or dioxygenases (Fig. 1) [28,29,32,56]. Ring cleavage reactions are catalyzed by extradiol-cleaving dioxygenases (ECDs) and intradiol cleaving dioxygenases (ICDs), which incorporate both atoms of dioxygen into the aromatic substrate cleaving the aromatic ring at positions *meta* and *ortho* to the hydroxyl substituents, respectively (Fig. 1) [7]. For example, catechol 2,3-dioxygenases (C2,3O) are Fe(II)-dependent ECDs

* Corresponding author.
E-mail address: didonato@unina.it (A. Di Donato).
1 These authors contributed equally to the paper.

0923-2508/$ – see front matter © 2005 Elsevier SAS. All rights reserved. doi: 10.1016/j.resmic.2005.04.001

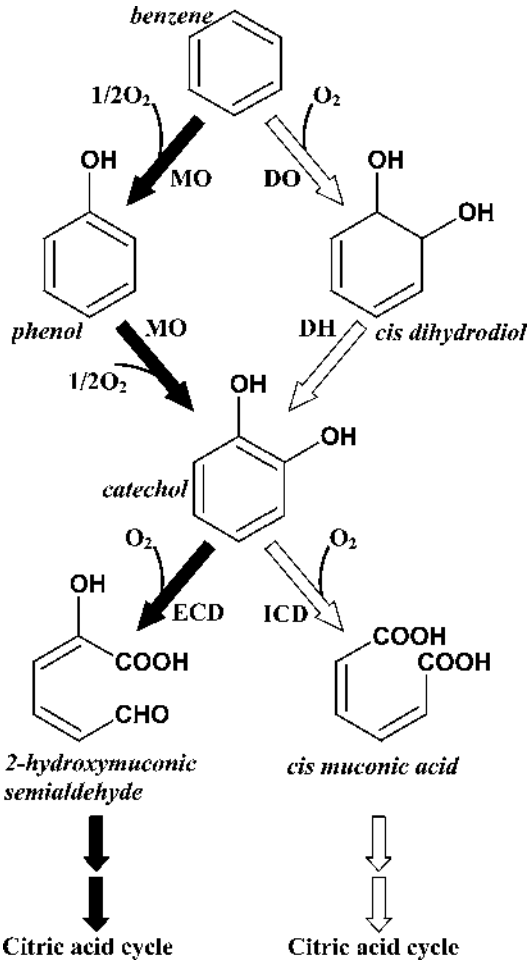

Fig. 1. Most frequently found degradation pathways of aromatic compounds. Black arrows indicate benzene metabolism in *B. pickettii*, *B. cepacia* JS150 and *P. stutzeri* OX1. MO, monooxygenase; DO, dioxygenase, DH, dehydrogenase; ECD, extradiol cleaving dioxygenase; ICD, intradiol cleaving dioxygenase.

which play a central role in the catabolism of benzene, toluene, and phenol, catalyzing the extradiol cleavage of (methyl)catechols formed by mono- and dioxygenases into 2-hydroxymuconic semialdehyde derivatives [7]. The wide distribution of relatively few families of mono- and dioxygenases among eubacteria has suggested that the genes coding for these enzymes are frequently mobilized to create new hybrid pathways, thus increasing the number and variety of strains able to degrade aromatic molecules [14,16,39].

Only two archaea have been reported to grow on aromatic molecules: the hyperthermophile *Ferroglobus placidus*, which anaerobically oxidizes several aromatics using Fe^{3+} as an electron acceptor [52], and the halophilic archaeon *Haloferax* sp. D1227, which grows under aerobic conditions on 3-phenylpropionic acid and benzoic acid [21]. The metabolic pathways for the degradation of aromatic compounds used by *F. placidus* are not known. The degradation of 3-phenylpropionic acid by *Haloferax* sp. D1227 probably proceeds through a two-carbon shortening of the substituent side chain by a mechanism similar to the 13-oxidation of fatty acids [21]. However, no archaeal mono- or dioxygenase specific for aromatic molecules has been characterized thus far.

The thermophilic archaeon *Sulfolobus solfataricus* [12], like other thermophilic organisms, is being extensively studied as a potential source of thermostable proteins for industrial applications or as a host microorganism for whole cell applications including cell-based bioreactors [42]. Recently, an analysis of its genome [39] revealed the existence of (i) a cluster of *orf*s coding for the subunits of a hypothetical bacterial multicomponent monooxygenase (BMM), (ii) an *orf* coding for a lower pathway protein of the catechol metabolism, and (iii) an *orf* coding for a putative catechol 2,3-dioxygenase (SsoC2,3O).

BMMs are a family of non-heme, diiron enzymes which use dioxygen to hydroxylate a variety of organic compounds [39]. All known BMMs, which can be grouped into 6 groups, are transcribed from single operons that code for 4–6 polypeptides, four of which— , 13, N, R—are always conserved [39]. The and 13 subunits and, in some cases, an additional y subunit, assemble into a complex known as the H complex endowed with hydroxylating activity. Subunit N oxidizes NADH providing electrons to the H complex. Group 2 BMMs, like toluene *o*-xylene monooxygenase (ToMO) from *Pseudomonas stutzeri* OX1, also possess a ferredoxin (T subunit, Fig. 2). The *orf*s found in the *S. solfataricus* genome coding for the hypothetical BMM are clustered together and their organization is the same as the *orf*s coding for group 2 BMMs (Fig. 2 and [39]). Two separate *orf*s code for N- and C-terminal domains of the subunit (N and C, respectively) and three *orf*s code for proteins homologous to subunits T, R, and 13 (Fig. 2). Another *orf*, located between the *orf*s coding for subunits C and T, codes for a protein—named X—which shows no similarity to other known proteins present in data bases [39]. Moreover, another *orf* is present [39] upstream from the sequences coding for subunit N, that codes for a putative ferredoxin reductase (subunit FR, ferredoxin reductase), belonging to a well known family of multicomponent dioxygenases which include benzene dioxygenase [51] and toluene dioxygenase [48,49]. The *orf* coding for the hypothetical *S. solfataricus* catechol 2,3-dioxygenases and for the *meta*-pathway protein are located immediately upstream from the *orf* coding for the FR subunit (Fig. 2).

Therefore, the *S. solfataricus* genome codes for a putative multicomponent monooxygenase (SsoMO) which seems to be different from other known BMMs. In fact, at least in its genome organization, this new BMM might be characterized by (i) the separation of the subunit domains into two separate subunits, (ii) the replacement of the usual monooxygenase-type reductase (N subunit) by a dioxygenase-type reductase (FR subunit), and (iii) the absence of a y2 subunit, or its replacement by a new type of subunit (X subunit) [39].

This genomic arrangement would suggest that *S. solfataricus* P2 possesses the metabolic machinery necessary to

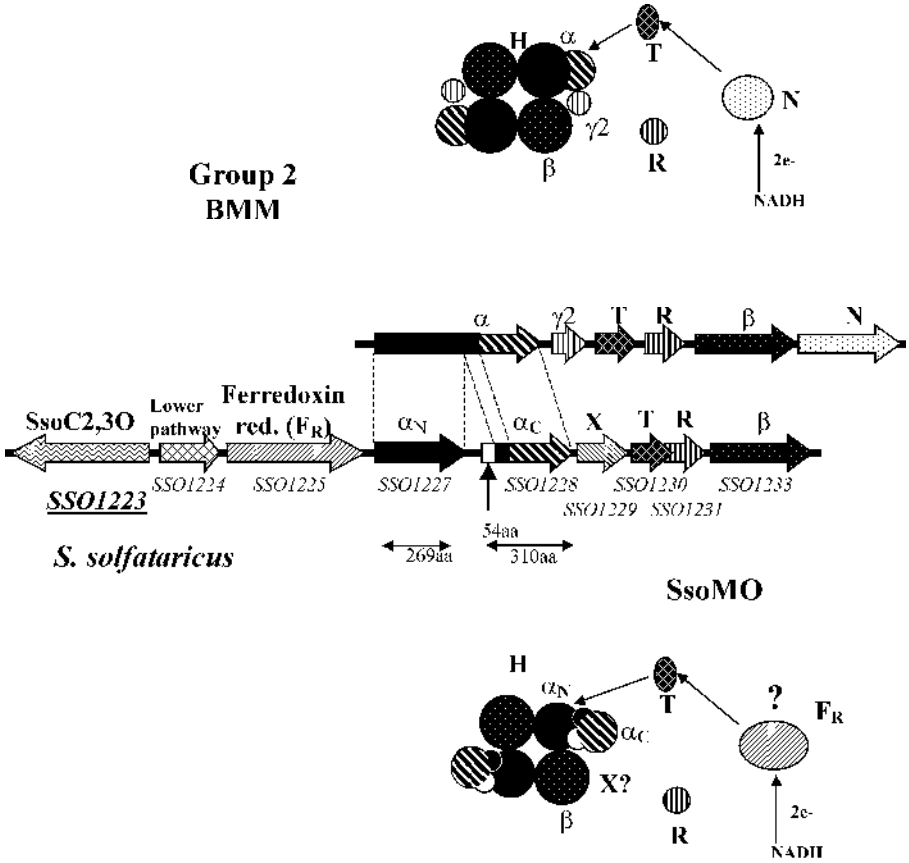

Fig. 2. Comparison between the operon coding for a generic group 2 BMM (top) and the region of *S. solfataricus* containing the homologous *orf*s (bottom). The names of the *orf*s are in italics, whereas the polypeptides are in bold. Identical filling motifs indicate homologous sequences. The schematic structure of the group 2 BMM and of the hypothetical SsoMO are shown. Arrows indicate electron flux.

metabolize benzene and/or benzene derivatives through a pathway similar to those found in *Burkholderia pickettii*, *Burkholderia cepacia* JS 150 and *P. stutzeri* OX1 (Fig. 1) [1,4,29,3 1].

In this paper we report that *S. solfataricus* can efficiently grow on phenol as the sole source of carbon and energy. Moreover, we show that the *orf*s coding for the SsoMO subunits, including FR and X subunits, are transcribed only in the presence of phenol. Finally, the cloning and heterologous expression and characterization of SsoC2,3O are reported.

To our knowledge, this is the first report of a thermophilic archaeon able to grow on an aromatic compound under aerobic conditions, and the first characterization of an archaeal ring cleavage dioxygenase.

2. Materials and methods

2.1. Materials

Bacterial cultures, plasmid purifications and transformations of *Escherichia coli* were performed according to Sambrook et al. [44]. The *E. coli* strain BL21(DE3) was purchased from AMS biotechnology. Vector pET22b(+) was from Novagen. *E. coli* strain JM101 was purchased from Boehringer. The *S. solfataricus* P2 strain was purchased from DSMZ (Deutsche Sammlung von Mikroorganismen und Zellkulturen GmbH). The Wizard SV Gel and PCR Clean-Up System for elution of DNA fragments from agarose gel were obtained from Promega. Enzymes and other reagents for DNA manipulation were from New England Biolabs. The oligonucleotides were synthesized at the Stazione Zoologica 'A. Dohrn' (Naples, Italy). All other chemicals were of the highest grade available and were from Pharmacia, Promega, New England Biolabs, Sigma, Fluka, or Applichem.

2.2. Growth curves

S. solfataricus P2 was routinely grown at 80 °C in minimal medium prepared according to Brock et al. [6], adjusted to pH 4.1 with $_{H2SO4}$ and supplemented with 0.2% sucrose as sole source of carbon and energy. Cell growth was followed spectrophotometrically at 600 nm. Saturated cultures (about 1.6 $OD_{600\ nm}$) were used to inoculate minimal medium supplemented with sucrose, phenol, *o*-, *m*-, or *p*-cresol at the appropriate concentrations as sole source of carbon and energy. *S. solfataricus* cells were consistently diluted to 0.08 $OD_{600\ nm}$ and grown at 80 °C. Concentrations of phenol and cresol isomers in the cultures

were measured spectrophotometrically. At the appropriate times, 1 ml aliquots of the cultures were collected, cells were removed by centrifugation at 17 000 *g* at room temperature for 10 min, and the supernatants diluted tenfold in 0.1% formic acid in water. The concentration of phenol in the diluted supernatants was measured using an extinction coefficient $\varepsilon_{271\ nm} = 1.62\ mM^{-1}\ cm^{-1}$. The concentration of cresol isomers was measured using an extinction coefficient $\varepsilon_{271\ nm} = 1.47\ mM^{-1}\ cm^{-1}$ for *o*-cresol, $\varepsilon_{272\ nm} = 1.35\ mM^{-1}\ cm^{-1}$ for *m*-cresol, and $\varepsilon_{277\ nm} = 1.62\ mM^{-1}\ cm^{-1}$ for *p*-cresol. The evaporation of phenol and cresols was evaluated by measuring their concentration in solutions prepared as described for bacterial cultures except that cells were not added to the minimal medium containing the aromatic compounds.

The average duplication time (*g*) was calculated by plotting the logarithm of cells density ($\ln OD_{600\ nm}$) as a function of time and using the equation:

$$g = \ln 2/k$$

in which *k* is the slope of the line fitting the experimental data.

The yield factor is expressed as $Y_{X/S} = AX/AS$, where *AX* is the variation of the cell mass (g of dry weight) and *AS* is the phenol consumed (g).

2.3. Total RNA purification and RT-PCR

S. solfataricus P2 cells grown on phenol or sucrose were harvested at 2400 *g* at 4 °C for 30 min at an optical density of about 0.37 and 0.96 $OD_{600\ nm}$, respectively. Cell pastes were stored at −80 °C until use. Total RNA was extracted with the TRI-Reagent kit (Sigma), using the manufacturer's protocol. Samples were then incubated with 10 $U\mu l^{-1}$ DNaseI (Boehringer) at 37 °C for 30 min and subjected to an acid phenol:chloroform extraction. RNA was recovered from the aqueous phase by precipitation with 3 M sodium acetate pH 5.3. Total RNA was dissolved in 60 µl of diethylpyrocarbonate-treated H_2O and stored at −80 °C. RNA concentration was estimated spectrophotometrically by measuring the absorbance at 260 nm ($1\ OD_{260\ nm} = 40\ \mu g\ ml^{-1}$) [44]. The integrity of RNA was verified on a denaturant 1.5% agarose gel. An aliquot of each RNA preparation was treated with 0.2 mg ml^{-1} RNase A at 37 °C for 1 h and used to run control RT-PCR reactions.

RT-PCR reactions were performed using the "Access RT-PCR System" kit (Promega), using 48 ng of RNA as template for each reaction and amplification products were examined on 1% agarose gels. RT-PCR reactions were performed using the following primers: 5-CCCCTCTAGAAGGAGAAATGTAGATGAAATGTGAAT-3 (upstream) and 5-CCCCCCATGGATCCCACTTATATTAAAAG-3 (downstream) for the amplification of *orf SSO1225*; 5-CCCGAGCTCAAGAAGGAGATTTACTTATGAAACCAGT-3 (upstream) and 5-CCCCGTCGACAAATTAAATTTTCTTTTCCA-3 (downstream) for *orf SSO1227*; 5-CCCCGTCGACAAGAAGGAGATACGACGATGAGTAGAG-3 (upstream) and 5-CCCAAGCTTTTGTTTTACGCCTCCG-3 (downstream) for *orf SSO1228*; 5-CCGGATCCAAGAAGGAGAAAAACAAATGAGTATAGAAG-3 (upstream) and 5-CCCGAATTCATAATCTCACGCTCTTA-3 (downstream) for *orf SSO1229*; 5-CCCAAGCTTAAGAAGGAGATGAGATTATGAATTACCCT-3 (upstream) and 5-CCCAAGCTTTCTAAAATTGTTTCAAGAGTTA-3 (downstream) for *orf SSO1230*; 5-CCCAAGCTTAAGAAGGAGAGTGATAAATGAGTTTGGA-3 (upstream) and 5-AAGGAAAAAAGCGGCCGCTTTCACCTCACAAGTC-3 (downstream) for *orf SSO1231*; 5-CCCGAATTCAAGAAGGAGAAAAGGATATGACTAGATTA-3 (upstream) and 5-CCCGAGCTCTCTCCTTCATAGTCCTA-3 (downstream) for *orf SSO1233*; 5-AGAATTCATATGGTAAATAAGTTACTTTCC-3 (upstream primer *sscat-up*) and 5-GGGGATCCAAGCTTATTAGATTTTTGCGCCTAA-3 (downstream primer *sscat-dw*) for *orf SSO1223*.

2.4. Phylogenetic analysis

Homology searches were performed using the programs BLAST and PSI-BLAST available at the web address http://www.ncbi.nlm.nih.gov/BLAST/. Default parameters were used to search the NCBI non-redundant (nr) database. Analysis of *S. solfataricus* genome was performed using tools available at the "*S. solfataricus* genome sequencing project" web site (http://www-archbac.u-psud.fr/projects/sulfolobus/). Multiple alignments were prepared using ClustalW (http://www.ebi.ac.uk/clustalw/). Alignments were visualized and examined using JalView (http://www.ebi.ac.uk/jalview/). Phylogenetic trees were prepared using Phylip and visualized using TreeView (http://taxonomy.zoology.gla.ac.uk/rod/treeview.html).

2.5. Cloning of SsoC2,3O

Genomic DNA was extracted from a 50 ml saturated culture of *S. solfataricus* as described [44]. *orf SSO1223* coding for SsoC2,3O was amplified by PCR using the specific primers *sscat-up* and *sscat-dw*. Primers *sscat-up* and *sscat-dw* were designed to add *Nde*I and *Hin*dIII restriction sites upstream and downstream, respectively, of the amplified *orf*. The amplified fragment was digested using *Nde*I and *Hin*dIII and ligated to the pET22b(+) commercial vector previously cut with the same enzymes. Ligated vectors were used to transform *E. coli* JM101. Clones harboring the recombinant plasmid were identified by PCR using the T7 promoter and T7 terminator primers which are complementary to sequences located upstream and downstream from the pET22b(+) multicloning site, respectively. Plasmid DNA from clones in which the expected 1000-bp fragment was detected were sequenced and found to contain a fragment whose sequence was identical to that of published *orf SSO1223*. The plasmid containing *orf SSO1223* was named pET22b(+)/S soC2,3O.

2.6. Expression and purification of SsoC2,3O

E. coli BL21 (DE3) cells transformed with plasmid pET22b(+)/SsoC2,3O were routinely grown in Luria–Bertani (LB) medium supplemented with 50 µg ml^{-1} ampicillin at 37°C for 19 h. Cells were collected by centrifugation at 5500 *g* for 20 min at 4°C, suspended in 50 mM Tris–HCl (pH 8.4) containing 10% ethanol, 10% glycerol, 200 µM $Fe(NH_4)_2(SO_4)_2$, 6mM vitamin C, and 1 $mgml^{-1}$ lysozyme, and lysed by sonication. Expression yielded about 200 mg of SsoC2,3O l^{-1} of culture as estimated from Coomassie blue-stained SDS–PAGE of cell lysates. Soluble and insoluble fractions of cell lysates were separated by centrifugation at 17000 *g* for 30 min at 4°C. About 20–30% of total SsoC2,3O was found to be present in the soluble fraction, as detected by SDS–PAGE (data not shown). Average dioxygenase-specific activity of the soluble fraction was found to be about 1.5–1.8 Umg^{-1} of SsoC2,3O, one unit being the amount of protein that converts 1 µmol of catechol to 2-hydroxymuconic semialdehyde under the condition described below.

Soluble SsoC2,3O in the supernatant was purified to about 95% homogeneity by a two-step procedure including a heat precipitation step followed by ion exchange chromatography. 200 µM $Fe(NH_4)_2(SO_4)_2$ and 6 mM vitamin C were added to the soluble fraction of cell lysate. The sample was purged with nitrogen, sealed and incubated at 60°C for 30 min, and then slowly cooled to 4°C. Precipitated proteins were removed by centrifugation at 17000 *g* for 30 min at 4°C. The average dioxygenase-specific activity of the soluble fraction after heat precipitation was found to be about 2.0–2.4 Umg^{-1} of SsoC2,3O. The soluble fraction containing SsoC2,3O was loaded onto a column (10 × 150 mm) of Q-Sepharose Fast Flow (Pharmacia) equilibrated with buffer A (50 mM Tris–HCl (pH 8.4), 10% ethanol, 10% glycerol). The column was washed with three column volumes of buffer A and eluted with a 260 ml linear gradient of NaCl from 0 to 0.4 M in buffer A at the flow rate of 15 ml h^{-1}. Fractions containing SsoC2,3O were pooled and concentrated by ultrafiltration in an Amicon apparatus equipped with a YM30 membrane (Millipore). This procedure yielded about 10 mg of SsoC2,3O l^{-1} of culture, i.e., 25% yield with respect to soluble expressed protein. When the protein was assayed on catechol, it was found to be inactive. Protein samples were stored at −80° C after having changed by ultrafiltration the buffer to 100 mM Tris–HCl (pH 7.0), containing 50% glycerol.

2.7. Reactivation of SsoC2,3O

Aliquots of the SsoC2,3O were heated as described above for the cell lysate. At the appropriate times the specific activity of the sample was determined as described in the following section. *2.8. Enzyme assays*

All assays were performed by measuring the amount of product of the reaction at temperatures between 25 and 80°C, in 50 mM Tris–HCl (pH 7.5) in 500 µl final volume. The pH of the buffers was always measured at the temperature of use. Freshly reactivated SsoC2,3O was used to start the reaction. The amount of products was measured spectrophotometrically by using their extinction coefficients. These were: $\varepsilon_{375\ nm}$ = 33000 M^{-1} cm^{-1} for 2-hydroxymuconic semialdehyde, the product of catechol; $\varepsilon_{388\ nm}$ = 13400 M^{-1} cm^{-1} for the product of 3-methylcatechol (3-MC); $\varepsilon_{382\ nm}$ = 28 100 M^{-1} cm^{-1} for the product of 4-methylcatechol (4-MC).

Kinetic parameters were determined by using the program GraphPad Prism (GraphPad Software, http://www.graphpad.com).

2.9. Thermostability measurements

Thermostability of SsoC2,3O was determined by incubating aliquots of the freshly reactivated protein at 60, 70, or 80°C for the appropriate times. At the end of the incubation samples were cooled on ice and immediately assayed on catechol at 25 °C.

2.10. Analytic methods

SDS–PAGE was carried out according to Laemmli [33]. The protein concentration was determined colorimetrically with the Bradford reagent [5], using bovine serum albumin as a standard. Total iron and Fe^{2+} content was determined colorimetrically by complexation with Ferene S in the presence and absence of vitamin C, respectively [37].

3. Results

3.1. Growth curves

In order to evaluate the ability of *S. solfataricus* P2 to grow on aromatic compounds, the microorganism was grown at 80°C in saline minimal medium containing 0.2% sucrose as the sole carbon source until saturation (about 1 $OD_{600\ nm}$ after 120 h). An inoculum of the saturated culture was diluted at 0.08 $OD_{600\ nm}$ final cell density in saline minimal medium containing phenol at a 2 mM (0.188 g l^{-1}) or 4 mM (0.376 g l^{-1}) concentration, as the sole source of carbon and energy. Control cultures were also grown by inoculating the same amount of cells (i) into minimal medium containing 0.2% sucrose and (ii) into minimal medium in the absence of any carbon source.

As shown in Fig. 3,*S. solfataricus* was able to grow in the presence of phenol at both concentrations tested. However, the lag period time was higher than that measured when cells

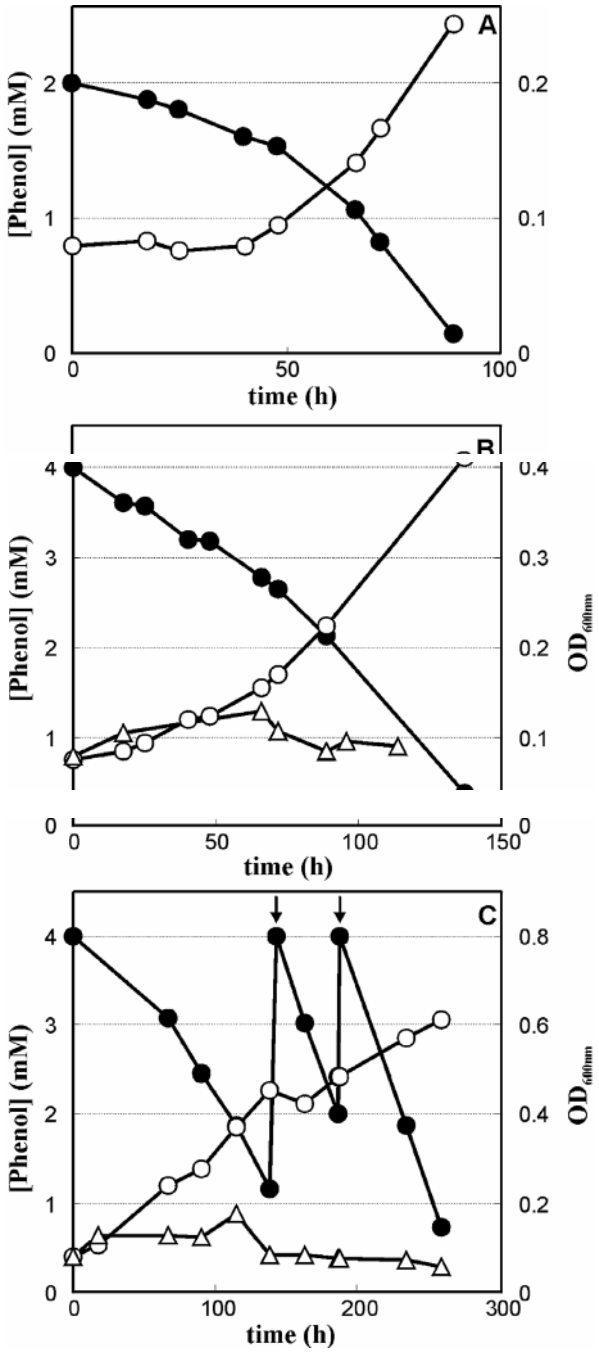

Fig. 3. Growth curves and phenol consumption of *S. solfataricus* cultures grown on 2(A) and 4mM (B and C) phenol. In A and B *S. solfataricus* cells grown in sucrose were used to inoculate the phenol-containing medium, whereas in C *S. solfataricus* cells grown on phenol were used. Arrows in C indicate the addition of fresh phenol to the culture. Filled circles indicate the concentration ofphenol, empty circles the optical density of the cultures, and empty triangles in B an C indicate the optical density of a control culture inoculated in a saline medium without any carbon source.

were grown on sucrose (40–50 h and about 10 h, respectively). In both cultures grown in the presence of phenol, its concentration decreased proportionally to the increase in cell density, and virtually reached zero after about 90 h in the presence of 2 mM phenol, and after about 150 h in the presence of 4 mM phenol. Moreover, the total amount of cells after phenol consumption was directly proportional to the initial phenol concentration. No cell growth could be measured when cells were grown in minimal medium in the absence of any carbon source. To evaluate the contribution of phenol evaporation to phenol consumption during cell growth, a solution of saline medium containing 4 mM phenol was incubated at 80°C under the same conditions used for cell growth experiments, and the phenol concentration was measured as a function of time. After 90 h the phenol concentration was about 82% of the initial value (data not shown), whereas, under the same conditions, in *S. solfataricus* cultures, the final phenol concentration was about 7% of the starting value. The average duplication time and biomass yield were calculated for cells grown in the presence of 4 mM phenol. The average duplication time was found to be about 47 h, twofold higher than that measured for cells grown in the presence of 0.2% sucrose (23 h). Biomass yield was 0.58 g of dried biomass per g of degraded phenol.

When *S. solfataricus* cells grown on phenol were diluted to 0.08 $OD_{600\ nm}$ in fresh minimal medium containing 4 mM phenol, a shorter lag period was observed (Fig. 3C). Moreover, further addition of phenol to cultures resulted in an extension of cell growth and in higher cell density. It should also be noted that phenol was very rapidly consumed after each addition (Fig. 3C).

To evaluate *S. solfataricus* sensitivity to phenol concentration, cells were cultured in minimal medium containing 4, 8, and 16 mM phenol. Growth rates in 4 and 8 mM phenol were found to be very similar. No growth was observed in 16 mM phenol (data not shown), thus indicating that phenol might be toxic to cells at this concentration.

During growth on phenol, *S. solfataricus* P2 cultures were found to accumulate a dark brown pigment. After centrifugation of the cultures at 17000 *g* at room temperature for 5 min, this pigment was found to form a black pellet stratified under the cell pellet. When pure catechol was incubated at 80°C in the saline minimal medium a similar pigment was obtained, suggesting that catechol, i.e., the hydroxylation product of phenol, accumulated during growth on this substrate.

In addition, *o*-, *m*-, and *p*-cresol were tested as growth substrates. *S. solfataricus* cells grown at saturation on sucrose were diluted and separately cultured in minimal media containing 2 mM of each of the three cresol isomers, at 80°C. Cell density was monitored for more than 300 h. No cell growth was observed in any of the cultures, thus indicating that cresol isomers could not sustain cell growth (data not shown).

3.2. Analysis of SsoMO and SsoC2,3O transcriptional levels

Given the ability of *S. solfataricus* cells to grow on phenol, we investigated whether this ability could depend on

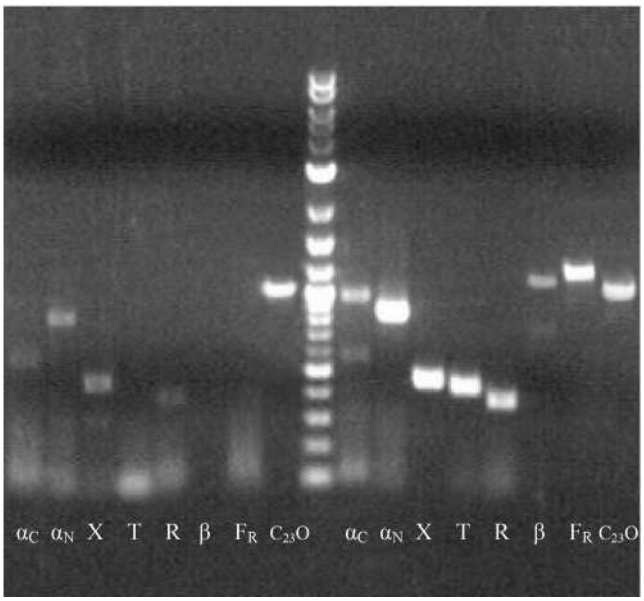

Fig. 4. Analysis on 1% agarose gel of the RT-PCR amplification products obtained using primers specific for SsoC2,3O and SsoMO *orf*s. Lanes 1–8: amplification products obtained using as template total RNA extracted from *S. solfataricus* cells grown on sucrose. Lane 9: 2 log ladder (New England Biolabs). Lanes 10–17: amplification products obtained using as template total RNA extracted from *S. solfataricus* cells grown on phenol.

the expression of putative genes for the catabolism of aromatic compounds present in the genome of the microorganism [39].

S. solfataricus cells grown on phenol or sucrose were lysed and total RNA was purified and subjected to RT-PCR as described in Section 2. Specific couples of primers were designed for the amplification of the *orf*s coding for the SsoMO subunits α_N, α_C, β, R, T, F_R, X, and for SsoC2,3O. For each couple, the upstream and the downstream primer were always complementary to the 5′ and to the 3′ end of an *orf*. The primer couples are expected to yield the amplification of fragments of 839 bp (α_N), 967 bp (α_C), 1,166 bp (β), 386 bp (R), 446 bp (T), 1,247 bp (F_R), 470 bp (X), and 1032 bp (SsoC2,3O). As shown in Fig. 4, RT-PCR experiments carried out using primers specific for the *orf*s coding for the SsoMO subunits yielded fragments of the expected length only when the RNA extracted from cells grown on phenol was used. Little or no amplification was detected in the case of cells grown on sucrose. Moreover, when the couple of primers designed for the *orf* coding for SsoC2,3O was used, the amplification of fragments of the expected size was observed in the case of cells grown both on phenol and on sucrose. No amplification was observed using DNaseI and RNase A-treated RNA samples nor when performing a PCR reaction on DNaseI-treated RNA samples, hence excluding DNA contamination of the RNA samples. These findings suggest that SsoC2,3O is constitutively transcribed in *S. solfataricus*, whereas the *orf*s coding for all the putative SsoMO subunits, including F_R and X subunits, are transcribed only in cells grown on phenol. *3.3. Sequence analysis of SsoC2,3O*

BLAST search with several ECD sequences in the genome of *S. solfataricus* revealed that it contained a second *orf* (*SSO2054*) homologous to ECDs. It should be underlined that this *orf* was adjacent to an *orf* coding for a hypothetical 4-hydroxyphenylacetate 3-monooxygenase (*orf SSO2053*). The protein sequence coded by *orf SSO2054*, named SsoECD-2, was aligned to the sequence of SsoC2,3O and the two proteins were found to possess 19% identity and 40% similarity. Therefore, it can be concluded that *S. solfataricus* genomes coded for two different but homologous ECDs. These two dioxygenase sequences were used to search homologous sequences by PSI-Blast. A set of 122 sequences conserving the three iron ligands, H153, H214, and E265, and the three catalytic residues, H199, H246, and Y255 [55] (*P. putida* MT2 C2,3O numbering), was obtained. Only four sequences out of the 122 in the set did not belong to eubacteria: the two *S. solfataricus* dioxygenases, a dioxygenase from *Sulfolobus tokodaii* (a thermophilic archaeon related to *S. solfataricus*), and a single eukaryotic sequence from *Neurospora crassa*. The sequences were aligned by ClustalW and multiple alignment was used to obtain the maximum parsimony (Fig. 5) and neighbor-joining (not shown) phylogenetic trees. Both trees showed that the majority of the sequences clustered into 6 groups sharing similar substrate specificity. Group 1 contained C2,3Os, including *Pseudomonas putida* MT2 and *P. stutzeri* OX1 C2,3Os [3, 55]. Group 2 contained dioxygenases acting on catechols with large substituents at positions 3 and/or 4. Group 3 included 3,4-dihydroxyphenylacetate-2,3-dioxygenases (DHPAD). The second *S. solfataricus* dioxygenases SsoECD-2, and the dioxygenase from *S. tokodaii* were very closely related—77% identity and 88% similarity—and formed the most divergent branch of this group. As bootstrap confidence was very high both in the maximum parsimony and the neighbor-joining trees, these two proteins were tentatively classified as DHPADs. Four out of seven members of Group 4 were from thermophilic organisms: SsoC2,3O from *S. solfataricus*, DHBD from *Bacillus* sp. JF8 (BP-BaciJF8), C2,3O from *Bacillus stearothermophilus* FDTP (C-BsteFDTP) and the hypothetical dioxygenase from *Chloroflexus aurantiacus* (D-Caur). Thus, it may be hypothesized that thermophilicity rather than substrate specificity is the distinctive feature of the members of this group. Group 5 included the 2,3-dihydroxy-*p*-cumate 3,4-dioxygenases [19, 38]. Group 6 included two dioxygenases acting on 2,4,5-trihydroxytoluene, an intermediate of 2,4-dinitrotoluene degradation [46,5 0], and the only known eukaryotic dioxygenase (D-Ncra in Fig. 5).

3.4. Cloning, expression and purification of SsoC2,3O

Preparative expression of SsoC2,3O, carried out as described in Section 2, enabled obtaining about 40–60 mg of SsoC2,3O l^{-1} in the soluble fraction of cell lysates. This

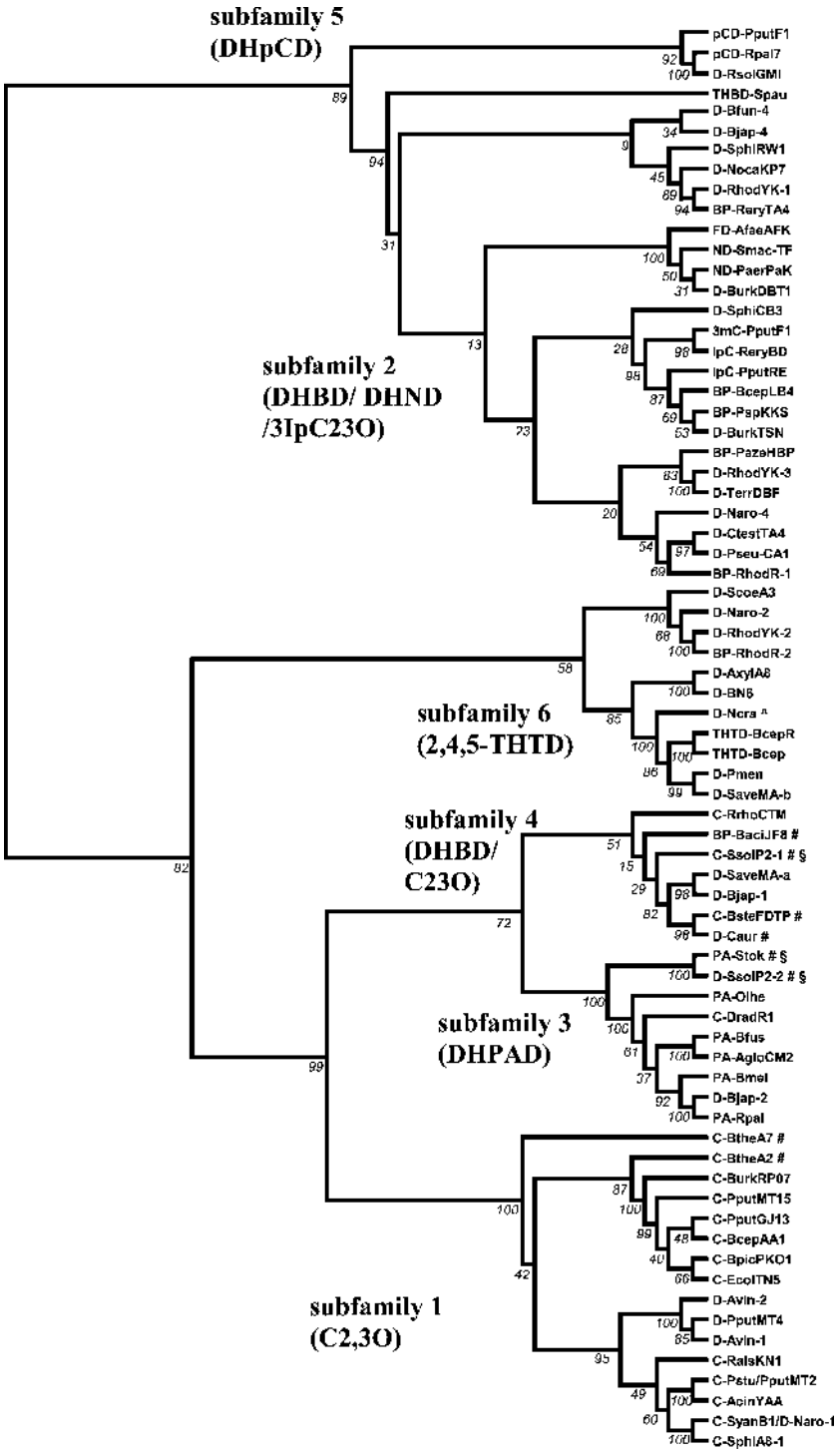

Fig. 5. Maximum parsimony tree of ECDs. Number in italics at each node is the percentage ofbootstrap replicates that possess that node. # indicates a sequence from a thermophile; § indicates a sequence from an archaea; ^ indicates a sequence from a eukarya. For clarity the names of the proteins were abbreviated as follows: D, non-characterized dioxygenase; C, C2,3O; 3mC, 3-methyl-C2,3O; IpC, 3-isopropyl-C2,3O; BP, DHBD; ND, dihydroxynaphthalene dioxygenase; PA, DHPAD; THBD, trihydroxybiphenyl dioxygenase; THTD, trihydroxytoluene dioxygenase; pCD, dihydroxy-*p*-cumate dioxygenase. Abbreviations of the names of the microorganisms were obtained from the first letter of the genus and the first three letters of the species; the strain is indicated only in case of ambiguity. When more sequences were identified in a single organism they were numbered progressively.

fraction showed catechol dioxygenase activity which increased about 20–30% after heat precipitation at 60 °C for 15–30 min under an N_2 atmosphere and in the presence of Fe^{2+} salts and DTT or vitamin C. Iron and reducing agents were added to avoid oxidation and/or loss of the catalytic metal. A slight decrease in activity was observed when heat precipitation was carried out at 70 °C (data not shown). When growth of *E. coli*/pET22b(+)/SsoC2,3O cells and heat

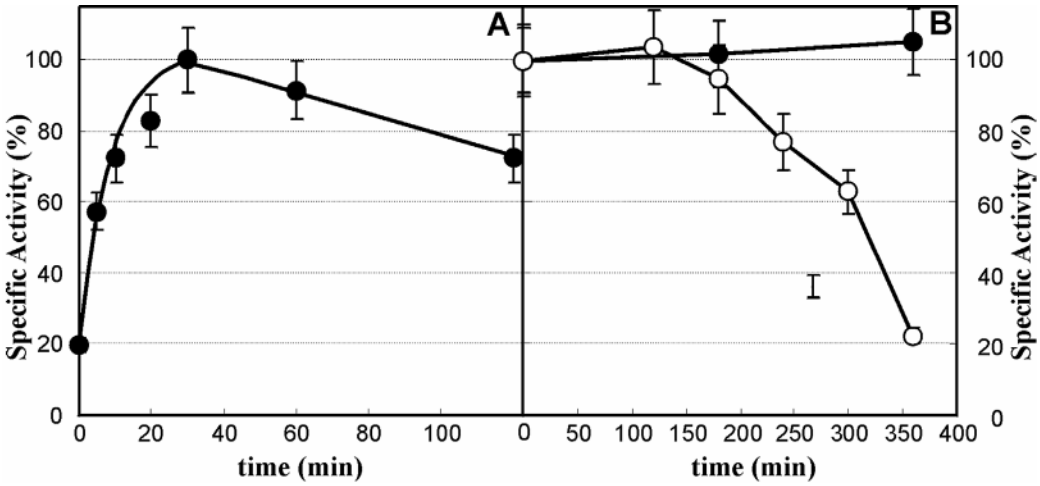

Fig. 6. (A) Reactivation of SsoC2,3O by Fe(II) and vitamin C at 60˚C. (B) inactivation caused by exposure to air at 4˚C. In A specific activity is reported as percentage of the maximum value. In B specific activity is reported as percentage of the initial value; empty and filled circles indicate specific activity of samples of reactivated SsoC2,3O after exposure to air and storage in an N_2 atmosphere, respectively.

precipitation of cell lysates was carried out in the presence of Mn^{2+} no activity was detected.

Recombinant SsoC2,3O was purified to about 95% homogeneity by heat precipitation followed by ion-exchange chromatography. This procedure led to obtaining about 10 mg of SsoC2,3O l^{-1} of culture, i.e., 25% yield with respect to soluble SsoC2,3O in the cell lysate, but with no dioxygenase activity.

3.5. Reactivation of SsoC2,3O and stability in storage

Based on the finding (data not shown) that during purification, SsoC2,3O was found to be active after heat precipitation, it was concluded that activity had been lost during the chromatographic step. Addition of 200 μM $Fe(NH_4)_2(SO_4)_2$ or 6 mM vitamin C or both to the elution buffer of the Q-Sepharose column did not lead to obtaining any active protein. However, determination of the iron content of the purified SsoC2,3O showed that only 0.25 moles of iron were present per mol of protein, fourfold less than expected [7]. Moreover, about 50% of iron was found to be in the Fe^{3+} form, thus indicating that the absence of activity was likely due either to the loss or to the oxidation of the catalytic iron. It has already been reported that other ECDs are inactive after purification because they lose the catalytic metal, and that they can be reactivated by addition of the appropriate metal ions [22,43]. We thus incubated purified SsoC2,3O for increasing times, at 60˚C under a nitrogen atmosphere, in the presence of variable concentrations of $Fe(NH_4)_2(SO_4)_2$ (100–200 μM), vitamin C (0.5–8.0 mM), and glycerol (10–5 0%), and measured the activity of the protein after incubation. Iron salts and vitamin C proved to be essential for reactivation; however, different concentrations did not significantly change activity recovery. Specific activity of the protein increased with glycerol concentration. Moreover, higher specific activities were found when performing reactivation at pH 7.0 than at pH 8.0 (data not shown). Also, the duration of the incubation at 60˚C proved to be crucial. As shown in Fig. 6A, specific activity rapidly increased, reached a maximum after 30 min of incubation and then decreased very slowly. On the basis of these findings SsoC2,3O reactivation was routinely carried out by incubating the purified protein at 60˚C under a nitrogen atmosphere for 30 min in Tris–HCl (pH 7.0) containing 50% glycerol, 200 μM $Fe(NH_4)_2(SO_4)_2$, and 6mM vitamin C. Specific activity at 25˚C of SsoC2,3O samples reactivated under these conditions always ranged between 1.8–2.2 U mg^{-1}. Reactivated SsoC2,3O was found to contain about 2 moles of iron per mole of protein. Iron was present as Fe^{2+}. Reactivated protein retained complete activity for more than 350 min when kept under an N_2 atmosphere at 4˚C, whereas it lost about 80% of its activity when stored for the same time at 4˚C in the absence of nitrogen (Fig. 6B).

Finally, the stability in storage of the inactive form of SsoC2,3O was investigated. The protein purified with the procedure described above was immediately stored at different temperatures and glycerol concentrations. At different times the protein was reactivated as described above and assayed for enzymatic activity. We found that both low temperatures and high glycerol concentrations improved its stability in storage. Storage at −80˚C in the presence of 50% glycerol was found to be the optimal condition.

3.6. Biochemical characterization ofSsoC2,3O

Thermostability of SsoC2,3O was studied by measuring residual activity on catechol of freshly reactivated protein after incubation at various temperatures. The half-life of SsoC2,3O was found to be about 230–240 min at 60˚C. This value decreased to 100–110 min at 70˚C, and to about 20 min at 80˚C (Fig. 7A). As all incubations were performed under a nitrogen atmosphere and in the presence of vitamin C, inactivation cannot be attributed to oxidation of

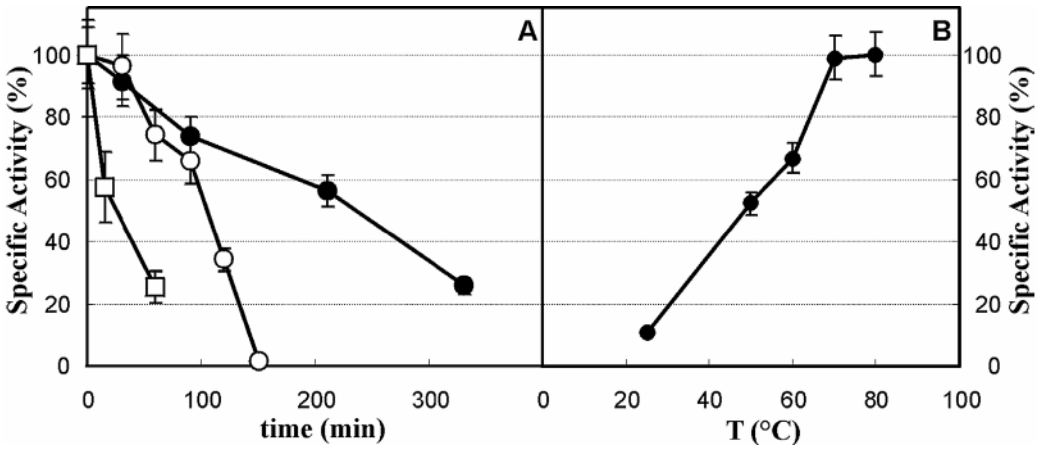

Fig. 7. Thermostability (A) and thermophilicity (B) of SsoC2,3O. In A specific activity is reported as percentage of the initial value. Thermostability was measured at 60 (filled circles), 70 (empty circles), and 80 °C (empty squares). In B specific activity is reported as percentage of the maximum value.

Table 1
Kinetic parameters measured at 25 and 60 °C for catechol, 3-MC, and 4-MC

Protein		Substrate		
		Catechol	3-MC	4-MC
*P.stutzeri*OX1	k_{cat}(s^{-1})	52±5	29±3	50±5
C2,3O	K_M (μM)	1.5± 0.3	3.8± 0.6	
(25 °C)[a]	k_{cat}/K_M (μM^{-1} s^{-1})	35	7.6	
SsoC2,3O	k_{cat} (s^{-1})	1.3± 0.1	0.58± 0.06	0.76± 0.07
(25 °C)	K_M (μM)	1.6±0.2	1.7±0.3	3.0±0.2
	k_{cat}/K_M (μ$M^{-1}s^{-1}$)	0.81	0.34	0.25
SsoC2,3O	k_{cat} (s^{-1})	7.8 ± 0.6	5.2 ± 0.2	4.7 ± 0.2
(60 °C)	K_M (μM)	5.9 ± 0.5	3.6 ± 0.4	11.7 ± 1.7
	k_{cat}/K_M (μ$M^{-1}s^{-1}$)	1.3	1.4	0.4
SsoC2,3O	k_{cat}[b]	6	9	6.2
(60/25 °C)	K_M[b]	3.7	2.1	3.9
	k_{cat}/K_M[b]	1.6	4.1	1.6

a Values from Ref. [55].
b Ratios between the kinetic parameters measured at 60 and 25 °C.

the catalytic iron, but is probably the consequence of heat denaturation of the protein.

The optimal temperature of SsoC2,3O was determined by assaying the activity of the freshly reactivated protein on catechol, at different temperatures. The specific activity increased linearly with temperature, reached a maximum at 70 °C, and remained constant up to 80 °C (Fig. 7B).

Kinetic parameters for catechol, 3-MC and 4-MC, were determined at 25 and 60 °C (Table 1). At 25 °C the highest specificity constant was measured when catechol was used as substrate, whereas the K_S values for 3-MC and 4-MC were very similar and about threefold lower than the K_S value for catechol. The K_M values for the three substrates were very similar to those measured for the mesophilic C2,3O from *P. stutzeri* OX1 at the same temperature (Table 1). On the contrary, the k_{cat} values were about 40–60-fold lower than those measured for the *P. stutzeri* C2,3O depending on the substrate. At 60 °C all the k_{cat} values increased 6–9-fold with respect to those measured at 25 °C, whereas the K_M values increased 2–4-fold. Moreover, at 60 °C the K_S values measured for catechol and 3-MC were identical within the experimental error.

4. Discussion

4.1. Phenol metabolism in S. solfataricus

S. solfataricus is a thermoacidophilic archaea that grows at temperatures between 80 and 90 °C and at pH values of around 4 [12]. Moreover, it is metabolically versatile, being able to oxidize, under aerobic conditions, several organic molecules and reduced sulfur compounds [6,15]. The occurrence in its genome of DNA sequences coding for putative proteins of the catabolism of aromatic compounds has led to the hypothesis that *S. solfataricus* might be able to grow on these molecules, an ability that has never been reported previously. Indeed, our data show that *S. solfataricus* is able to use phenol as the sole source of carbon and energy, with an average duplication time which is only twofold higher

than that observed on sucrose. Moreover, the biomass yield for growth on phenol—0.58 g per g of phenol—is comparable to that reported for other phenol-consuming organisms (0.4–0.52 g per g of phenol) [20], thus confirming that this compound is a good growth substrate for *S. solfataricus*.

During growth on phenol, we observed the accumulation of a dark polymer similar to that obtained by the spontaneous oxidation of catechol in the *S. solfataricus* saline medium. This latter finding supports the hypothesis that phenol is metabolized via oxidation to catechol. Indeed, the accumulation of dark pigments in cultures of organisms producing catechols has already been reported [17] and catechols are known to undergo oxidative polymerization in the presence of molecular oxygen as oxidant and transition metals which act as catalysts [13]. It is worth noting that *S. solfataricus* saline medium contains several transition metal salts [6].

The finding that the *orf*s coding for SsoMO are specifically transcribed only in cells grown on phenol but not in cells grown on sucrose strongly suggests that this enzyme is the catalyst involved in the hydroxylation of the substrate, the first reaction of most of the known pathways for the degradation of phenol [1,17,18,25,45]. Moreover, the finding that the dioxygenase gene coding for SsoC2,3O is also transcribed in *S. solfataricus* reinforces the hypothesis that the microorganism makes use of a catabolic pathway for the degradation of aromatic molecules similar to those found in other microorganisms (Fig. 1) [1,17,18,25, 45]. However, constitutive transcription of the *orf* coding for SsoC2,3O is unexpected and cannot be easily explained. It has been reported [2] that in *P. stutzeri* OX1 the enzymes responsible for its ability to grow on toluene are induced by the cresols formed by the low constitutive expression of toluene-*o*-xylene monooxygenase. Thus, the hypothesis can be advanced that a similar role might be played in *S. solfataricus* by SsoC2,3O, which could be involved in regulation of the metabolic process. It should also be added that, even though the selective transcription of the SsoMO *orf*s strongly suggests the involvement of the monooxygenase in phenol metabolism in *S. solfataricus*, it does not rule out that other monooxygenases might be involved in the process. We have searched the *S. solfataricus* genome for sequences coding for proteins homologous to other oxygenases of aromatic compounds. Only two new *orf*s were found, *orf SSO2053* coding for a 4-hydroxyphenylacetate 3-monooxygenase, and the adjacent *orf SSO2054* coding for a second ECD (SsoECD-2). Phylogenetic analysis of a large set of ECDs showed that SsoC2,3O belongs to a small heterogeneous subfamily including both a C2,3O and a dihydroxybiphenyl dioxygenase, whereas SsoECD-2 and the very similar dioxygenase from *S. tokodaii* form the most divergent branch of the subfamily of DHPADs. Thus, it may be concluded that both *orf SSO2053* and *orf SSO2054* code for enzymes involved in phenylacetate metabolism, whereas SsoMO and SsoC2,3O would appear to be the oxygenases involved in phenol metabolism.

It is worth noting that the genome of *S. tokodaii* contains a cluster of *orf*s similar to the *S. solfataricus orf*s coding for the oxygenases that we have hypothesized to be involved in phenylacetate metabolism, but it does not contain *orf*s coding for proteins homologous to SsoMO or SsoC2,3O. Moreover, no other known archaeal genome contains *orf*s homologous to that coding for SsoMO or for SsoC2,3O [39]. Thus, it would appear that these two genes are a specific acquisition of the *S. solfataricus* P2 genome, perhaps obtained through a horizontal gene transfer event similar to those hypothesized for the genes of the metabolic pathways of aromatics of several bacteria [14,16,39]. This hypothesis is reinforced by the finding that the *S. solfataricus* genome is very rich in mobile elements (IS, insertion sequence elements) which represent more than 10% of the genome, making it extremely variable [8,9]. Nine *orf*s homologous to *orf*s of known transposons (including two *orf*s coding for transposases) have been found downstream of the last SsoMO *orf* (on the right of SsoMO β in Fig. 2) and two other transposon *orf*s are located upstream of the SsoC2,3O *orf*. These findings support the hypothesis that the entire region is the result of a genomic rearrangement.

Finally, we found that the three cresol isomers do not support *S. solfataricus* growth. This finding is surprising given the ability of SsoC2,3O to use methylcatechols, i.e., the hydroxylation products of cresols, as substrates. The inability of *S. solfataricus* to use cresols as growth substrates may be subject to different explanations, including a restricted substrate specificity of SsoMO, which acts upstream from the C2,3O dioxygenase or of the enzymes which act downstream from SsoC2,3O.

4.2. Characterization of SsoC2,3O

We have found that *orf SSO1223*, when expressed in *E. coli*, yields a protein, SsoC2,3O, active toward catechol, 3-MC and 4-MC. In the SsoC2,3O sequence all the residues that are known to play a role in dioxygenases catalysis, i.e., the three iron ligands, the two active site histidine residues and the tyrosine residue [55], are present. SsoC2,3O has a very low enzymatic activity at 25 °C, as observed for several other thermophilic proteins [54] (Table 1), with a k_{cat} value 40-fold lower than that of the mesophilic C2,3O from *P. stutzeri* OX1. However, its $_{kcat}$ value increases with temperature, reaching a maximum at a temperature near the optimal growth temperature. At 80 °C SsoC2,3O is only 4– 5-fold less active than the *P. stutzeri* C2,3O at 25 °C.

SsoC2,3O activity, like that of many other ECDs, is dependent on the presence of Fe(II). In the recombinant protein the catalytic metal seems to be very easily oxidized and labile. The purified protein contains only 25% of the expected iron and half of the metal ions are in the Fe(III), non-catalytic form. A similar feature has been observed for other ECDs [22,43]. Sensitivity to oxidation of the recombinant protein is further confirmed by the fact that recombinant SsoC2,3O can be reactivated by providing Fe(II) in a reduc-

ing environment but the reactivated protein rapidly loses its activity when exposed to air and not when it is stored under a nitrogen atmosphere. It should be noted, however, that cytosol is a reducing environment and hence SsoC2,3O could be at least partially protected from oxidation in vivo. Moreover, inside the cell, protective molecules could be present, like the small ferredoxines which have been found to reactivate several ECDs from mesophiles [27,40,41,53].

SsoC2,3O is a thermostable enzyme with a half-life longer than 200 min at 60˚C and about 110 min at 70˚C. These values are comparable to those reported for the most thermostable known ECD, the DHBD from *Bacillus* sp. JF8 [24]. Interestingly, at 80˚C the half-life of SsoC2,3O is only 20 min. Above this temperature, the dioxygenase undergoes rapid inactivation in spite of the fact that the optimal growth temperature of *S. solfataricus* P2 is around 87˚C [6,15]. However, the half-life at this temperature could be longer inside the cell due to the presence of stabilizing molecules. It has been demonstrated that *B. stearothermophilus* A2, which degrades phenol at 60˚C, produces a thermolabile C2,3O and compensates for the inactivation of the enzyme by increased protein production [36]. A similar mechanism might be present in *S. solfataricus*.

Acknowledgements

This work was supported by grants from the Ministry of University and Research (PRIN/2002 and PRIN/2004).

References

[1] F.L. Arenghi, D. Berlanda, E. Galli, G. Sello, P. Barbieri, Organization and regulation of *meta*-cleavage pathway gene for toluene and *o*-xylene derivative degradation in *Pseudomonas stutzeri* OX1, Appl. Environ. Microbiol. 67 (2001) 3304–3308.

[2] F.L. Arenghi, M. Pinti, E. Galli, P. Barbieri, Identification of the *Pseudomonas stutzeri* OX1 toluene-*o*-xylene monooxygenase regulatory gene (*touR*) and of its cognate promoter, Appl. Environ. Microbiol. 65 (1999) 4057–4063.

[3] I. Bertini, F. Briganti, S. Mangani, H.F. Nolting, A. Scozzafava, X-ray absorption studies on catechol 2,3-dioxygenase from *Pseudomonas putida* mt2, Biochemistry 33 (1994) 10777–10784.

[4] G. Bertoni, F. Bolognesi, E. Galli, P. Barbieri, Cloning of the genes for and characterization of the early stages of toluene catabolism in *Pseudomonas stutzeri* OX1, Appl. Environ. Microbiol. 62 (1996) 3704–3711.

[5] M.M. Bradford, A rapid and sensitive method for the quantitation of microgram quantities of protein utilizing the principle of protein–dye binding, Anal. Biochem. 72 (1976) 248.

[6] T.D. Brock, K.M. Brock, R.T. Belly, R.L. Weiss, *Sulfolobus*: A new genus of sulfur-oxidizing bacteria living at low pH and high temperature, Arch. Mikrobiol. 84 (1972) 54–68.

[7] J.B. Broderick, Catechol dioxygenases, Essays Biochem. 34 (1999) 173–189.

[8] K. Brugger, P. Redder, Q. She, F. Confalonieri, Y. Zivanovic, R.A. Garrett, Mobile elements in archaeal genomes, FEMS Microbiol. Lett. 206 (2002) 13 1–141.

[9] K. Brugger, E. Torarinsson, P. Redder, L. Chen, R.A. Garrett, Shuffling of *Sulfolobus genomes* by autonomous and non-autonomous mobile elements, Biochem. Soc. Trans. 32 (2004) 179–183.

[10] L. Cavalca, E. Dell'Amico, V. Andreoni, Intrinsic bioremediability of an aromatic hydrocarbon-polluted groundwater: Diversity of bacterial population and toluene monoxygenase genes, Appl. Microbiol. Biotechnol. 64 (2004) 576–587.

[11] L. Cavalca, P. Di Gennaro, M. Colombo, V. Andreoni, S. Bernasconi, I. Ronco, G. Bestetti, Distribution of catabolic pathways in some hydrocarbon-degrading bacteria from a subsurface polluted soil, Res. Microbiol. 151 (2000) 877–887.

[12] M. Ciaramella, F.M. Pisani, M. Rossi, Molecular biology of extremophiles: Recent progress on the hyperthermophilic archaeon *Sulfolobus*, Antonie Van Leeuwenhoek 81(2002) 85–97.

[13] M.L. Colarieti, G. Toscano, G. Greco Jr., Soil-catalyzed polymerization ofphenolics in polluted waters, Water Res. 36(2002) 3015–3022.

[14] S.D. Copley, Evolution of a metabolic pathway for degradation of a toxic xenobiotic: The patchwork approach, Trends Biochem. Sci. 25 (2000) 261–265.

[15] M. De Rosa, A. Gambacorta, J.D. Bu'lock, Extremely thermophilic acidophilic bacteria convergent with *Sulfolobus acidocaldarius*, J. Gen. Microbiol. 86 (1975) 156–164.

[16] E. Diaz, Bacterial degradation of aromatic pollutants: A paradigm of metabolic versatility, Int. Microbiol. 7 (2004)173–180.

[17] F.M. Dong, L.L. Wang, C.M. Wang, J.P. Cheng, Z.Q. He, Z.J. Sheng, R.Q. Shen, Molecular cloning and mapping of phenol degradation genes from *Bacillus stearothermophilus* FDTP-3 and their expression in*Escherichia coli*, Appl. Environ. Microbiol. 58(1992)2531–2535.

[18] F.M. Duffner, U. Kirchner, M.P. Bauer, R. Muller, Phenol/cresol degradation by the thermophilic *Bacillus thermoglucosidasius* A7: Cloning and sequence analysis of five genes involved in the pathway, Gene 256 (2000) 215–221.

[19] R.W. Eaton, *p**-Cumate catabolic pathway in *Pseudomonasputida* Fl: Cloning and characterization of DNA carrying the *cmt* operon, J. Bacteriol. 178 (1996) 1351–1362.

[20] H. Feitkenhauer, S. Schnicke, R. Muller, H. Markl, Determination of the kinetic parameters of the phenol-degrading thermophile *Bacillus thermoleovorans* sp. A2, Appl. Microbiol. Biotechnol. 57(2001) 744–750.

[21] W. Fu, P. Oriel, Degradation of 3-phenylpropionic acid by *Haloferax* sp. D1227, Extremophiles 3 (1999) 45–53.

[22] K. Furukawa, N. Arimura, Purification and properties of 2,3-dihydroxybiphenyl dioxygenase from polychlorinated biphenyl-degrading *Pseudomonaspseudoalcaligenes* and *Pseudomonas aeruginosa* carrying the cloned *bphC* gene, J. Bacteriol. 169(1987)924–927.

[23] J. Gibson, C.S. Harwood, Metabolic diversity in aromatic compound utilization by anaerobic microbes, Annu. Rev. Microbiol. 56 (2002) 345–369.

[24] T. Hatta, G. Mukerjee-Dhar, J. Damborsky, H. Kiyohara, K. Kimbara, Characterization of a novel thermostable Mn(II)-dependent 2,3-dihydroxybiphenyl 1,2-dioxygenase from a polychlorinated biphenyl- and naphthalene-degrading *Bacillus* sp. JF8, J. Biol. Chem. 278 (2003) 21483–2 1492.

[25] K. Heesche-Wagner, T. Schwarz, M. Kaufmann, Phenol degradation by an enterobacterium: A *Klebsiella* strain carries a TOL-like plasmid and a gene encoding a novel phenol hydroxylase, Can. J. Microbiol. 45 (1999) 162–171.

[26] E. Heinaru, J. Truu, U. Stottmeister, A. Heinaru, Three types of phenol and *p*-cresol catabolism in phenol- and *p*-cresol-degrading bacteria isolated from river water continuously polluted with phenolic compounds, FEMS Microbiol. Ecol. 31(2000)195–205.

[27] N. Hugo, J. Armengaud, J. Gaillard, K.N. Timmis, Y. Jouanneau, A novel –2Fe–2S– ferredoxin from *Pseudomonas putida* mt2 promotes the reductive reactivation of catechol 2,3-dioxygenase, J. Biol. Chem. 273 (1998) 9622–9629.

[28] E. Jindrova, M. Chocova, K. Demnerova, V. Brenner, Bacterial aerobic degradation of benzene, toluene, ethylbenzene, and xylene, Folia Microbiol. (Praha) 47 (2002) 83–93.

[29] G.R. Johnson, R.H. Olsen, Multiple pathways for toluene degradation in *Burkholderia* sp. strain JS150, Appl. Environ. Microbiol. 63 (1997) 4047–4052.

[30] P. Jothimani, G. Kalaichelvan, A. Bhaskaran, D.A. Selvaseelan, K. Ramasamy, Anaerobic biodegradation of aromatic compounds, Indian J. Exp. Biol. 41(2003) 1046–1067.

[31] J.J. Kukor, R.H. Olsen, Genetic organization and regulation of a meta cleavage pathway for catechols produced from catabolism of toluene, benzene, phenol, and cresols by*Pseudomonaspickettii* PKO1, J. Bacteriol. 173 (1991) 4587–4594.

[32] J.J. Kukor, R.H. Olsen, Molecular cloning, characterization, and regulation of a*Pseudomonaspickettii* PKO1 gene encoding phenol hydroxylase and expression of the gene in *Pseudomonas aeruginosa* PAO1c, J. Bacteriol. 172 (1990) 4624–4630.

[33] U. Laemmli, Cleavage of structural proteins during the assembly of the head of bacteriophage T4, Nature 227 (1970) 680–685.

[34] R. Margesin, S. Gander, G. Zacke, A.M. Gounot, F. Schinner, Hydrocarbon degradation and enzyme activities of cold-adapted bacteria and yeasts, Extremophiles 7 (2003) 451–458. Epub 2003 Aug 2026.

[35] R. Margesin, F. Schinner, Biodegradation and bioremediation of hydrocarbons in extreme environments, Appl. Microbiol. Biotechnol. 56 (2001) 650–663.

[36] R.E. Milo, F.M. Duffner, R. Muller, Catechol 2,3-dioxygenase from the thermophilic, phenol-degrading *Bacillus thermoleovorans* strain A2 has unexpected low thermal stability, Extremophiles 3 (1999) 185–190.

[37] L.M. Newman, L.P. Wackett, Purification and characterization of toluene 2-monooxygenase from *Burkholderia cepacia* G4, Biochemistry 34 (1995) 14066–14076.

[38] H.Z. Ninnekar, Purification and properties of 2,3-dihydroxy-*p*-cumate-3,4-dioxygenase from *Bacillus* species, Biochem. Int. 28 (1992) 97–103.

[39] E. Notomista, A. Lahm, A. Di Donato, A. Tramontano, Evolution of bacterial and archaeal multicomponent monooxygenases, J. Mol. Evol. 56 (2003) 435–445.

[40] D.W. Park, J.C. Chae, Y. Kim, T. Iida, T. Kudo, C.K. Kim, Chloroplast-type ferredoxin involved in reactivation of catechol 2,3-dioxygenase from *Pseudomonas* sp. S47, J. Biochem. Mol. Biol. 35 (2002) 432–436.

[41] A. Polissi, S. Harayama, In vivo reactivation of catechol 2,3-dioxygenase mediated by a chloroplast-type ferredoxin: A bacterial strategy to expand the substrate specificity of aromatic degradative pathways, EMBO J. 12 (1993) 3339–3347.

[42] H. Radianingtyas, P.C. Wright, 2-Propanol degradation by *Sulfolobus solfataricus*, Biotechnol. Lett. 25 (2003) 579–583.

[43] U. Riegert, G. Heiss, A.E. Kuhm, C. Muller, M. Contzen, H.J. Knackmuss, A. Stolz, Catalytic properties of the 3-chlorocatechol-oxidizing 2,3-dihydroxybiphenyl 1,2-dioxygenase from *Sphingomonas* sp. strain BN6, J. Bacteriol. 181 (1999) 4812–4817.

[44] J. Sambrook, E.F. Fritsch, T. Maniatis, Molecular Cloning. A Laboratory Manual, second ed., Cold Spring Harbor Laboratory Press, Cold Spring Harbor, NY, 1989.

[45] V. Shingler, J. Powlowski, U. Marklund, Nucleotide sequence and functional analysis of the complete phenol/3,4-dimethylphenol catabolic pathway of *Pseudomonas* sp. strain CF600, J. Bacteriol. 174 (1992) 71 1–724.

[46] R.J. Spanggord, J.C. Spain, S.F. Nishino, K.E. Mortelmans, Biodegradation of 2,4-dinitrotoluene by a *Pseudomonas* sp., Appl. Environ. Microbiol. 57 (1991) 3200–3205.

[47] A.M. Spormann, F. Widdel, Metabolism of alkylbenzenes, alkanes, and other hydrocarbons in anaerobic bacteria, Biodegradation 11 (2000) 85–105.

[48] V. Subramanian, T.N. Liu, W.K. Yeh, M. Narro, D.T. Gibson, Purification and properties of NADH-ferredoxin TOL reductase: A component of toluene dioxygenase from *Pseudomonasputida*, J. Biol. Chem. 256 (1981) 2723–2730.

[49] V. Subramanian, T.N. Liu, W.K. Yeh, C.M. Serdar, L.P. Wackett, D.T. Gibson, Purification and properties of ferredoxin TOL: A component of toluene dioxygenase from *Pseudomonas putida* F1, J. Biol. Chem. 260 (1985) 2355–2363.

[50] W.C. Suen, J.C. Spain, Cloning and characterization of *Pseudomonas* sp. strain DNT genes for 2,4-dinitrotoluene degradation, J. Bacteriol. 175 (1993) 1831–1 837.

[51] H.M. Tan, H.Y. Tang, C.L. Joannou, N.H. Abdel-Wahab, J.R. Mason, The *Pseudomonas putida* ML2 plasmid-encoded genes for benzene dioxygenase are unusual in codon usage and low in G + C content, Gene 130 (1993) 3 3–39.

[52] J.M. Tor, D.R. Lovley, Anaerobic degradation of aromatic compounds coupled to Fe(III) reduction by *Ferroglobus placidus*, Environ. Microbiol. 3 (2001) 28 1–287.

[53] D. Tropel, C. Meyer, J. Armengaud, Y. Jouanneau, Ferredoxin-mediated reactivation of the chlorocatechol 2,3-dioxygenase from *Pseudomonas putida* GJ31, Arch. Microbiol. 177 (2002) 345–351. Epub 2002 Feb 2002.

[54] C. Vieille, G.J. Zeikus, Hyperthermophilic enzymes: Sources, uses, and molecular mechanisms for thermostability, Microbiol. Mol. Biol. Rev. 65 (2001) 1–43.

[55] A. Viggiani, L. Siani, E. Notomista, L. Birolo, P. Pucci, A. Di Donato, The role of conserved residues H246, H199 and Y255 in the catalysis of catechol 2,3-dioxygenase from *Pseudomonas stutzeri* OX1, J. Biol. Chem. 279 (2004) 48630–48639.

[56] G.M. Whited, D.T. Gibson, Separation and partial characterization of the enzymes of the toluene-4-monooxygenase catabolic pathway in *Pseudomonas mendocina* KR1, J. Bacteriol. 173 (1991) 3017–3020.